The Environmental Impacts of Scaling a Microfinancial Product: Index-Based Livestock Insurance and East African Rangelands

Steven W. Wilcox, Christopher B. Barrett, Nathaniel Jensen, Patrick E. Clark, Francesco Pietro Fava, Gerardo E. Soto, Njoki Kahiu, Ying Sun*

July 2026

Abstract

Expanded access to financial products has ambiguous effects on natural resources, especially in environments lacking clear property rights. Index-based livestock insurance (IBLI) is a micro-insurance product originally developed to help pastoralists in East Africa manage catastrophic drought risk. Rigorous impact evaluations have clearly established welfare and productivity gains from IBLI. Open questions remain, however, regarding IBLI's potential environmental impacts. Might IBLI encourage overstocking or change grazing behaviors that harm the rangeland systems on which pastoralists rely, ultimately undermining the product's effectiveness in reducing livestock mortality risk? Or does IBLI encourage production strategies that ultimately improve rangeland health, for example through smaller and more productive herds? We address this question empirically by combining administrative data on the roll-out of IBLI with remotely-sensed rangeland condition measures spanning approximately 643,000 km^2 over the period 2000-2020. Using a staggered differences-in-differences estimator we find evidence for neutral to positive impacts of IBLI on East African rangelands.

Keywords: microfinance, drought, rangelands, pastoralism, remote sensing

JEL classification: O16, O13, Q24, C23

*Wilcox: Department of Agricultural and Resource Economics, Utah State University (USU), and faculty affiliate of the USU Ecology Center and the Berryman Institute, Logan, UT 84322, USA, steven.wilcox@usu.edu. Barrett: Charles H. Dyson School of Applied Economics and Management, Jeb E. Brooks School of Public Policy, and Cornell Atkinson Center for Sustainability, Cornell University, Ithaca, NY 14853, USA, cbb2@cornell.edu. Jensen: University of Edinburgh, Edinburgh, UK, EH8 9YL, njensen@ed.ac.uk. Clark: USDA-Agricultural Research Service, Boise, ID 83702, USA pat.clark@usda.gov. Fava: Department of Environmental Science and Policy (ESP), Università degli Studi di Milano, Via Celoria 2, 20133 Milan, Italy, fava@unimi.it. Soto: Instituto de Estadística, Universidad Austral de Chile, Chile, gerardo.soto@uach.cl. Kahiu: Department of Plant and Environmental Sciences, New Mexico State University, NM, USA, nkahiu@nmsu.edu. Sun: School of Integrative Plant Science, Soil and Crop Sciences Section, Cornell University, Ithaca, NY 14853, USA, ys776@cornell.edu. We gratefully acknowledge financial support from the CGIAR Standing Panel on Impact Assessment, data support from the International Livestock Research Institute, excellent research assistance from Shilvaan Patel and Joseba Iribarrren, and contributions from Benjamin Porter, and Chuan Liao. We are grateful for helpful comments received from Kathy Baylis, Joel Ferguson, John Gardner, David Just, C.-Y. Cynthia Lin Lawell, Ariel Ortiz-Bobea, Liz Tennant, several anonymous reviewers, and seminar participants at AAEA, Cornell, ICAE, NC-1034, SPIA, Texas A&M, WAEA, and CEAR. All errors are our own.

1 Introduction

Recent decades have witnessed a microfinance revolution aimed at empowering the poor to save, borrow, and insure so that they can invest in sustainable improvements in living standards and weather the shocks that buffet them (Besley 1995; Robinson 2001). A sizeable literature documents generally favorable impacts of microfinance interventions on incomes, investment and other indicators of human well-being (for reviews, see Van Rooyen et al. 2012 and Cull and Morduch 2018). Far less attention has been paid to whether improved access to financial products might generate unintended negative impacts on the natural systems that disproportionately support the livelihoods of the rural poor.

Among the variety of microfinance programs, interventions and products that directly or indirectly impact agricultural production, herding and/or harvesting activities may be the most plausible to generate unintended impacts on natural systems. A prominent and promising subset of the broader microfinance movement that fits this description is index insurance against crop and livestock loss (Carter et al. 2017), but may include other related programs that offer improved access to financial services (e.g., credit). By increasing risk-adjusted returns, improved access to financial services could boost investments that expand or intensify extractive operations, with plausibly adverse impacts on forest, land, water and/or wildlife resources, perhaps especially in settings where property rights are insecure, common pool resource settings dominate, or open access tenure prevails (Bhattacharya and Osgood 2014; Assunção et al. 2020; Noack and Costello 2024). Conversely, newfound access to financial services could facilitate environmentally favorable changes, for example by enabling sustainable agricultural intensification that reduces extensification into fragile ecosystems, per the Borlaug hypothesis (Stevenson et al. 2013; Villoria 2019a,b), supporting transitions out of natural resource extraction industries, or reducing risk management behaviors that degrade nature (Barrett 1999; Gollin et al. 2021; Feng et al. 2021; Wilcox et al. 2025). These potential outcomes illustrate that the environmental impacts of microfinance are analytically ambiguous, sensitive to local conditions, and can be globally important.

The scant evidence on this topic originates partly from the paucity of data that reliably link microfinance interventions and environmental outcomes, and partly due to the small spatial scale and short duration of most microfinance interventions. Two recent studies (Assunção et al. 2020; Noack and Costello 2024) have overcome these barriers in regards to the impacts of credit markets on fisheries and deforestation. We know of no evidence regarding the effects of microinsurance or other traditional micro-financial products on natural systems and the environment generally.

Index-based insurance, a form of microfinance, has been widely promoted in low-income, rural settings where adverse selection, moral hazard and high transaction costs limit access to conventional indemnity insurance (Carter et al. 2017; Jensen and Barrett 2017). Many index insurance products have generated favorable outcomes for policyholders, including increased incomes, productivity, subjective well-being, children's education, as well as reduced conflict, distress sales and meal skipping (Karlan et al. 2014; Jensen et al. 2017; Janzen and Carter 2019; Tafere et al. 2019; Janzen and Carter 2019; Stoeffler et al. 2022; Barrett et al. 2025; Gehring and Schaudt 2024; Jensen et al. 2025; Sakketa et al. 2025).

Given rural livelihoods' heavy reliance on natural resources, however, the sustainability of any observed gains from index insurance – or any microfinance product – depends in part on avoidance of unintended, negative environmental externalities. Multiple candidate mechanisms might cause environmental spillovers. For example, in the case of index insurance, by increasing risk-adjusted returns, an index insurance product might encourage expansion of the cultivated frontier or grazing lands into fragile areas, resulting in loss of natural habitats, e.g. forests, protected areas, wetlands. Index insurance might also encourage more intensive production on existing working lands, perhaps via reduced mobility and intensified local grazing, or general overstocking and overgrazing of rangelands, leading to rangeland degradation, erosion, or soil nutrient loss, etc. These possibilities mimic the Jevons Paradox of agricultural productivity growth, wherein higher returns induce extensification into previously uncultivated lands. Conversely, the provision of formal, financial insurance could reduce environmentally-damaging self-insurance behaviors, such as precautionary savings 'on the hoof' that result in overgrazing (Jensen et al. 2017; Cissé and Barrett 2018; Bulte and Haagsma 2021), over-application of pesticides (Feng et al. 2021), or overuse of natural resources as a means of self-insuring against producer price risk (Barrett 1999; Wilcox et al. 2025). Insurance access might also induce investments in boosting livestock productivity with less intensive rangelands use, per the Borlaug hypothesis (Jensen et al. 2017). The net environmental impacts of index insurance, and closely related micro-financial products, are therefore analytically ambiguous and an open empirical question.[1]

In this paper, we advance understanding on these important issues by examining the impacts of long-term access to index insurance at scale on rangelands. We do so by exploiting a new, high spatial resolution data set from 2000-2020 that covers 745,840 km2 of East African rangelands (Soto et al. 2024) that span the gradual roll-out of a successful micro-insurance product, index-based livestock insurance (IBLI). IBLI has now insured more than 3.2 million livestock herders in Ethiopia and Kenya against catastrophic drought losses,

[1]Analogous ambiguities and thin empirical evidence have also been reported for general crop insurance effects in developed country settings, such as in the US (Smith and Goodwin 2013).

including through the Kenyan government's national Kenya Livestock Insurance Program (Jensen et al. 2024) and the World Bank-led De-risking, Inclusion, and Value Enhancement of Pastoral Economies in the Horn of Africa (DRIVE) project (https://zep-re.com/drive-project/about-drive/). The spatial and temporal scale of IBLI's diffusion across southern Ethiopia and northern Kenya, combined with high spatial resolution data on rangeland conditions spanning IBLI's pre- and post-introduction periods, enable rigorous causal identification of microfinance's impacts at scale on a key natural resource. No comparable study is known to exist for the environmental impact of a microfinancial product.

IBLI offers an uncommon opportunity to test the environmental impacts of a long-term and scaled microfinance product that has and continues to support insurance coverage for hundreds of thousands of clients across a massive landscape. IBLI introduced drought insurance to low-income pastoralists who graze livestock on East Africa's rangelands, where drought-related herd mortality is the primary source of wealth loss (Lybbert et al. 2004; Barrett et al. 2006; Santos and Barrett 2011; Chantarat et al. 2013; Toth 2015; Santos and Barrett 2019). Initially piloted in northern Kenya in 2010, IBLI expanded into southern Ethiopia in 2012, and subsequently across northern, eastern and central Kenya (Jensen et al. 2024). Several impact evaluations have demonstrated IBLI's benefits, including improved livestock productivity, children's nutritional status and educational attainment, household income and subjective well-being, and reduced conflict and adverse coping strategies, among others (Jensen et al. 2017, Janzen and Carter 2019, Tafere et al. 2019; Barrett et al. 2025; Gehring and Schaudt 2024; Jensen et al. 2025; Sakketa et al. 2025). But if IBLI adversely affects rangelands, it might ultimately cause the very herd losses against which it ostensibly insures.

Theory- and simulation-based studies have predicted that IBLI and rangeland-oriented index insurance might have negative impacts on rangelands (Müller et al. 2011; John et al. 2019; Bulte and Haagsma 2021). The central mechanism at the heart of each of those models is that livestock drought insurance might induce risk averse herders to expand their herds, overall and/or in the immediate post-drought recovery period when rangelands vegetation is especially sensitive to grazing pressures. These models also all assume that rangeland vegetation dynamics are driven by biotic processes affected by grazing pressure, with abiotic phenomena, like drought, generating stochastic variation around dynamic equilibrium rangeland conditions. Jointly, these assumptions yield unambiguous predictions that livestock drought insurance induces overgrazing.

A potential weakness of these models is that they assume away other mechanisms that might partly or wholly offset any such partial equilibrium effects. For example, if herders can

invest not only in herd accumulation but also in improving animal productivity, as through greater veterinary care, the quality boosting incentive may dominate the herd accumulation incentive, permitting intensification and reduced congestion externalities or overgrazing. Or, in the absence of low-cost savings or insurance products, herders might have preferences that favor precautionary savings, which would likely take the form of additional livestock. In that case, a financial insurance product might induce reduced herd size, relaxing grazing pressures on rangelands. And none of the known simulation models explores induced changes in the spatial distribution of livestock. But if insurance reduces trekking animals – a costly form of self-insurance – then IBLI could induce improved range conditions in areas more distant from permanent settlements, perhaps at the expense of greater localized range degradation near settlements (McPeak 2003). Jensen et al. (2017) find precisely those sorts of intensification and precautionary savings effects in empirically evaluating IBLI's impacts on herder behaviors, while other studies likewise find strong evidence of precautionary savings in the absence of IBLI (Cissé and Barrett 2018) and induced destocking among those who take up the insurance (Barrett et al. 2025). Using data from GPS collars placed on insured and uninsured cattle, Toth et al. (2020) indeed find that IBLI induces reduced trekking distances. So the assumed preferences and choice sets of the models that predict adverse rangelands effects may be mistaken in ways that matter to predicting the environmental impacts of livestock drought insurance.

The true nature of range vegetation dynamics in East Africa has also been hotly debated by range scientists for decades. Ellis and Swift (1988) and other range scientists studying this region have emphasized that abiotic shocks like droughts may regulate rangeland conditions, not grazing pressure, leading to nonequilibrium ecological system. If nonequilibrial dynamics characterize this setting, that would dampen or decouple any induced increases in herd size's effects on rangeland conditions. Recent work focused on Mongolia has also shown that while human-mediated factors such as herd size and market liberalization can have negative effects on rangelands, weather and climate can exert far larger influence (Purevjav et al. 2025).

To address the issue empirically, we use the aforementioned new data set of remotely-sensed rangeland quality indicators from 2000-2020 (Soto et al. 2024) and administrative data on the staggered roll-out of IBLI across Kenya and southern Ethiopia from 2010-2020 to estimate IBLI's impacts across approximately 643,000 km^2. We tap recent advances in differences-in-differences (DiD) estimation in settings with effectively-random, staggered roll-out and potentially-heterogeneous treatment effects while controlling for pre- and post-treatment variation in exogenous covariates (Roth et al. 2023; Gardner et al. 2025). In our setting, it is crucial to control for seasonal weather variation to credibly isolate the effect of IBLI from other processes that may drive much of the observed variation in rangeland

conditions (Purevjav et al. 2025). We estimate models at multiple spatial scales and account for herder movement by inverse distance weighting IBLI exposure within a neighborhood defined by GPS-tracking of livestock migration in the study area (Liao et al. 2018b).

Across a series of rangeland health indicators (described in Section 3.3), we find no evidence of negative impacts to rangelands from IBLI. On the contrary, IBLI's impacts on rangelands range from neutral to statistically significantly positive. At the extensive margin – meaning when IBLI is first introduced in a location – we find mostly precisely-estimated null results with the exception of small but statistically significant increases in rangeland biological productivity indicators (e.g., reflectance-based vegetation indices). At the intensive margin – i.e., as the number of insured livestock increases after the initial introduction – not only do vegetation indices increase significantly with increased IBLI exposure but so does the fraction of land cover in photosynthetic vegetation. There are also signs of reduced bare ground, though these results are not as robust, and continued generally null effects on non-photosynthetic vegetation cover. These findings are encouraging and allay concerns regarding IBLI's potential to induce negative impacts on rangeland systems.

In providing the first known empirical test of the environmental effects of a microfinancial product at scale, we contribute to existing literature in several ways. Beyond relationships to the aforementioned literature, we highlight three particular contributions. First, our work provides an important answer to long-standing questions regarding the potential unintended environmental spillovers of IBLI. By showing that the worst concerns about IBLI are not supported by the evidence, our work allays longstanding concerns that have been raised by prior theoretical and simulation studies (Bhattacharya and Osgood 2014; Müller et al. 2011; John et al. 2019; Bulte and Haagsma 2021). This is crucial because IBLI is scaling rapidly to other locations across Africa. The DRIVE project is rapidly expanding IBLI coverage not only in Ethiopia and Kenya, but into Djibouti and Somalia as well. The World Food Program (WFP) is scaling its existing use of IBLI in Ethiopia, Zambia, and other countries under its R4 Rural Resilience Initiative. IBLI has been proposed for a 12 country region of west Africa (Estefania-Salazar and Iglesias 2026) and Nigeria has already approved the launch of an IBLI product. Mongolia has a longstanding IBLI product and multiple central Asian countries with significant extensive livestock grazing are now exploring IBLI as a climate risk management tool. While contract specifications and rangeland conditions vary among and within each of these areas – as they do within our study zone – the present findings are of general interest regionally and globally given that roughly two-thirds of all agricultural lands on Earth are used for extensive grazing and climate change is exciting interest in tools to help manage drought risk. While we cannot be certain these findings may hold in other systems with different rangeland ecology, the mechanisms we suspect may be in play are

potentially generalizable (e.g., reduced precautionary savings).

Second, our work provides a novel empirical study as it pertains to renewable resource sustainability by helping to extend empirical applications to rangelands. Economists have been conducting research on rangelands and herders for generations (e.g., Standiford and Howitt 1992; Batabyal et al. 2001; McPeak 2003; Lybbert et al. 2004; Finnoff et al. 2008; Epanchin-Niell et al. 2009; Mu et al. 2013), but empirical work applying quasi-experimental methods with explicit measurement of rangeland outcomes at scale is a recent development (Constenla-Villoslada et al. 2022; Purevjav et al. 2025). Relatedly, while classic works on the tragedy of the commons, and the tension between the Borlaug Hypothesis and Jevons Paradox have often reflected on a variety of environmental impacts, and livestock husbandry and rangelands have received attention in related discussion, associated empirical work has often focused on other classic renewable resources such as fisheries, forests, and water (Hardin 1968; Stevenson et al. 2013; Villoria 2019a; Pelletier et al. 2020; Assunção et al. 2020; Ayres et al. 2021; Balboni et al. 2023; Noack and Costello 2024). A potential reason for the lack empirical work is that the relative health of rangelands is not readily measured by any single measure and it is only in recent years that remotely sensed methods have become credible for monitoring these systems (Pellant et al. 2020; Reeves et al. 2015; Retallack et al. 2023).

Finally, our findings offer a notable contrast to recent work studying the effects of credit access on natural resources, particularly as regards conditions with property rights. The aforementioned studies by Assunção et al. (2020) and Noack and Costello (2024) provide important empirical evidence on the effects of credit markets on deforestation and fisheries. A core implication of both of these studies is that greater credit access causes resource degradation in the presence of incomplete and imperfect property rights. By contrast, we find that increased insurance access does not cause rangelands degradation – if anything, range conditions improve as herders take up drought insurance – despite similarly incomplete and imperfect property rights. This finding highlights a subtle, but important difference between credit and insurance. Rangelands, like forests, can be over-exploited when financial market failures induce second-best self-insurance behaviors that damage the environment (Barrett 1999; McCarthy et al. 1999; McPeak and Barrett 2001). In settings such as ours, resolving insurance market failures may not prompt environmental damage; indeed, it may even reduce resource over-exploitation by offering an alternative risk management tool.

2 East African Pastoralism and IBLI

The arid and semi-arid lands (ASALs) of East Africa are characterized by limited physical and institutional infrastructure and low human population densities. Combined with poor

soils and low and variable rainfall, the main livelihood is pastoralism, the extensive grazing of livestock on communal lands with complex, contested property rights (McCarthy et al. 1999; McPeak et al. 2011). Livestock are pastoralists' main store of wealth and generate most of their income, social status, and nutrient intake.[2] Livestock productivity depends fundamentally on rangeland conditions, which is adversely affected by overgrazing, leading Garrett Hardin to famously reference extensive livestock grazing to motivate his 'tragedy of the commons' hypothesis.[3] Pastoralists in the region have historically used mobility to manage drought risk exposure by adjusting seasonal and daily movements in response to drought-induced impacts to forage quality and quantity, though in the modern era a variety of factors are working to reduce herder mobility.[4] Any intervention that might change pastoralists' investment in livestock or their grazing patterns could therefore plausibly affect rangelands. Although the study area's human population densities are low, varying from roughly 7 persons/km^2 in Marsabit County, Kenya, to 74 in West Pokot County,[5] rangelands degradation and its feedback effects on livestock productivity and survival have been a concern in our northern Kenya - southern Ethiopia study area for decades, if not longer (Ellis and Swift 1988; Coughenour et al. 1990; Coppock et al. 1994; McCarthy et al. 1999; McPeak 2003; McPeak et al. 2011).

IBLI was originally designed to help pastoralists in this region rebuild their herds after catastrophic drought events.[6] Pastoralists can buy IBLI policies specific to the 'index insurance unit' (IU) – approximately equivalent to a sub-county in today's Kenya – in which they principally reside (Figure 1). IU-specific premium rates and indemnity payments are based on historical and current realizations of normalized difference vegetation index (NDVI) data generated from moderate resolution imaging spectroradiometer (MODIS) satellite imagery in near-real-time by the US government's National Oceanic and Atmospheric Administration. IBLI contracts last 12 months and are sold during each of two semi-annual sales periods, in January-February and in August-September. That timing reflects the region's bimodal rainfall patterns, with a long rainy season that typically runs March-June followed by a long dry season that lasts through September, then a weaker, short rainy season that runs October-December, followed by the January-February short dry season. When the NDVI-based index

[2]See McPeak et al. (2011) or Jensen et al. (2024) for rich descriptions of this area.

[3]Hardin (1968), p.1244 wrote "The tragedy of the commons develops in this way. Picture a pasture open to all. It is to be expected that each herdsman will try to keep as many cattle as possible on the commons."

[4]Liao et al. (2017) measured the distance herds migrate in our study area using GPS collars placed on cattle. They found a mean grazing range diameter of 40 km, with a standard deviation of 23 km, and a maximum range of 122 km. We discuss our analysis of this same data and how we account for herder movement in our empirical analysis in Section 3.2.

[5]Estimates from `geo-ref.net`

[6]See Jensen et al. (2024) for details on the development, adaptation, and expansion of IBLI.

falls beneath a contractually-specified seasonal trigger – originally calibrated to reflect a 15 percent expected loss (Chantarat et al. 2013) – policyholders receive a cash payout.

IBLI was piloted in Marsabit District of northern Kenya in January 2010. After IBLI worked as designed during a major drought in 2011, a very similar IBLI product was introduced into the neighboring Borana region of southern Ethiopia in August 2012. Subsequently, IBLI incrementally rolled-out into other parts of the Kenyan ASALs, with new commercial underwriters taking up the product, and to additional kebeles (the smallest administrative unit in Ethiopia) within the Borana Zone of Ethiopia. In 2015, the Kenyan government launched the Kenya Livestock Insurance Program (KLIP), a state-subsidized purchase of IBLI on behalf of qualified, low-income herders. By 2018, IBLI was available for purchase in every IU shown in Figure 1, and by 2020 KLIP was present in all IUs in Kenya.

The timing and order of IBLI's roll-out across IUs was unrelated to rangeland conditions, driven chiefly by insurance underwriters' operational capacity, their retail sales agents, and regulators (Johnson et al. 2019; Jensen et al. 2024). This generates plausible exogeneity in the timing of rangelands IBLI exposure at the extensive margin, enabling evaluation of microinsurance's impacts on rangelands. Exposure at the intensive margin, however, was potentially endogenous to rangeland conditions that affect pastoralists' demand for IBLI (Jensen et al. 2018). We discuss in Section 4 how we deal with that prospective endogeneity.

To enhance our study area, we identify plausible control areas in ASALs with very similar vegetation, climate, land-use and ethnic groups that border the IUs where IBLI was sold during the study period (Figure 1). These prospective IUs were identified and studied by the research team that developed and adapted IBLI during its expansion for the purpose of enabling introduction of IBLI there as well (Jensen et al. 2024). But for supply-side reasons related largely to underwriters' pre-existing coverage, the cost of initial product design, and staffing, IBLI was not offered in those regions by 2020. IBLI is now expanding into these plausible control areas, however, under a large, World Bank-led, multi-country expansion under the De-risking, Inclusion and Value Enhancement of Pastoral Economies in the Horn of Africa (DRIVE) project, which launched in 2022. So these prospective IUs offer suitable natural control sites for our purposes, as they are not-yet-treated areas testably comparable to the sites where IBLI rolled out over its first decade.

There are a variety of complicating factors in understanding IBLI's impacts on rangelands in the ASALs, including challenges with rangeland heterogeneity and scale. Soto et al. (2024) map eight land cover classes that reflect rangeland heterogeneity in the region. This variation is a function of a variety of biophysical properties, including topography and hydrology. A natural way to address these issues is to incorporate this variation in our measurement

of rangeland conditions and to leverage units of analysis that are associated with this heterogeneity as well as herder movement. Watershed units offer a natural fit in this regard as they reflect local biophysical properties of the landscape and avoid potential scale mismatch issues that come with administrative unit boundaries. We elaborate on how we approach issues with scale, units of analysis, and rangeland heterogeneity in Sections 3.2 and 3.3.

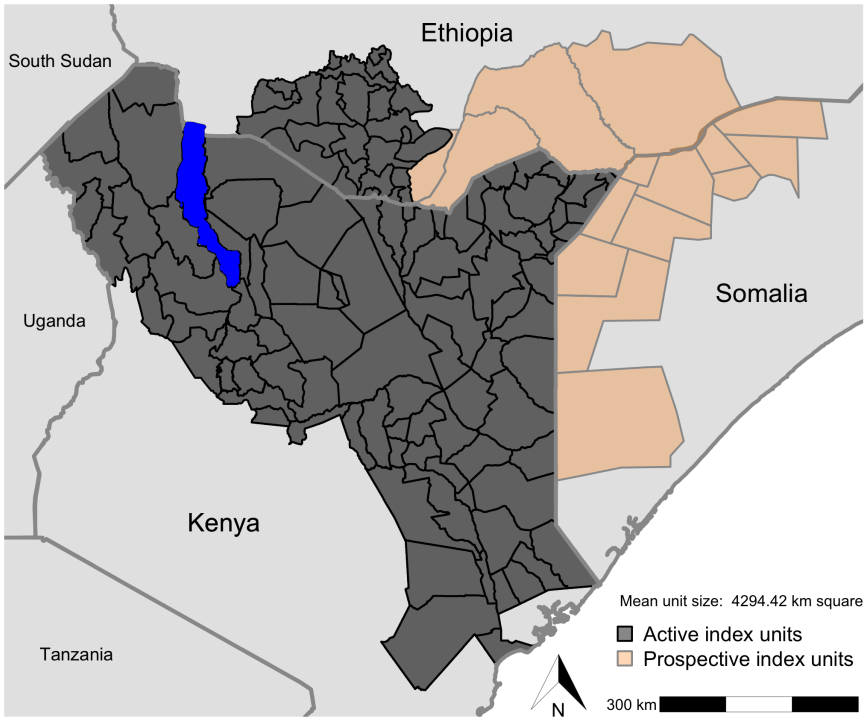


Figure 1: Active IUs span the northern and eastern portions of Kenya and part of southern Ethiopia, and are shaded in dark grey. Prospective IUs in which IBLI was not yet introduced during our study period in southern Ethiopia and western Somalia provide plausible control units and are shaded orange.

3 Data

3.1 IBLI administrative data and uptake over time

We measure IBLI exposure using administrative sales data from the insurance underwriters that sell IBLI. Individual herders purchase policies from insurance agents who live in or visit their community. Those agents submit to the underwriter the premium payment and administrative data on the purchaser: purchaser name, village name, index insurance unit, mobile phone number (for receiving payment), the quantity and species insured. Once KLIP launched in 2015, eligible individuals were identified through engagements between

community representatives and county governments. Those individuals were then registered for IBLI coverage for approximately USD 700 of insurance coverage and KLIP would pay the underwriter directly on behalf of eligible individuals. Note that pastoralists also continued purchasing insurance themselves while and after KLIP was active, and KLIP beneficiaries could, and frequently did, purchase additional insurance coverage.

The data frequency is semi-annual, reflecting the March-September long rains and long dry (LRLD) and the October-February short rains and short dry (SRSD) seasons corresponding to the IBLI contracts. We construct a time series of IU-level exposure to IBLI from 2000-2020 in both binary (i.e., presence/absence, the extensive margin) and continuous (i.e., the intensive margin in tropical livestock units (TLUs) insured). TLU is a standard measure of livestock that sums across species based on average metabolic weight: 1 TLU = 1 cow = 0.7 camel = 10 sheep/goats. The average cumulative exposure was 521 TLUs over the 2010-20 period. Since IBLI was first sold in January 2010, all 2000-2009 observations take value zero, representing the pre-exposure period.

Figure 2 shows IBLI's expansion in total TLUs insured by year and season, as well as private IBLI purchase versus purchase through KLIP. Juxtaposed against these trend lines is the rangeland area in km^2 exposed to IBLI by year and season as measured within IU boundaries. KLIP substantially expanded coverage overtime (Figure 2),[7] while private purchases of IBLI fluctuated substantially. We also see in Figure 2 that the area exposed to IBLI starts to level-out around 2015. Appendix A.1 provides analogous two-way plots, which feature additional measures of rangeland area exposed by low and high forage quality rangeland types (Figure A.1.1), measures of the total number of policies (Figure A.1.2), cumulative TLUs, policies, and exposed rangeland area (Figure A.1.3), and an animation of contemporaneous IBLI coverage over space and time at the IU level (Figure A.1.4).

[7]The subsidy provided by KLIP is based on population. Once a local population received KLIP, it remains in place, hence the monotonic increase.

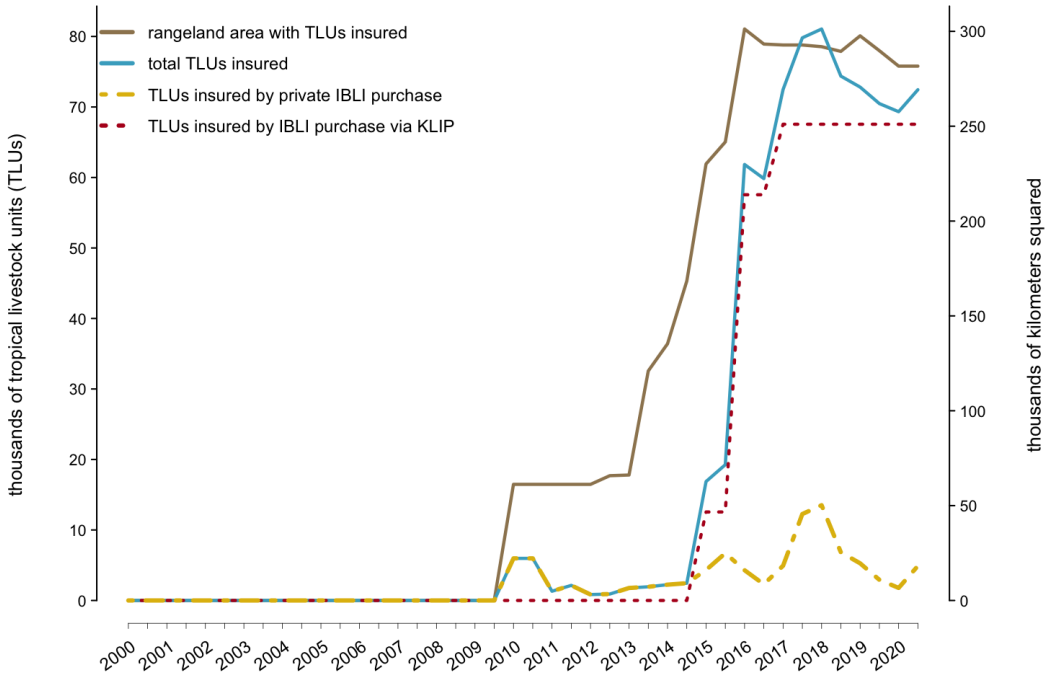


Figure 2: IBLI expansion in thousands of TLUs insured and area of rangelands exposed in thousands km^2.

3.2 Spatial units of analysis, herder movement, and IBLI exposure

In our study area, there are challenges to capturing meaningful variation in rangeland and herding processes and with measuring exposure to IBLI. One challenge comes with the fact that IUs are quite large while meaningful variation in rangeland conditions and quality (Section 3.3) and herding processes likely occurs at a smaller spatial scale. Another challenge comes with the potential for spillover effects from herders grazing across IUs. This is an issue because pastoralists regularly move their herds in search of forage and water (Coppock et al. 1994; Lybbert et al. 2004; Toth 2015; Jensen et al. 2017). But unlike fully nomadic populations elsewhere, here herding is predominantly transhumant, organized around a permanent base camp, where some family members remain throughout the year, while other family members episodically trek herds to satellite camps where they stay for varying lengths of time depending on rangeland and biophysical conditions.

To address scale issues, we study four different levels of spatial aggregation. This approach helps address trade-offs embodied in what geographers term the "modifiable areal unit problem" as it relates to prospective aggregation bias (Openshaw and Taylor 1979; Avelino et al. 2016). At the largest aggregate level we use IUs (Figure 1), and we also study sub-watershed unit levels 8, 9, and 12, also known as hydrologic unit code boundaries

(HUCs, hereafter) from Lehner and Grill (2013). Watersheds have geophysical boundaries set by the biophysical processes (e.g., hydrology, geology, topography) that drive underlying rangeland ecosystems and grazing patterns, thereby offering natural spatial units of analysis for this study. The number of unique units that intersect our study area within each level of aggregation and their average size in terms of area are: 130 and 4,294 km^2 (IUs); 870 and 739 km^2 (HUC-8); 2339 and 263 km^2 (HUC-9); 4753 and 125 km^2 (HUC-12). Figure 3 depicts our HUC-12 units (Appendix Figures A.1.5 - A.1.6 show respective maps for HUC-8 and HUC-9). Final panels are nearly perfectly balanced at each watershed unit level; slight panel imbalance occurs for several innocuous reasons (see further details in Section 5).

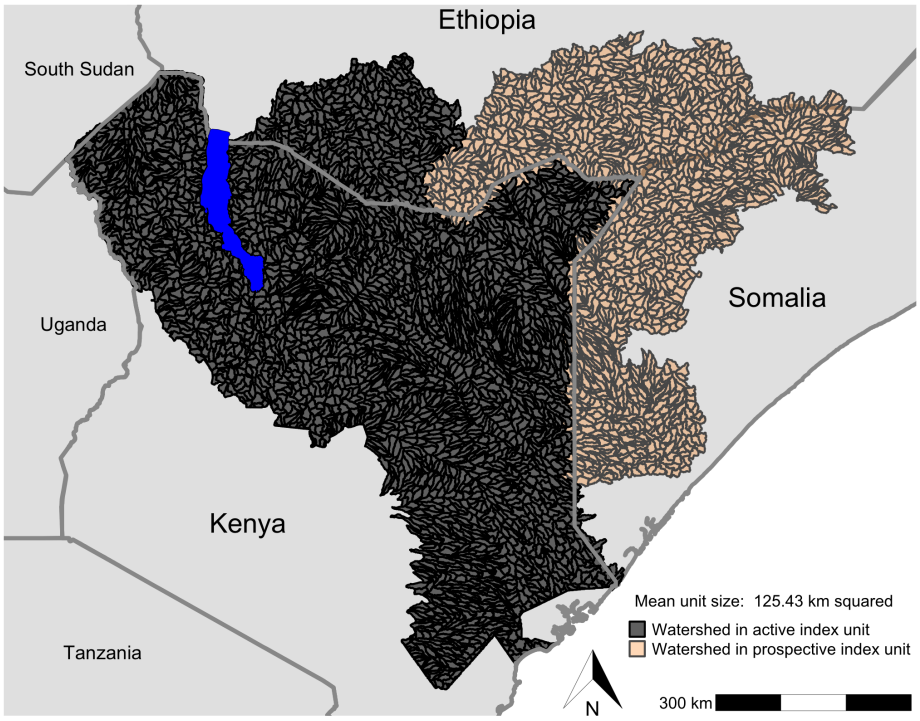


Figure 3: Map of study area and intersecting HUC-12 units from Lehner and Grill (2013).

To account for potential spillover effects from herders grazing across unit boundaries, we apply an inverse distance weighting (IDW)[8] algorithm, which accounts for exposure to IBLI within units (i.e., IU, HUCs) and within a surrounding neighborhood. To empirically ground neighborhood size we use data from GPS collars placed on livestock within pastoralists' herds in the Borana region of southern Ethiopia during 2011-2015 (Clark et al. 2006; Liao et al. 2017, 2018a). Specifically, we apply a neighborhood distance of 63 km, which reflects the sum of the mean and standard deviation of observed herding distances during each

[8]IDW amounts to an application of a gravity model (Carrère et al. 2020) and has been used in spatial statistics and other econometric studies of rangelands (Purevjav et al. 2025).

SRSD season over 2011-2015. This is a conservative distance as herding distances tend to be a bit larger in the SRSD. Respective equations and algorithms to implement IDW in our setting are detailed in Appendix A.2. Appendix Figure A.2.1 shows boxplots of seasonal livestock herding distance distributions and Appendix Figure A.2.2 shows example neighborhood buffers for a watershed unit near Lake Turkana.

To study IBLI exposure we focus on cumulative TLUs insured at the extensive and intensive margins and we study exposure as an irreversible state. Specifically, we consider a unit to be exposed to IBLI in the first period when ≥ 1 cumulative TLU is insured within a unit as measured by our IDW approach. Cumulative exposure accounts for the fact that any effects on rangelands are likely to be a function of the livestock units insured over time and the aggregate effects of herders' exposure to IBLI. Treating exposure as an irreversible state also accounts for the fact that there have been no disruptions to IBLI exposure during our study period. In our staggered exposure estimation design (see details in Section 4), we take advantage of variation at the extensive and intensive margins by comparing exposed units to never-exposed and not-yet-exposed units. These comparisons include units located in areas in southern Ethiopia and western Somalia, which were not directly exposed to IBLI during our study period that are scheduled to receive IBLI coverage in the future.

Figure 4 provides counts of the number of exposed versus unexposed units over time at the HUC-12 level and provides contrasting counts with and without IDW. The top panel of Figure 4 contrasts measures of extensive margin IBLI exposure at the HUC-12 level, with and without IDW. Notably, the number of exposed units increases with IDW. The bottom panel shows the distribution of treated versus control units at increasing levels of intensive margin exposure using IDW (e.g., ≥ 500 cumulative TLUs insured). At both the extensive and intensive margins, a large number of never-exposed and not-yet-exposed units are present in each period. The average level of inverse distance weighted cumulative exposure at the HUC-12 level over 2010-2020 was about 521 TLUs. Appendix A.2 provides a variety of additional supporting information, including: spatial animations at the HUC-12 level showing how our IDW approach impacts contemporaneous and cumulative IBLI exposure (Figures A.2.3-A.2.4); the cumulative distribution function of cumulative IDW exposure (Figure A.2.5); and a table of summary statistics on IBLI exposure (Table A.2.1) over 2010-2020 for each level of aggregation and by differing approaches to measuring exposure (e.g., contemporaneous without IDW versus cumulative with IDW).

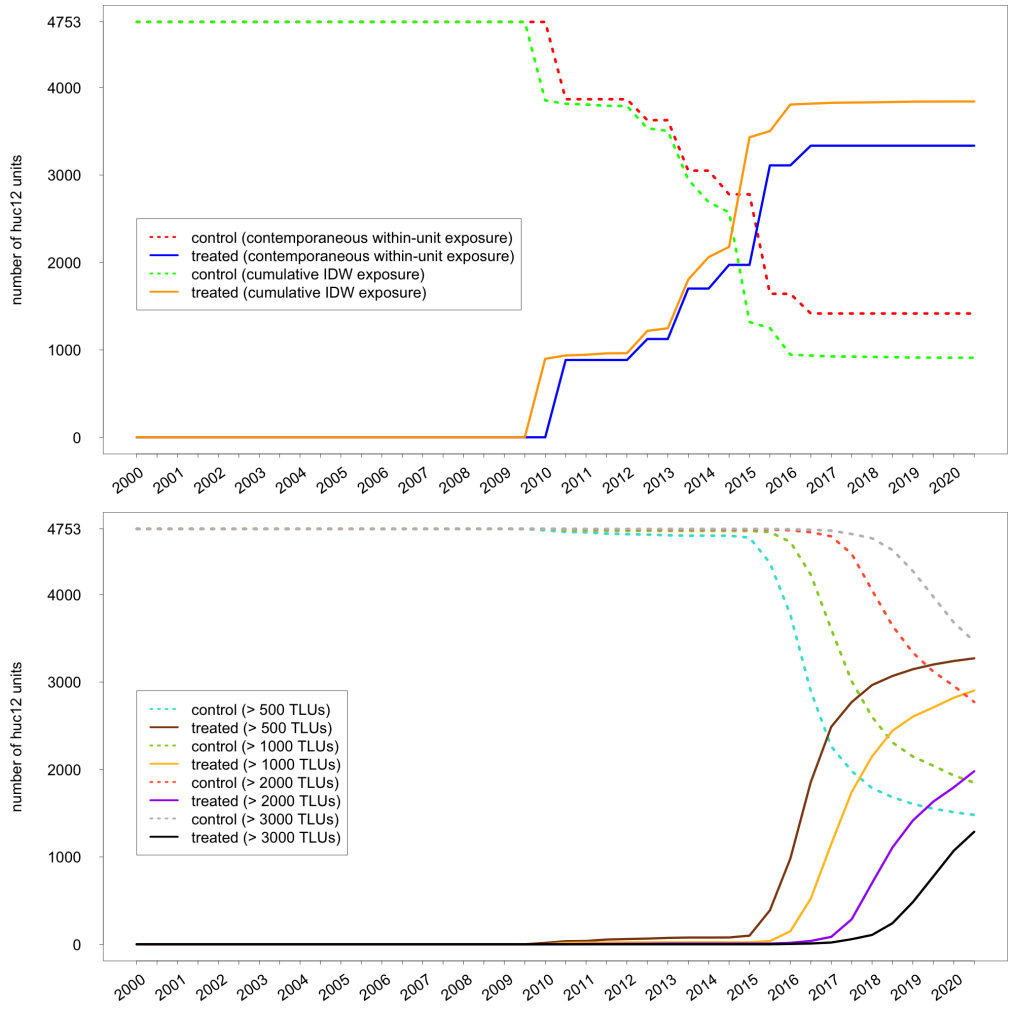


Figure 4: Top panel: Counts of extensive margin treated and control units over time at the HUC-12 level, contrasting contemporaneous IBLI exposure without IDW (contemporaneous within-unit exposure) and with cumulative IDW (cumulative IDW exposure). Bottom panel: Counts of treated and control units over time at the HUC-12 level for different intensive margins of exposure using IDW.

3.3 Rangeland condition measurement and other covariates

No unique measure of the health of rangelands exists; it is a latent variable. A widely adopted framework in rangeland science is rangeland health (RH), which is conceptualized as being a function of three primary attributes: biotic integrity, hydrologic function, and soil/site stability (Pellant et al. 2020). RH indicator measurement has historically relied heavily on field-based data collection. In much of the world, including our study area, available ground-based data are insufficient to answer research questions such as ours and collecting the needed data is cost-prohibitive and/or impossible to gather retrospectively.

Remote sensing advances, however, now enable the development of validated RH indicators at scale (Reeves et al. 2015; Retallack et al. 2023).[9]

We use a combination of publicly available, remotely sensed data series and measures from Soto et al. (2024) who provide a new multi-decadal high-resolution dataset on RH in East Africa that spans the entirety of our study area over the period 2000-2022. These data include ten years of observations prior to IBLI's introduction and a similar duration post-introduction. By studying these series at the four aforementioned levels of aggregation (i.e., IU and HUC levels) we can recover meaningful variation in rangeland conditions and forage quality over time and address potential aggregation bias from the modifiable areal unit problem (Openshaw and Taylor 1979; Avelino et al. 2016).

The dependent variables that we employ consist of fractional land cover measures and vegetation indices. For fractional land cover, we use the 30m series from Soto et al. (2024) that provide sub-pixel estimates of the proportion ($\in$[0,1]) of each pixel belonging to three classes: bare ground (BG), photosynthetic vegetation (PV), and non-photosynthetic vegetation (NPV). Due to high cloud cover in the region's LRLD season, these series are only available during the SRSD season each year. Generally speaking, more PV is desirable, more BG undesirable, and NPV can be neutral in that NPV offers limited forage value during the dry to wet season transition and can offer shade and help to reduce erosion and maintain soils and hydrology.

For vegetation indices, we use standard reflectance-based indices from publicly available 250m resolution MODIS data (Didan et al. 2021).[10] We favor the enhanced vegetation index (EVI), which is widely viewed as an improvement over other similar indices but we study several for completeness.[11] These indices generally fall in the 0-1 range for vegetated surfaces, with values closer to 1 indicating higher levels of greenness and productivity. The advantage of MODIS-based indices, as opposed to Landsat, is that the shorter return interval mitigates data gaps from cloud contamination and sensor failure. As such, MODIS-based series offer more complete temporal and spatial coverage than the fractional land cover series and are available in the LRLD and SRSD.

To summarize these series, we create aggregate fractional cover and vegetation measures

[9]Examples include work to characterize phenology and surface features like bare ground (Poitras et al. 2018; Wang et al. 2019; Rigge et al. 2021; Soto et al. 2024), measure woody shrub encroachment and state transitions (Liao et al. 2018a), and model structural and site potential deviations and trends in fractional cover (Reeves and Baggett 2014; Rigge et al. 2019; Shi et al. 2022).

[10]Didan et al. (2021) construct 16-day composites of high quality daily MODIS imagery.

[11]Additional series that we study include the Normalized Difference Vegetation Index (NDVI), the modified soil adjusted vegetation index (MSAVI), and near-infrared reflectance of vegetation (NIR_v). These series demonstrate very similar variation, so we focus our analysis on EVI.

within each areal unit using 30m resolution rangeland type maps from Soto et al. (2024). We use these maps to construct spatial masks, which we use as binary raster layers indicating usable pixels to capture rangeland variation of interest. Our main analysis relies on three spatial masks that permit study of heterogeneity across our study area: (i) an 'all' rangelands spatial mask that incorporates all rangeland types; (ii) a 'low' forage quality mask that reflects rangeland types with lower forage production potential for livestock; and (iii) a 'high' forage quality mask that reflects rangeland types with higher forage production potential for livestock.[12] Because year-to-year land cover can be susceptible to false state changes, and land cover change generally proceeds slowly in these systems, we use the modal land cover class over annually classified pixels for four five-year periods – 2000-2005, 2006-2010, 2011-2015, and 2016-2020 – and construct the all, low, and high masks for each period. The final RH measures we employ are the proportion of each unit in each fractional cover class (BG, PV, NPV) and the mean vegetation index value for each time period and mask.[13] This combination of measures provides credible data on important variation in RH at scale. Appendix B.1 provides further details how these measures relate to the RH framework and standard ground-based approaches to measuring RH attribute indicators (Table B.1.1), summary statistics on fractional cover measures and EVI by each aggregated mask (all, high, and low) and three specific rangeland types to underscore underlying variation (Table B.1.2), and example maps of the three aforementioned rangeland masks (Figures B.1.1 - B.1.3).

Other time-varying natural processes impact RH, are likely to determine significant variation in biological productivity (Purevjav et al. 2025), and may be correlated with IBLI uptake. We therefore control for seasonal weather variation, which drives significant variation in rangeland biological productivity in this region, as precipitation generates pulses in plant growth that attenuate over time and more rapidly with higher temperatures (Ellis and Swift 1988; Coughenour et al. 1990). For temperature data we construct binned temperature exposure variables scaled to growing degree days (GDDs) using 9km resolution, hourly temperature data from the reanalysis ERA-Land5 product (Muñoz-Sabater et al. 2021). For precipitation, we use 5km resolution data from CHIRPS (Funk et al. 2015), which uses remotely sensed and ground based station data to construct spatially continuous measures of precipitation. Using data from CHIRPS we gather measures of the average and standard de-

[12] Soto et al. (2024) classify these rangeland types: closed canopy woodland (CCW), dense scrubland (DS), bushland (BU), open canopy woodland (OCW), sparse scrubland (SS), cultivated land (CL), grassland (GR), and sparsely vegetated land (SV). Every class is included in the 'all' rangelands group, including CL since cultivated land in the region is often grazed and difficult to distinguish from classes like GR. The 'low' quality group includes SV, BU, DS, and CCW. The 'high' quality group includes OCW, GR, SS, and CL.

[13] For example, to gather a summarized vegetation index at an areal unit level for high forage quality rangelands in 2006, we apply the 'high' rangeland mask for 2006-2010.

viation of precipitation. Using these series, we construct control variables for each unit, year, season and level of aggregation over 2000-2020. Appendix B.1 provides summary statistics on these weather covariates by each level of aggregation (Table B.1.3).[14]

3.4 Trends in rangeland conditions

Figure 5 shows unconditional trends in the mean share of BG, PV, NPV, and the value of EVI for all rangelands, along with the contemporaneous trend in average precipitation. Analogous figures in Appendix B.2 show the contrasting trends across all, low, and high forage quality rangelands for fractional cover (Figure B.2.1) and EVI (Figure B.2.2). Figure 5 offers clear evidence of regular swings in the area share of BG, PV, and NPV that match closely with changes in precipitation. This is evident in 2006, 2011, and 2019, with notable increases in PV and decreases in BG and NPV. Likewise, a strong positive correlation between EVI and fluctuations in seasonal precipitation is also readily apparent. The corresponding figures in Appendix B.2 do not show marked differences between high and low forage quality rangelands, though in fractional cover measures we do see support for our masking strategy in that we see the share of BG is generally higher than that of PV in the low forage quality rangelands group, and vice versa for high forage quality rangelands. Overall, Figure 5 suggests that on average, BG and PV shares are slowly increasing while the NPV share is slowly declining. The apparent neutral trend in EVI also suggests that average biological productivity has held fairly constant in our study region over our study period, though subject to periodic, large swings in conjunction with variation in precipitation. These trends suggests some ambiguity as to whether rangeland conditions/health are improving or declining on average over time. Appendix B.2 features additional spatial and temporal variation in the unconditional values of these RH indicators via spatial animations at the HUC-12 level over 2000-2020 (Figures B.2.3 - B.2.5).

[14]Fire also impacts RH. However, in this region fire can be intentionally set to achieve different management objectives making it endogenous with rangeland conditions and thus a bad control.

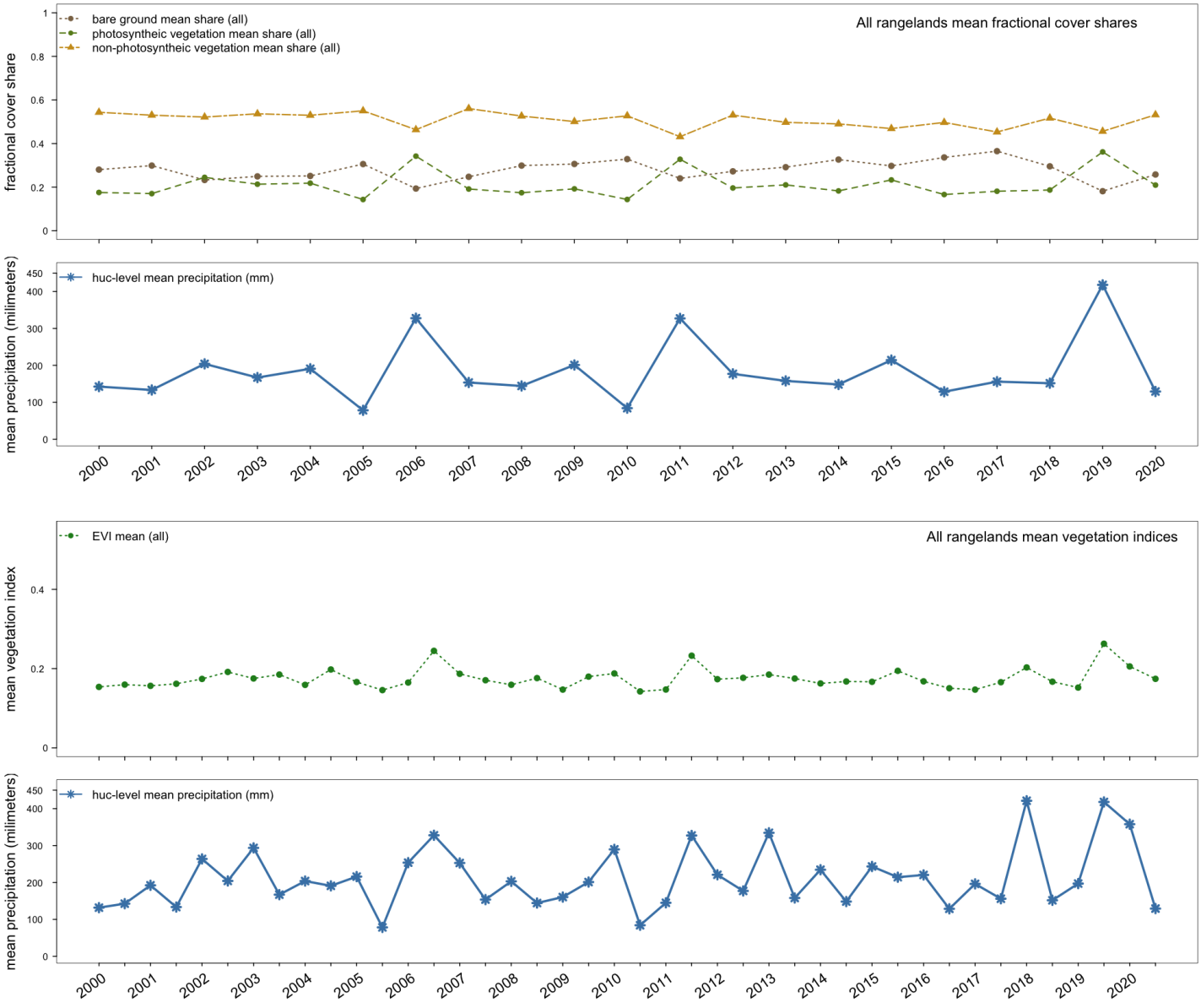


Figure 5: Trends at the HUC-12 level for mean fractional cover shares for all rangelands in the SRSD (top), mean precipitation in the SRSD (second from top), mean EVI in the SRSD and LRLD for all rangelands (third from top), and seasonal average precipitation in the SRSD and LRLD (bottom panel).

Figures 6 and 7 provide comparisons of average trends in RH indicators conditional on exposure to IBLI as measured via our IDW strategy (see Section 3.2). Figure 6 compares exposed and unexposed HUC-12 units at the extensive margin (i.e., a unit is exposed once ≥ 1 cumulative TLU is insured). Figure 7 compares exposed and unexposed HUC-12 units at the intensive margin where a unit is considered exposed once ≥ 500 cumulative TLUs are insured, which is very close to the mean cumulative exposure of 521 TLUs at the HUC-12 level over

2010-2020. Both figures depict variation in conditional average fractional cover shares and conditional average EVI across all rangeland types. Analogous figures featuring comparisons in conditional average trends for all, high, and low groups are provided in Appendix B.2 at both the extensive margin and increasing levels of intensive margin exposure for the HUC-12 level (Figures B.2.6 - B.2.9), and the same kind of variation is captured in companion figures at the HUC-8 level (Figures B.2.10 - B.2.13). The associated trends are very similar across masked variation (i.e., all, high, and low).

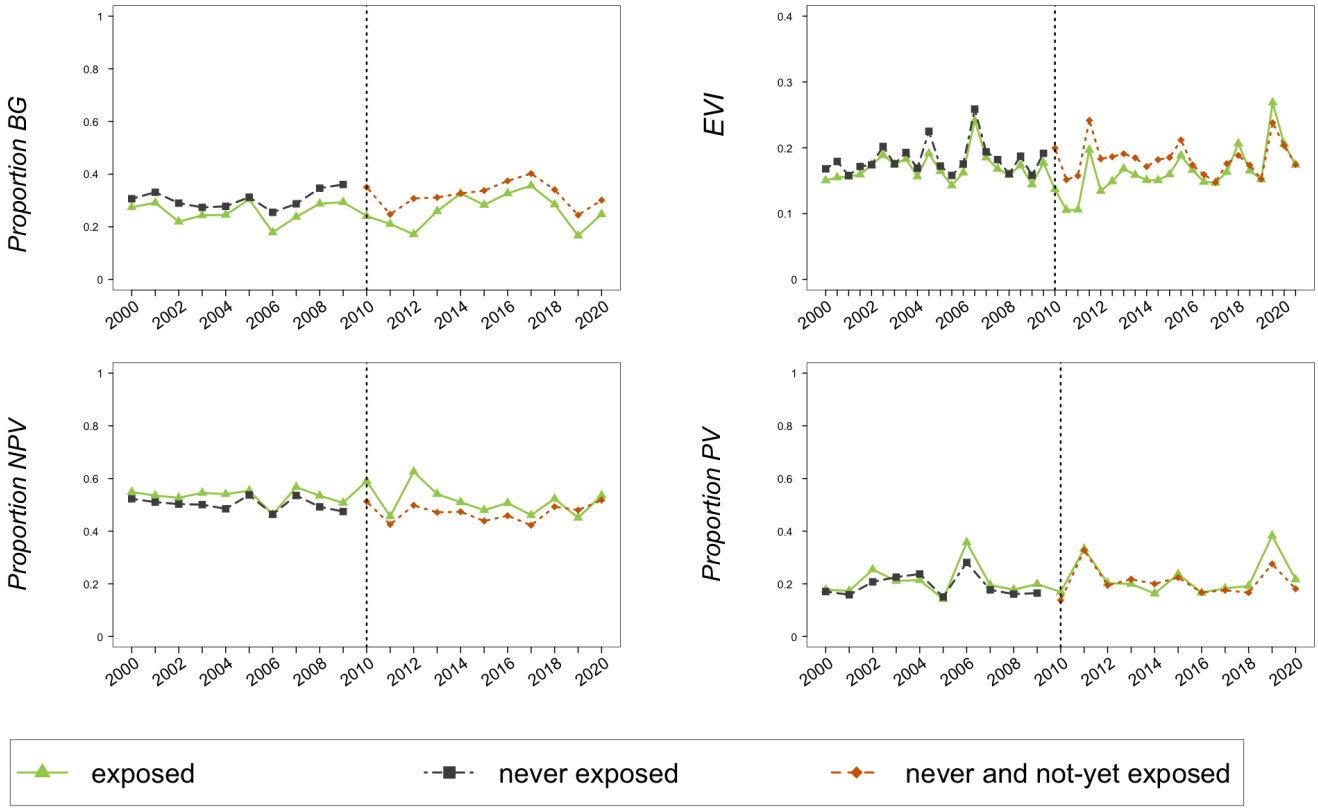


Figure 6: Extensive margin conditional trends in RH indicators measured across all rangeland types at the HUC-12 level; exposure is defined as ≥ 1 cumulative TLU insured. Vertical dashed lines indicate IBLI's 2010 launch. Top row: average proportion of bare ground (BG); average enhanced vegetation index (EVI). Bottom row: average proportion of non-photosynthetic vegetation (NPV); average proportion of photosynthetic vegetation (PV). Prior to exposure, comparison groups are fixed: the 'exposed' group includes any unit that is ever exposed; the 'never exposed' group includes never treated units only. For time periods including and following the vertical line, comparison groups vary each period per staggered exposure: the 'exposed' group is updated each period; and the 'never and not-yet exposed' group includes units in the 'never exposed' group and units that aren't yet exposed.

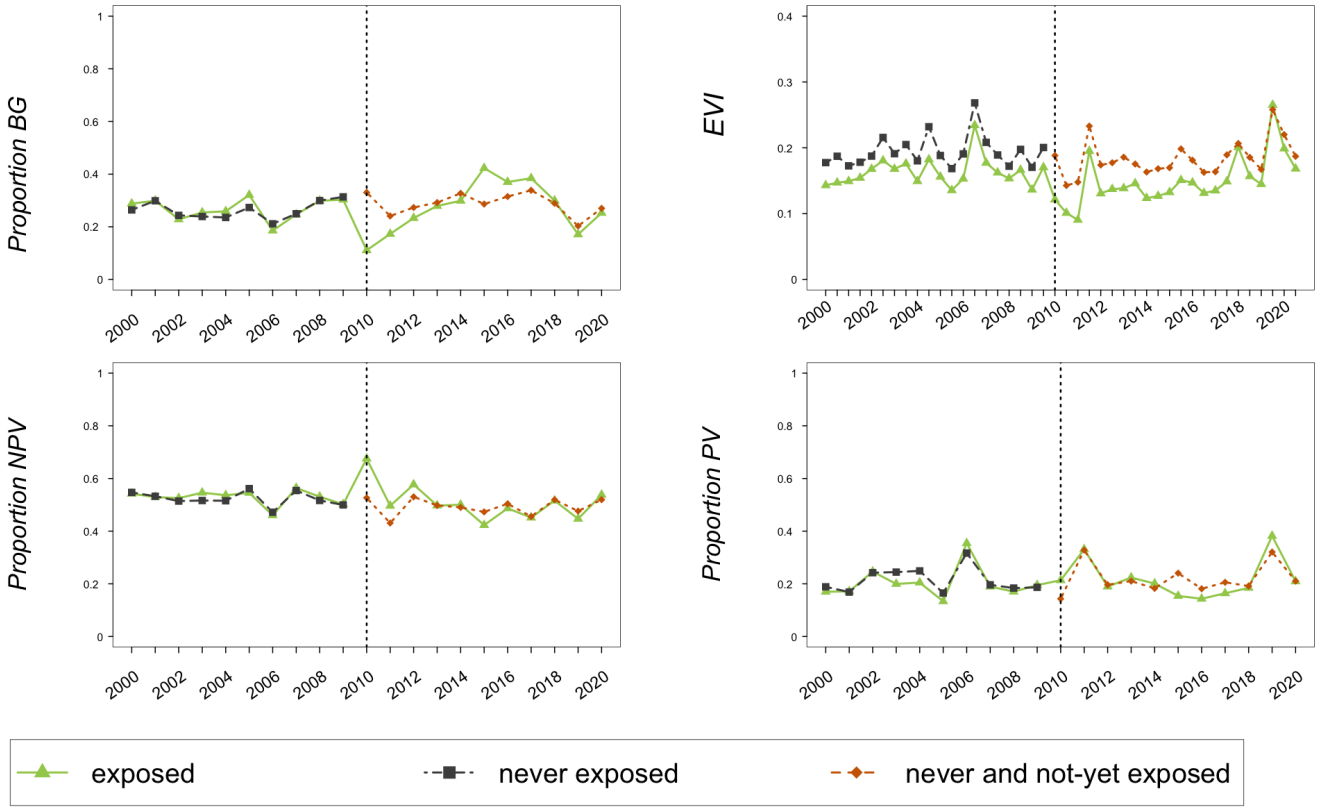


Figure 7: Intensive margin conditional trends in RH indicator measures across all rangeland types at the HUC-12; exposure defined as $\geq$ 500 cumulative TLUs insured. Vertical dashed lines indicate when the first HUC-12 units were exposed to $\geq$ 500 cumulative TLUs insured in 2010. Top row: average proportion of bare ground (BG); average enhanced vegetation index (EVI). Bottom row: average proportion of non-photosynthetic vegetation (NPV); average proportion of photosynthetic vegetation (PV). Prior to exposure, comparison groups are fixed: the 'exposed' group includes any unit that is ever exposed; the 'never exposed' group includes never treated units only. For time periods including and following the vertical line, comparison groups vary each period per staggered exposure: the 'exposed' group is updated each period; and the 'never and not-yet exposed' group includes units in the 'never exposed' group and units that aren't yet exposed.

While these figures do not offer formal tests of either parallel trends pre-IBLI between exposed and unexposed units nor of the impacts of IBLI on these RH indicators, Figures 6 and 7 do provide very useful information. First, these figures show that exposed and never exposed averages followed very similar time paths prior to the 2010 launch of IBLI. Second, for a few indicators and years, observable differences seem to appear following exposure to IBLI, which are somewhat more apparent at the intensive margin (Figure 7). Overall, Figures 6 and 7 do not provide strong suggestive evidence of any significant pre-exposure deviations in trends, nor do they suggest a large impact on rangelands from IBLI. The lack

of any discernible aggregate conditional trends also suggests that the fixed effect terms in the econometric estimation are not hiding or obviously controlling for some salient trend.

Another informative feature of variation captured in Figures 6 and 7, and the suite of companion figures in Appendix B.2, is that they demonstrate how event-time differs depending on the level of intensive margin exposure and level of aggregation. For example, at the HUC-12 level, the initial period of exposure can differ by several years with increasing levels of intensive margin exposure. For example, at the HUC-12 level, Figure B.2.7 shows intensive margin exposure at $\geq$ 500 cumulative TLUs first occurs in 2010, while Figure B.2.9 shows that exposure at $\geq$ 3000 cumulative TLUs first occurs in 2016. In addition, the initial year of exposure can also differ by level of aggregation for the same level of intensive margin exposure. For example, at the HUC-12 level Figure B.2.9 shows that exposure at $\geq$ 3000 cumulative TLUs first occurs in 2016, while Figure B.2.13 shows the the same level of exposure at the HUC-8 level first occurs in 2011. This perspective highlights how the underlying variation can differ spatially and temporally in staggered DiD estimation with varying levels of exposure and levels of aggregation.

4 Econometric Methods

Did the introduction and scaling of the microfinance product IBLI have unintended effects on the rangelands that support pastoralism? To motivate our staggered exposure estimation strategy to answer this question we first estimate standard two-way fixed effects (TWFE) specifications and implement tests for the appropriateness of TWFE (Jakiela 2021). These tests for the presence of negative weights and treatment effect heterogeneity confirm that TWFE is inappropriate in our setting (see Appendix C for details). We therefore rely on the two-stage approach developed by Gardner et al. (2025), which (unlike other staggered DiD estimators) accommodates time-varying covariates.[15]

At a sub-annual level, controlling for local seasonal weather variation is especially essential, not least of which because the widespread impression in this region is that droughts have occurred with increasing frequency and intensity since 2000 (Haile et al. 2020). Recent work on rangelands also demonstrates the critical nature of weather variation in driving long-run changes in rangeland biological productivity (Purevjav et al. 2025). If the background weather process has been evolving with climate change during the post-exposure period,

[15]The estimator of Borusyak et al. (2024) yields treatment effect estimates that are numerically equivalent to those of Gardner et al. (2025) in the canonical staggered-adoption setting, although the approaches differ in their variance estimation. The regression-based two-stage framework of Gardner et al. (2025) also provides a convenient implementation for models with continuous treatment intensity, time-varying exogenous covariates, and treatment effect heterogeneity.

failure to control for it may bias our estimates of the impact of IBLI on rangelands.

Gardner et al. (2025) introduce a two stage estimator in which the first stage regresses Y on all covariates and fixed effects using only untreated observations in order to residualize outcomes Y. In the second stage, the estimator regresses residualized Y from all observations on a treatment dummy or event-time dummies to obtain overall and event-time average treatment effects on the treated (ATT) respectively, following the steps outlined below.

Step 1: For a given binary measure of treatment D_{ist} (e.g., an extensive or intensive margin cumulative IDW exposure margin indicator), subset to the unbalanced panel of never and not-yet-exposed observations (i.e., such that $D_{ist} = 0$) and regress $Y_{i,r,s,t}$ on fixed effects and controls $\mathbf{X}_{i,s,t}$:

$$Y_{i,r,s,t} = \mathbf{X}'_{\mathbf{i,s,t}}\theta + \gamma_i + \sigma_t + \mu_{i,r,s,t} \tag{1}$$

where $Y_{i,r,s,t}$ reflects the pre-exposure RH outcome for areal unit i in rangeland type r in season s and IBLI-year t[16], vector $\mathbf{X}'$ includes measures of average precipitation and/or precipitation variability and binned hours of temperature exposure, γ_i and σ_t represent unit and time fixed effects, respectively, and μ captures the error term.

Step 2: Use the estimates of $\widehat{\theta}$, $\widehat{\gamma_i}$, and $\widehat{\sigma_t}$ from step 1 to residualize $Y_{i,r,s,t}$, defined as $\ddot{Y}_{i,r,s,t} \equiv Y_{i,r,s,t} - \mathbf{X}'_{\mathbf{i,s,t}}\widehat{\theta} - \widehat{\gamma_i} - \widehat{\sigma_t}$, and regress it on treatment dummy D_{ist}:

$$\ddot{Y}_{i,r,s,t} = D_{ist}\beta + \ddot{\varepsilon}_{i,r,s,t} \tag{2}$$

In the second step β reflects the overall ATT across group-time cohorts, a weighted ATT across all potentially heterogeneous treatment effects and exposure cohorts at a given level of exposure. Other ATTs can be computed in similar fashion with dummy variables that reflect heterogeneity of interest (e.g., specific group-time cohorts), including by time period for event studies. The event study version is obtained by replacing D_{ist} with a vector of event-time dummies $\mathbf{W}'_{ist}$ for testing pre-trends and dynamic treatment effects in each post-treatment period across all group-time cohorts.

The identifying assumption is that conditional on the time-varying covariates, IBLI exposure is orthogonal to any time-and-spatially-varying heterogeneity that is correlated with rangeland conditions. All DiD estimation relies on satisfaction of a credible version of the parallel trends assumption for causal identification. In the staggered DiD setting, comparatively strong and weak versions of the parallel trends assumption exist, depending on the estimator. Gardner et al. (2025) rely on estimation of pre-treatment leads on the residu-

[16] An 'IBLI-year' begins March 1. Thus our year 2010 reflects the first year of IBLI exposure, from March 1, 2010, through February 28, 2011.

alized outcome from the first stage. Coefficients for dummies estimated for pre-treatment leads within $\mathbf{W}'_{ist}$ provide suitable placebo tests for the plausibility of parallel trends (i.e., the null hypothesis that respective coefficients equal zero). Respective coefficients have the interpretation of measuring average deviations from never-treated trends.

There are two primary challenges to our causal identification strategy. First, for all of our remotely sensed variables – both our weather controls and our RH outcome variables – there exists a possibility of nonrandom prediction error that could bias estimates (Jain 2020). Garcia and Heilmayr (2024) and Alix-García and Millimet (2023) develop methods to mitigate these kinds of issues when outcome variables are binary at the pixel level. Since we use aggregated variables at an areal unit level as discussed in Section 3.3 these alternatives do not apply. As such, we note that our estimates are conditional on the maintained assumption of non-classical-error-free remote sensing measures. Classical measurement error should not bias our estimates, since there is no measurement error in the main explanatory variable of interest, exposure to IBLI. Second, if the parallel trends assumption is not satisfied, our estimated ATTs may be biased. We therefore implement Rambachan and Roth (2023)'s robustness checks that account for various violations of parallel trends. Our implementation utilizes software from Butts and Gardner (2021).

5 Staggered Differences-in-Differences Results

5.1 Extensive Margin Tests

Figure 8 presents results for all rangelands with 95% confidence intervals estimated using Gardner et al. (2025)'s two-stage DiD estimator, where the treatment dummy of interest captures IBLI exposure based on IDW at the extensive margin defined as ≥ 1 cumulative TLU insured at the HUC-12 level (see Section 3.2). All estimates include unit fixed effects and period fixed effects and time varying weather controls. All standard errors are clustered at the index unit level.

These findings indicate that we cannot reject the null hypothesis of no effects on any fractional land cover measure at the extensive margin. Not only are all estimated treatment effects for BG, NPV and PV statistically insignificantly different from zero, but the magnitude of each point estimate is no more than one percent in absolute magnitude. These are rather precisely estimated zero effects. We do, however, reject the no effects null for mean EVI. Specifically, we find a positive effect from IBLI exposure on mean EVI of around 0.006, which is statistically significant at the 1% level. This is consistent with previous empirical findings that IBLI reduced precautionary savings in kind, i.e., in the form of livestock

(Jensen et al. 2017; Barrett et al. 2025).

Additional estimates in Appendix D.1 provide qualitatively similar estimates at the extensive margin and show comparisons of effects across all, low, and high rangeland subsets (see Section 3.3). Respective figures show extensive margin results with and without IDW across all the aforementioned rangeland subsets (Figure D.1.1 versus D.1.2), as well as results at the HUC-9, HUC-8, and IU levels (Figures D.1.3 - D.1.5). Results shown in Figure 8 and in Appendix D.1 reflect nearly perfectly balanced panels at watershed unit levels where some marginal missingness reflects clouds or other quality filters for fractional cover and vegetation indices, and/or a few instances of very small units with odd geometry that did not intersect cleanly with larger pixels. Sample sizes also differ across rangeland forage quality masks because underlying rangeland types are not smoothly distributed in space.

The unbiasedness of these estimates depends on satisfying the parallel trends assumption during the pre-exposure period. Figure 9 presents event study plots for BG, PV, and EVI within all rangelands that trace the dynamic treatment effects across all group-time cohorts and estimated coefficients sufficient for a test of the presence of pre-trends. Respective estimations also include unit and period fixed effects and time varying weather controls in the first stage.

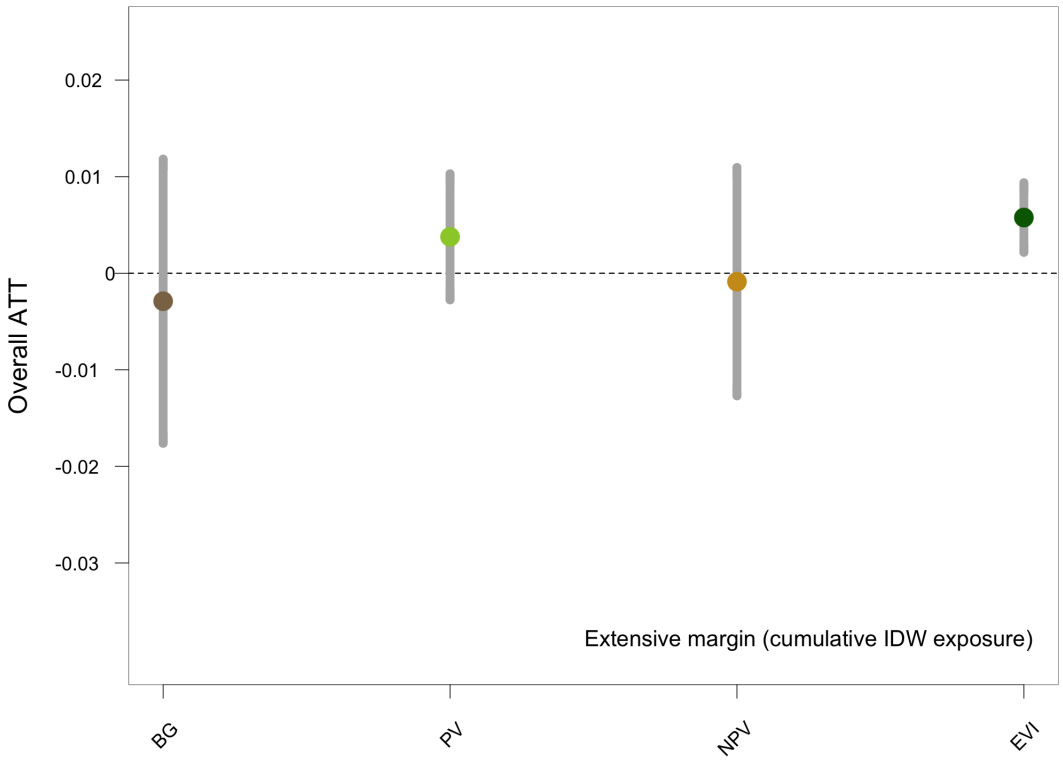


Figure 8: Overall ATTs with 95% confidence intervals for tests of impacts at HUC-12 level from IBLI exposure at the extensive margin based on cumulative IDW exposure (≥ 1 cumulative TLU insured). ATTs reflect point estimates of β in equation (2) (see Section 4). Standard errors are clustered at the index unit level. From left to right, estimated coefficients reflect IBLI's impacts on BG, PV, NPV and EVI within all rangelands (see Section 3.3). The number of observations for respective estimations are: fractional cover all mask, $n = 99,426$; EVI all mask, $n = 199,416$. First stage covariates are the same across models and include: the mean and standard deviation of seasonal precipitation (mm), and mean GDD in 5° C bins with the exception of two 10° C bins from 5-10° C and 30-45° C due to limited exposure from 5-10° C and 35-40° C. Each model includes unit and period fixed effects.

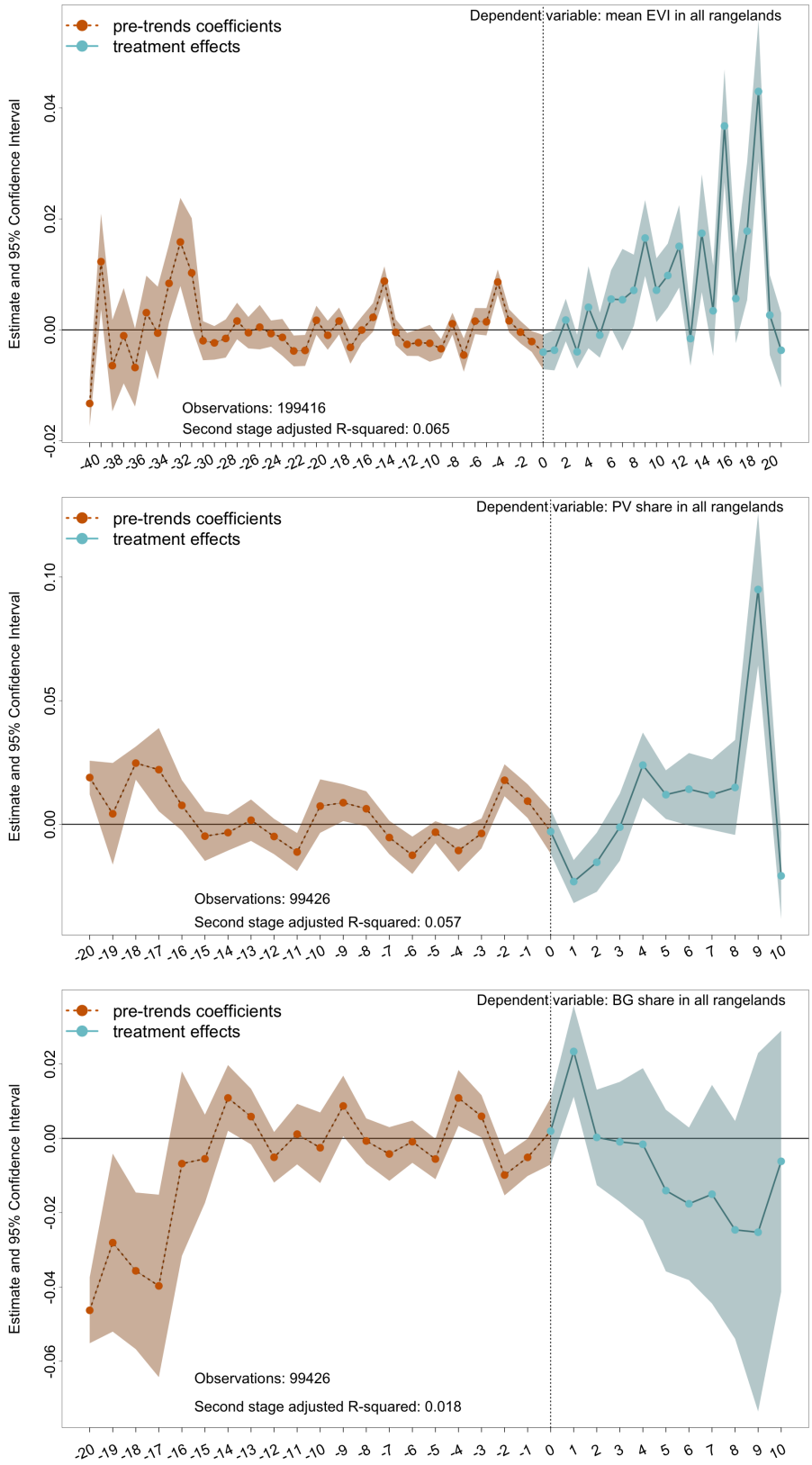


Figure 9: Event studies for the effect of IBLI at the extensive margin based on cumulative IDW exposure ($\geq$ 1 cumulative TLU insured) on EVI, PV, and BG within all rangelands (see Section 3.3). Estimation is from an event study version of equation (2) (see Section 4). Standard errors are clustered at the index unit level.

Although most pre-exposure coefficient estimates are statistically insignificantly different from zero (Figure 9), several are statistically different from zero. Thus estimated treatment effects at the extensive margin may be biased. However, the dynamics apparent in these event study plots may reflect, in part, natural variation in RH measures, which fluctuate in conjunction with time-varying unobserved factors (e.g., wildlife grazing pressures, lightning strikes, or human initiated fire) unrelated to IBLI rollout. The earliest event-time coefficients are also likely to be more imprecisely estimated simply because there are few units within the earliest pre-trend periods.

These results are consistent with IBLI having a neutral to positive impact on rangelands. However, since pre-exposure parallel trends tests do not uniformly support the parallel trends assumption at the extensive margin, these estimates may be biased. A more realistic test of IBLI's impacts on rangelands will account for variation at the intensive margin of IBLI exposure.

5.2 Intensive Margin Tests

We implement tests of IBLI's effect at the intensive margin using two complementary approaches supported by Gardner et al. (2025): continuous and binned. Table 1 presents results at the HUC-12 level based on a continuous measure of exposure, defined as the cumulative sum of IDW exposure across all rangelands. Figure 10 presents results for binned intensive margin exposure defined as exposure to $\geq$ 500 cumulative TLUs insured, which is very to close the 2010-2020 mean exposure level of 521 TLUs. Figure 11 provides the corresponding event studies for BG, PV, and EVI for all rangelands. All estimates include unit and period fixed effects and time varying weather controls. All standard errors are clustered at the index unit level. As with our extensive margin tests, intensive margin tests reflect nearly perfectly balanced panels. Marginal amounts of missingness reflects clouds or other quality filters, and/or a few instances of very small units with odd geometry. Sample sizes also differ across rangeland masks because rangeland types are not smoothly distributed in space.

Both the binned and continuous approaches tell the same story, which is apparent via comparison of column 3 in Table 1 and the overall ATTs captured in Figure 10. As with the extensive margin results, there remains no evidence against the null of no effect on the proportion of land in BG or NPV. However, in addition to evidence for a statistically significant positive effect for EVI, there are now statistically significant, positive effects for PV at the 1% level, which is consistent with the increased greenness finding per the mean EVI measure. The binned exposure estimates also scale in a consistent manner with the continuous estimates. For example, the ATT for the effect on mean EVI in all rangelands

at the $\geq$ 500 cumulative TLUs insured level is 0.011. The mean exposure level among the HUC-12 units that have been exposed to $\geq$ 500 cumulative TLUs insured level is 1785.19 TLUs. The corresponding ATT (0.011) divided by this mean level of exposure (1785.19) is approximately 0.000006, which is very close to the 0.000005 coefficient estimate in column (3) of Table 1. In addition, there are also indications of negative effects on BG and NPV, though these estimates are not consistently statistically significant.

The event studies captured in Figure 11 suggest stronger evidence for conditional parallel trends as more coefficient estimates are statistically indistinguishable from zero and pre-trend movement between periods is greatly diminished. These findings offer reasonable support for the identifying assumption that conditional parallel trends hold for above-mean intensive margin exposure to IBLI.

To study additional variation at the intensive margin we conduct a variety of alternative specifications, including models with unit-specific linear trends in addition to unit and period fixed effects. Table 1 column 4 shows the results; Appendix D.2 reports the corresponding first stage of the results presented in Table 1 (Tables D.2.1 - D.2.4). When unit-specific linear trends are included, goodness-of-fit statistics (e.g., RMSE, AIC, BIC, Adjusted R-squared) for the first and second stages are somewhat worse, associated coefficient estimates change sometimes markedly so in terms of sign, magnitude, and significance, and event studies do not appreciably differ from a conditional parallel trends perspective. These findings lead us to favor estimations with seasonal weather controls and unit and period fixed effects, the predictive power of which is somewhat stronger. This approach is featured in column (3) of Table 1 and Figure 10.

The overall finding that emerges from these intensive margin results is consistent with our extensive margin findings. Specifically, the evidence points towards a neutral to positive effect of IBLI on rangeland conditions. Increasing greenness in both fractional cover and greenness is generally a encouraging finding, and potentially reduced BG is encouraging. These findings alone are insufficient to claim IBLI has a clear positive impact on RH, but the overall results are not consistent with the worst fears that IBLI might undermine rangeland systems and thereby induce the kinds of losses it is seeking to insure against.

Table 1: Intensive margin tests (overall ATTs) for the effect of IBLI on rangelands using inverse distance weighted (IDW) continuous measures of the total cumulative TLUs insured at the HUC-12 level (see Gardner et al. (2025) pg. 17-18).

	Dependent variable: Bare ground (BG) share all rangelands			
Total cumulative TLUs insured (IDW)	0.000010**	-0.000006***	-0.000004	0.000003
	(0.000004)	(0.000002)	(0.000005)	(0.000003)
BG second stage statistics				
Observations	99,426	99,426	99,426	99,426
Adjusted R^2	0.001	0.005	0.002	0.001
	Dependent variable: Photosynthetic vegetation (PV) share all rangelands			
Total cumulative TLUs insured (IDW)	-0.000005**	0.000009***	0.000009***	-0.000003
	(0.000002)	(0.000001)	(0.000002)	(0.000004)
PV second stage statistics				
Observations	99,426	99,426	99,426	99,426
Adjusted R^2	0.002	0.015	0.014	0.002
	Dependent variable: Non-photosynthetic vegetation (NPV) share all rangelands			
Total cumulative TLUs insured (IDW)	-0.000006*	-0.000003*	-0.000005	0.0000009
	(0.000004)	(0.000002)	(0.000004)	(0.000004)
NPV second stage statistics				
Observations	99,426	99,426	99,426	99,426
Adjusted R^2	0.0007	0.001	0.004	0.00009
	Dependent variable: Mean enhanced vegetation index (EVI) all rangelands			
Total cumulative TLUs insured (IDW)	-0.0000009	0.000002***	0.000005***	0.000003**
	(0.000001)	(0.0000005)	(0.000001)	(0.000001)
EVI second stage statistics				
Observations	199,416	199,416	199,416	199,416
Adjusted R^2	0.0001	0.004	0.024	0.010
First stage specifications (BG, PV, NPV, EVI)				
Unit fixed effects	No	Yes	Yes	Yes
Period fixed effects	No	No	Yes	Yes
Unit-specific trends	No	No	No	Yes

Note: Estimation is via a continuous exposure version of equation (2) (see Section 4). First stage covariates are the same across models and include: the mean and standard deviation of seasonal precipitation (mm), and mean GDD in 5° C bins with the exception of two 10° C bins from 5-10° C and 30-45° C due to limited exposure from 5-10° C and 35-40° C. Standard errors are clustered at the index unit level. *p<0.1; **p<0.05; ***p<0.01.

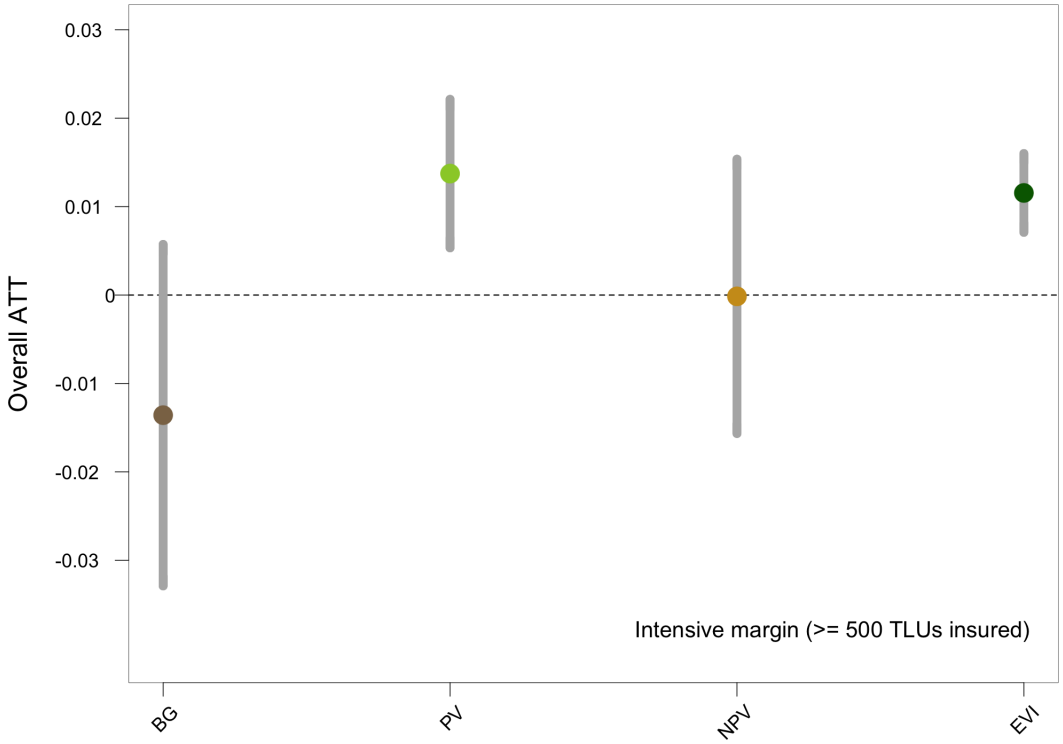


Figure 10: Overall ATTs with 95% confidence intervals for tests of impacts at HUC-12 level from IBLI exposure at the intensive margin of $\geq$ 500 cumulative IDW TLUs insured. ATTs reflect point estimates of β in equation (2) from Gardner et al. (2025) (see Section 4). Standard errors are clustered at the index unit level. From left to right, estimated coefficients reflect IBLI's impacts on BG, PV, NPV and EVI within all rangelands (see Section 3.3). The number of observations for respective estimations are: fractional cover all mask, $n = 99,426$; EVI all mask, $n = 199,416$. First stage covariates are the same across models and include: the mean and standard deviation of seasonal precipitation (mm), and mean GDD in 5° C bins with the exception of two 10° C bins from 5-10° C and 30-45° C due to limited exposure from 5-10° C and 35-40° C. Each model includes unit and period fixed effects.

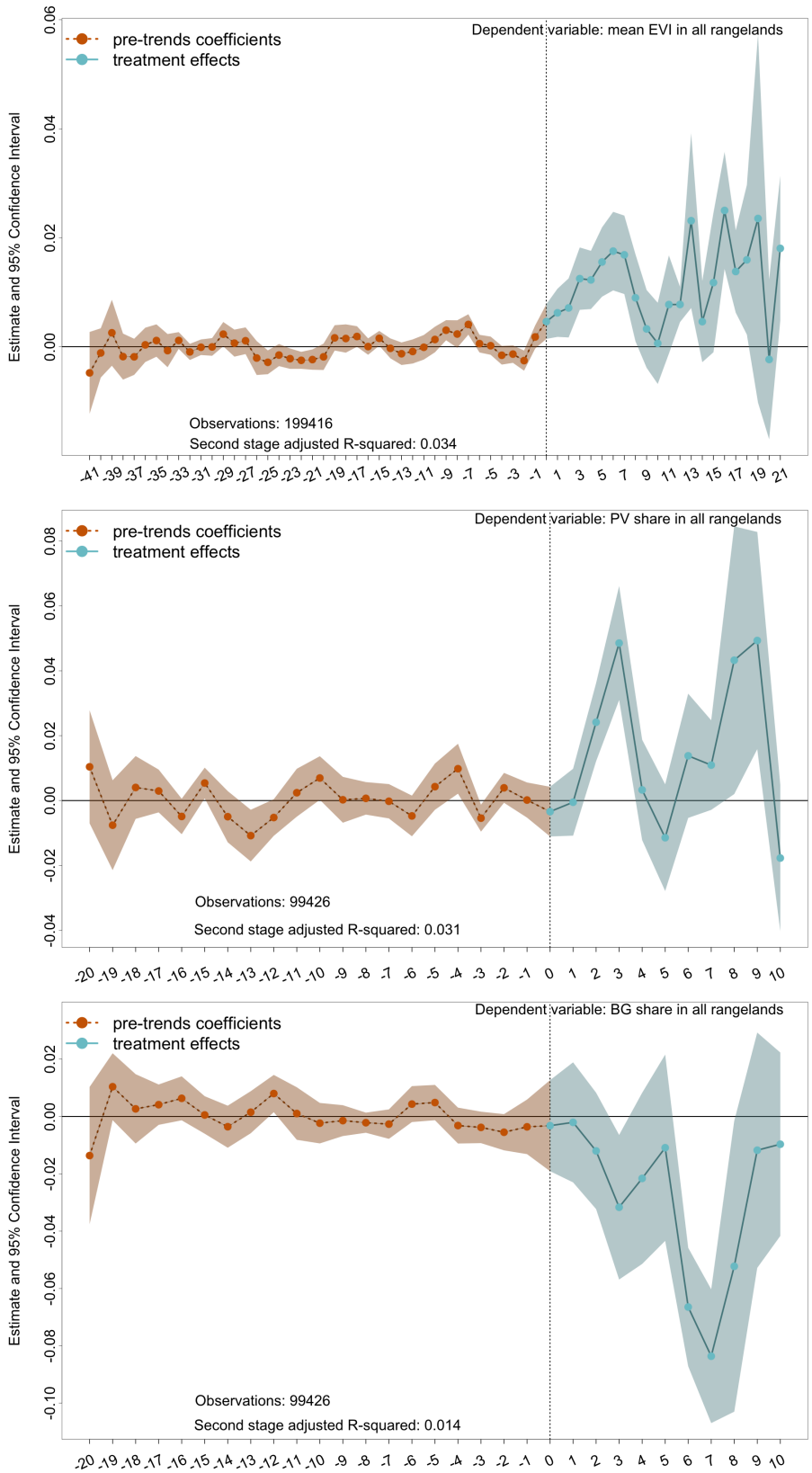


Figure 11: Event studies for the effect of IBLI at the intensive margin ($\geq$ 500 cumulative IDW TLUs insured) on EVI, PV, and BG within all rangelands (see Section 3.2). Estimation is from an event study version of equation (2) (see Section 4). Standard errors are clustered at the index unit level.

5.3 Robustness checks

Beyond the estimations referenced above, we implement four primary robustness checks to assess the stability of our core finding that IBLI has neutral to positive effects on rangelands. First, we implement a variety of estimations using the continuous and binned exposure levels at different levels of spatial aggregation which are provided in Appendix D.3. Table D.3.1 shows analogous output to Table 1 at the HUC-9 level and the results are very similar. Figures D.3.1-D.3.4 estimate overall ATTs in analogous fashion to Figure 10 focused on the same intensive margin exposure (i.e., $\geq$ 500 cumulative IDW TLUs insured) and show the corresponding results across all, low, and high rangeland types for HUC-12, HUC-9, HUC-8, and index unit levels respectively. While HUC-9 and HUC-8 level results are comparable to the HUC-12 level, all effects become null at the IU level. This seems a potential indication of the aggregation bias that can result at a larger areal unit level.

Second, we study the binned exposure approach at increasing levels of intensive margin exposure at the HUC-12 level across all, low, and high rangeland types. In Appendix D.3, overall ATTs are provided in Figures D.3.5-D.3.7 for the intensive margin effect at $\geq$ 1000, 2000, and 3000 cumulative IDW TLUs insured. Results at the $\geq$ 1000 cumulative TLUs insured level are comparable to those in Figure 10. At the $\geq$ 2000 cumulative IDW TLUs insured level, EVI is no longer statistically significant, results for increased PV are larger in magnitude and still significant, and there are statistically significant results for decreased bare ground. This pattern generally remains at the $\geq$ 3000 cumulative IDW TLUs insured level, though statistically significant reduced bare ground only remains for high forage quality rangelands. A limitation that emerges with increasing levels of binned exposure in this regard is that respective group-time cohorts are observed for increasingly fewer periods, therefore limited observations at these increasing levels of exposure are available. However, since results at the fully continuous margin of exposure are consistent with our general findings and increasing intensive margin results are also generally consistent with neutral to positive impacts on rangelands from IBLI, this should continue to allay concerns about the consistency of these findings.

Third, given the presence of some variation in the statistical significance of results focused on EVI and PV at differing margins of exposure, we study potential for heterogeneous effects by season for EVI as this is the only outcome which features variation in the SRSD and LRLD. Table D.3.2 shows the results for respective tests which feature EVI measures across our three rangeland masks, an interaction between a dummy for the LRLD season and an extensive margin exposure dummy, and an interaction between a dummy for the LRLD season and continuous intensive margin exposure. In all cases, point estimates are

positive but we cannot reject the null of no difference in effects by season. The presence of some differences in statistical significance between EVI and PV might raise concerns about the consistency of the general finding a small but positive effects as regards cover of PV and greenness. However, the dominant picture is very consistent. Across the range of preferred two-stage DiD estimates we present, all overall ATT point estimates for PV and EVI are positive. This is not surprising given the high correlation between these measures, which capture different dimensions of live vegetation.[17] Occasional differences in statistical significance for these outcomes likely arise from some combination of differences in measurement (e.g., spatial and temporal variation in these variables), and also variation in exposed cohorts which necessarily vary with differing intensive margins of exposure.

Finally, we also apply the methods from Rambachan and Roth (2023) that implement robust confidence intervals, which incorporate potential violations of parallel trends in post-treatment periods. In Appendix D.3, Figures D.3.8 - D.3.10 show the corresponding results for each post-treatment ATT for BG, PV, and EVI in all rangelands focused on binned intensive margin exposure of $\geq$ 500 cumulative TLUs insured. These figures show results for robust 95% confidence intervals for each post-treatment ATT using the "relative magnitude" approach from Rambachan and Roth (2023). This approach uses the maximum observed deviation M from parallel trends in the pre-treatment period to bound potential post-treatment deviations from parallel trends and thereby produce confidence intervals that account for the potential bias. In our case, since the largest Each figure features the estimated original confidence interval followed by a set of alternative confidence intervals that incorporate an increasing share of the full value of the observed M. For point estimates that reject the null, these confidence intervals show how incorporation of increasing shares of maximum potential deviation alter statistical significance and offer additional perspective on potential effect sizes. For point estimates that are already null, these confidence intervals provide an enhanced sense of the potential effect sizes once more robust confidence intervals are constructed. In these figures although we find that our statistically significant results do eventually become statistically insignificant with increasing deviations from parallel trends in the post-treatment period, the overall finding of a broadly neutral to positive effect of IBLI on rangelands remains. These alternative confidence intervals also suggest that the potential effect sizes could be somewhat more economically meaningful that the modest point estimates featured in our main results. The results are also intuitive based on the strength of the results discussed so far.

[17]The bivariate correlation between PV and EVI using unresidualized variation across the rangeland masks we apply, is very high ranging from 0.52 to 0.72. For residualized variation, the correlation is similar to slightly higher ranging from 0.62 to 0.71. The close relationship is also apparent in Figures 5-7 and analogous Appendix figures.

5.4 Implications and potential mechanisms

The general pattern of impacts at the intensive margin on a continuous basis and above-mean IBLI exposure is consistent with, and even somewhat clearer than the prior extensive margin results. IBLI has neutral to positive impacts on rangelands. The estimates at the intensive margin more strongly support the hypothesis that IBLI may have modestly positive effects, particularly for increasing the prevalence of photosynthetic vegetation and the biological productivity of the rangelands. These effects also do not differ by broad quality differences (i.e., high vs. lower forage quality rangelands).

By no means do these results suggest IBLI generated a strong, broad-based improvement in RH. Such a determination would require a wider range of measures capturing a more credible suite of the elements that influence the three primary attributes of RH (Pellant et al. 2020). However, our findings allay widespread fears – and model-based simulations (Müller et al. 2011; John et al. 2019; Bulte and Haagsma 2021) – predicting that IBLI, or analogous livestock-focused index insurance, would cause rangeland degradation. The fact that the intensive margin estimates are stronger, and more positive, than the extensive margin effects is especially comforting in that if the ordering were the opposite, one might reasonably worry that continued scaling of IBLI might bring about adverse, but not yet realized effects.

In contrast to the model-based studies' warnings about likely adverse effects of IBLI on rangeland conditions, our findings are consistent with either or both of two phenomena. First, perhaps nonequilibrial vegetation dynamics characterize the bulk of the study area, as claimed by multiple range ecology studies (Ellis and Swift 1988; Coughenour et al. 1990; Coppock et al. 1994). If so, herder behavior has little, if any, feedback on rangeland conditions. Testing that hypothesis falls well beyond the scope of this paper. But if that is the dominant mechanism explaining our findings, then the generalizability of our results to other locations that are launching IBLI turns on the nature of a venue's rangeland ecology dynamics.

The second phenomena are human behavioral and, we suspect, are more readily generalizable. Prior, careful empirical studies of IBLI's impacts on herder behaviors have established that IBLI induced increased investment in livestock care rather than in herd accumulation (e.g., via veterinary care), reduced precautionary savings in livestock, and prompted herders to shrink grazing ranges (Jensen et al. 2017; Toth et al. 2020; Barrett et al. 2025). Such behaviors – all assumed away in the model-based simulations that caution IBLI might generate unintended adverse environmental impacts – may have allowed rangelands to go unaffected, on net, or even to respond favorably to reduced grazing pressure. This is the extensive live-

stock grazing analog to findings from crop agriculture that support the Borlaug hypothesis that improvements in the returns to farming can reduce land degradation.

6 Conclusions

Microfinance, including agricultural index insurance, has become extremely popular over the past quarter century, to the point that Muhammad Yunus, the founder of Grameen Bank, won the 2006 Nobel Peace Prize. If microfinance stimulates economic activity and investment, however, it could also have unintended environmental consequences, perhaps especially in lands without clear, strong private property rights (Bhattacharya and Osgood 2014; Assunção et al. 2020; Noack and Costello 2024). In the case of microinsurance against catastrophic drought losses, the central premise is that insurance does not cause serious adverse impacts on the natural environment that support human well-being. By rigorously testing for IBLI's impacts on rangelands, we directly confront this key question as the product scales rapidly across East African rangelands and elsewhere around the world.

The question requires empirical investigation because IBLI's potential impacts on rangelands are analytically ambiguous. It could increase or decrease herd sizes and expand or shrink grazing ranges. Empirical work to date yields conflicting findings for the direction of impact on herd sizes (Jensen et al. 2017, Matsuda et al. 2019, Barrett et al. 2025) and herding effort (Toth et al. 2020, Son 2025). We merge newly available, high quality data on East African rangeland health indicators and rangeland types over an extended period (Soto et al. 2024) with administrative data on IBLI exposure to directly test what effects, if any, IBLI has had on rangelands.

Using a DiD estimator designed for staggered roll-out while controlling for time-varying exogenous controls (Gardner et al. 2025), we find strong evidence against the hypothesis that IBLI has adversely affected East African rangelands. Rather, the evidence suggests neutral-to-positive impacts on rangelands, at both the extensive margin of initial exposure to IBLI and, especially, at the intensive margin, once locations accumulate sufficient exposure to IBLI for any induced effects to become more observable. We find statistically significant improvements in rangeland biological productivity, as well as an increased share of land covered in photosynthetic vegetation.

These reduced form findings offer reassurance that the worst fears about IBLI have not come to fruition nor is there any support in the data that they are likely to materialize as the product scales further. Our findings after eleven years of IBLI's staggered roll-out to nearly 3.2 million herders across a vast area of southern Ethiopia and Kenya disprove the IBLI-induced "tragedy of the commons" hypothesis. Insurance companies, governments, and

international donors can continue to promote IBLI comfortable in the knowledge that offering microfinancial protection against catastrophic drought risk is not degrading the rangelands on which pastoralists' livelihoods depend.

A natural extension to this work would explore the structural foundations of this empirical result. What combination of returns to livestock keeping, pastoralist risk preferences and grazing behaviors, along with product characteristics – specifically, loss reduction based on the strike level and basis risk – plausibly result in induced reductions in precautionary savings in kind that neutralize, perhaps even dominate insurance's investment inducing effects? That sort of structural exploration can inform a broader understanding of the conditions under which our empirical findings might prove generalizable, that is, when microfinance expansion can be reasonably expected not to adversely impact the natural environment.

Furthermore, there also seems high value to extending our general approach of seeking to test the effects of microfinancial products on the environment in other settings. Indeed, gaining a better understanding of the conditions in which increased access to financial resources do or do not impact the natural environment in some way that undercuts net gains of otherwise successful poverty-reducing innovations is of great general importance. For example, our finding that addressing financial market failures does not appear to lead to resource degradation, despite lack of clearly defined property rights, is a notable contrast to other recent work on credit markets (Assunção et al. 2020; Noack and Costello 2024). Identifying where and when these and other conditions conditions might apply to make microfinance and other poverty-mitigating tools environmental sustainable seems a vital endeavor for future work.

References

Alix-García, Jennifer, and Daniel L Millimet. 2023. Remotely incorrect? accounting for nonclassical measurement error in satellite data on deforestation. *Journal of the Association of Environmental and Resource Economists* 10 (5): 1335–1367. DOI: https://www.journals.uchicago.edu/doi/full/10.1086/723723.

Assunção, Juliano, Clarissa Gandour, Romero Rocha, and Rudi Rocha. 2020. The effect of rural credit on deforestation: Evidence from the brazilian amazon. *Economic Journal* 130 (626): 290–330. DOI: https://doi.org/10.1093/ej/uez060.

Avelino, Andre Fernandes Tomon, Kathy Baylis, and Jordi Honey-Rosés. 2016. Goldilocks and the raster grid: Selecting scale when evaluating conservation programs. *PloS one* 11 (12): e0167945. DOI: https://doi.org/10.1371/journal.pone.0167945.

Ayres, Andrew B., Kyle C. Meng, and Andrew J. Plantinga. 2021. Do environmental markets improve on open access? evidence from california groundwater rights. *Journal of Political Economy* 129 (10): 2817–2860. DOI: 10.1086/715075.

Balboni, Clare, Aaron Berman, Robin Burgess, and Benjamin A. Olken. 2023. The economics of tropical deforestation. *Annual Review of Economics* 15: 723–754. DOI: 10.1146/annurev-economics-090622-024705.

Barrett, Christopher B. 1999. Stochastic food prices and slash-and-burn agriculture. *Environment and Development Economics* 4 (2): 161–176. DOI: https://doi.org/10.1017/S1355770X99000133.

Barrett, Christopher B., Nathaniel Jensen, Karlijn Morsink, Yuma Noritomo, Hyuk Harry Son, Rupsha Banerjee, and Nils Teufel. 2025. Long-run effects of catastrophic drought insurance. Working paper. Available at: https://barrett.dyson.cornell.edu/files/papers/Long_term_effects_of_IBLI.

Barrett, Christopher B, Paswel Phiri Marenya, John McPeak, Bart Minten, Festus Murithi, Willis Oluoch-Kosura, Frank Place, et al. 2006. Welfare dynamics in rural kenya and madagascar. *Journal of Development Studies* 42 (2): 248–277. DOI: https://doi.org/10.1080/00220380500405394.

Batabyal, Amitrajeet A., Basudeb Biswas, and E. Bruce Godfrey. 2001. On the choice between the stocking rate and time in range management. *Environmental and Resource Economics* 20 (3): 211–223. DOI: 10.1023/A:1012647003818.

Besley, Timothy. 1995. Savings, credit and insurance. *Handbook of development economics* 3: 2123–2207. DOI: https://doi.org/10.1016/S1573-4471(05)80008-7.

Bhattacharya, Haimanti, and Daniel E Osgood. 2014. Weather index insurance and common property resources. *Agricultural and Resource Economics Review* 43 (3): 438–450. DOI: https://doi.org/10.1017/S1068280500005530.

Borusyak, Kirill, Xavier Jaravel, and Jann Spiess. 2024. Revisiting event-study designs: robust and efficient estimation. *Review of Economic Studies* 91 (6): 3253–3285. DOI: https://doi.org/10.1093/restud/rdae007.

Bulte, Erwin, and Rein Haagsma. 2021. The welfare effects of index-based livestock insurance: Livestock herding on communal lands. *Environmental and Resource Economics* 78 (4): 587–613. DOI: https://doi.org/10.1007/s10640-021-00545-1.

Butts, Kyle, and John Gardner. 2021. did2s: Two-stage difference-in-differences. DOI: https://arxiv.org/abs/2109.05913.

Carrère, Céline, Monika Mrázová, and J Peter Neary. 2020. Gravity without apology: the science of elasticities, distance and trade. *Economic Journal* 130 (628): 880–910. DOI: https://doi.org/10.1093/ej/ueaa034.

Carter, Michael, Alain de Janvry, Elisabeth Sadoulet, and Alexandros Sarris. 2017. Index insurance for developing country agriculture: A reassessment. *Annual Review of Resource Economics* 9: 421–438. DOI: https://doi.org/10.1146/annurev-resource-100516-053352.

Chantarat, Sommarat, Andrew G Mude, Christopher B Barrett, and Michael R Carter. 2013. Designing index-based livestock insurance for managing asset risk in northern kenya. *Journal of Risk and Insurance* 80 (1): 205–237. DOI: https://doi.org/10.1111/j.1539-6975.2012.01463.x.

Cissé, Jennifer Denno, and Christopher B Barrett. 2018. Estimating development resilience: A conditional moments-based approach. *Journal of Development Economics* 135: 272–284. DOI: https://doi.org/10.1016/j.jdeveco.2018.04.002.

Clark, Patrick E, Douglas E Johnson, Mark A Kniep, Phillip Jermann, Brad Huttash, Andrew Wood, Michael Johnson, et al. 2006. An advanced, low-cost, gps-based animal tracking system. *Rangeland Ecology & Management* 59 (3): 334–340. DOI: https://doi.org/10.2111/05-162R.1.

Constenla-Villoslada, Susana, Yanyan Liu, Jiaming Wen, Ying Sun, and Shun Chonabayashi. 2022. Large-scale land restoration improved drought resilience in ethiopia's degraded watersheds. *Nature Sustainability* 5: 488–497. DOI: 10.1038/s41893-022-00861-4.

Coppock, David Layne, et al. 1994. *The Borana Plateau of Southern Ethiopia: Synthesis of Pastoral Research, Development, and Change, 1980-91*, volume 5. ILRI (aka ILCA and ILRAD).

Coughenour, Michael B, David L Coppock, and James E Ellis. 1990. Herbaceous forage variability in an arid pastoral region of kenya: importance of topographic and rainfall gradients. *Journal of Arid Environments* 19 (2): 147–159. DOI: https://doi.org/10.1016/S0140-1963(18)30813-9.

Cull, Robert, and Jonathan Morduch. 2018. Microfinance and economic development. In *Handbook of finance and development*. Edward Elgar Publishing, 550–572. DOI: https://doi.org/10.4337/9781785360510.00030.

Didan, Kamel, Armando Barreto Munoz, Ramón Solano, and Alfredo Huete. 2021. Modis/terra vegetation indices 16-day l3 global 250m sin grid v061 [dataset]. DOI https://doi.org/10.5067/MODIS/MOD13Q1.061.

Ellis, James E, and David M Swift. 1988. Stability of african pastoral ecosystems: Alternate paradigms and implications for development. *Rangeland Ecology & Management/Journal of Range Management Archives* 41 (6): 450–459. DOI: https://doi.org/10.2307/3899515.

Epanchin-Niell, Rebecca, Jeffrey Englin, and Darek Nalle. 2009. Investing in rangeland restoration in the arid west, usa: Countering the effects of an invasive weed on the long-term fire cycle. *Journal of Environmental Management* 91 (2): 370–379. DOI: 10.1016/j.jenvman.2009.09.004.

Estefania-Salazar, Enrique, and Eva Iglesias. 2026. Enhancing drought resilience: An index insurance scheme for west african pastoralists. *Climate Risk Management* 52: 100808. DOI: 10.1016/j.crm.2026.100808.

Feng, Shuaizhang, Yujie Han, and Huanguang Qiu. 2021. Does crop insurance reduce pesticide usage? evidence from china. *China Economic Review* 69: 101679. DOI: https://doi.org/10.1016/j.chieco.2021.101679.

Finnoff, David, Aaron Strong, and John Tschirhart. 2008. A bioeconomic model of cattle stocking on rangeland threatened by invasive plants and nitrogen deposition. *American Journal of Agricultural Economics* 90 (4): 1074–1090. DOI: 10.1111/j.1467-8276.2008.01166.x.

Funk, Chris, Pete Peterson, Martin Landsfeld, Diego Pedreros, James Verdin, Shraddhanand Shukla, Gregory Husak, et al. 2015. The climate hazards infrared precipitation with stations—a new environmental record for monitoring extremes. *Scientific data* 2 (1): 1–21. DOI: 10.1038/sdata.2015.66.

Garcia, Alberto, and Robert Heilmayr. 2024. Impact evaluation with nonrepeatable outcomes: The case of forest conservation. *Journal of Environmental Economics and Management* 125: 102971. DOI: https://doi.org/10.1016/j.jeem.2024.102971.

Gardner, John, Neil Thakral, Linh T. Tô, and Luther Yap. 2025. Two-stage differences in differences. Working paper, Available at: https://neilthakral.github.io/files/papers/2sdd.pdf.

Gehring, Kai, and Paul Schaudt. 2024. Insuring peace: Index-based livestock insurance, droughts, and conflict. CESifo Working Paper, DOI: http://dx.doi.org/10.2139/ssrn.4702292.

Gollin, Douglas, Casper Worm Hansen, and Asger Mose Wingender. 2021. Two blades of grass: The impact of the green revolution. *Journal of Political Economy* 129 (8): 2344–2384. DOI: 10.1086/714444.

Haile, Gebremedhin Gebremeskel, Qiuhong Tang, Guoyong Leng, Guoqiang Jia, Jie Wang, Diwen Cai, Siao Sun, et al. 2020. Long-term spatiotemporal variation of drought patterns over the greater horn of africa. *Science of the Total Environment* 704: 135299. DOI: https://doi.org/10.1016/j.scitotenv.2019.135299.

Hardin, Garrett. 1968. The tragedy of the commons: the population problem has no technical solution; it requires a fundamental extension in morality. *Science* 162 (3859): 1243–1248. DOI: https://doi.org/10.1126/science.162.3859.1243.

Jain, Meha. 2020. The benefits and pitfalls of using satellite data for causal inference. *Review of Environmental Economics and Policy* 14 (1): 157–169. DOI: https://doi.org/10.1093/reep/rez023.

Jakiela, Pamela. 2021. Simple diagnostics for two-way fixed effects. Working paper, DOI: https://doi.org/10.48550/arXiv.2103.13229.

Janzen, Sarah A, and Michael R Carter. 2019. After the drought: The impact of microinsurance on consumption smoothing and asset protection. *American Journal of Agricultural Economics* 101 (3): 651–671. DOI: https://doi.org/10.1093/ajae/aay061.

Jensen, Nathaniel, and Christopher Barrett. 2017. Agricultural index insurance for development. *Applied Economic Perspectives and Policy* 39 (2): 199–219. DOI: https://doi.org/10.1093/aepp/ppw022.

Jensen, Nathaniel D, Christopher B Barrett, and Andrew G Mude. 2017. Cash transfers and index insurance: A comparative impact analysis from northern kenya. *Journal of Development Economics* 129: 14–28. DOI: https://doi.org/10.1016/j.jdeveco.2017.08.002.

Jensen, Nathaniel D, Francesco P Fava, Andrew G Mude, Christopher B Barrett, Brenda Wandera-Gache, Anton Vrieling, Masresha Taye, et al. 2024. *Escaping Poverty Traps and Unlocking Prosperity in the Face of Climate Risk: Lessons from Index-Based Livestock Insurance*. Cambridge University Press. DOI: https://doi.org/10.1017/9781009558280.

Jensen, Nathaniel D, Jose D López-Rivas, Karlijn Morsink, and Emma E Rikken. 2025. Weathering conflict: The effect of resource shocks on livestock raids. CSAE Working Paper 2025-02. Oxford: University of Oxford Centre for the Study of African Economies. DOI: https://orcid.org/0000-0002-2946-5771.

Jensen, Nathaniel D, Andrew G Mude, and Christopher B Barrett. 2018. How basis risk and spatiotemporal adverse selection influence demand for index insurance: Evidence from northern kenya. *Food Policy* 74: 172–198. DOI: https://doi.org/10.1016/j.foodpol.2018.01.002.

John, Felix, Russell Toth, Karin Frank, Jürgen Groeneveld, and Birgit Müller. 2019. Ecological vulnerability through insurance? potential unintended consequences of livestock drought insurance. *Ecological Economics* 157: 357–368. DOI: https://doi.org/10.1016/j.ecolecon.2018.11.021.

Johnson, Leigh, Brenda Wandera, Nathan Jensen, and Rupsha Banerjee. 2019. Competing expectations in an index-based livestock insurance project. *Journal of Development Studies* 55 (6): 1221–1239. DOI: https://doi.org/10.1080/00220388.2018.1453603.

Karlan, Dean, Robert Osei, Isaac Osei-Akoto, and Christopher Udry. 2014. Agricultural decisions after relaxing credit and risk constraints. *Quarterly Journal of Economics* 129 (2): 597–652. DOI: https://doi.org/10.1093/qje/qju002.

Lehner, Bernhard, and Günther Grill. 2013. Global river hydrography and network routing: baseline data and new approaches to study the world's large river systems. *Hydrological Processes* 27 (15): 2171–2186. DOI: https://doi.org/10.1002/hyp.9740.

Liao, Chuan, Patrick E Clark, and Stephen D DeGloria. 2018a. Bush encroachment dynamics and rangeland management implications in southern ethiopia. *Ecology and evolution* 8 (23): 11694–11703. DOI: https://doi.org/10.1002/ece3.4621.

Liao, Chuan, Patrick E Clark, Stephen D DeGloria, and Christopher B Barrett. 2017. Complexity in the spatial utilization of rangelands: Pastoral mobility in the horn of africa. *Applied Geography* 86: 208–219. DOI: https://doi.org/10.1016/j.apgeog.2017.07.003.

Liao, Chuan, Patrick E Clark, Mohamed Shibia, and Stephen D DeGloria. 2018b. Spatiotemporal dynamics of cattle behavior and resource selection patterns on east african rangelands: evidence from gps-tracking. *International Journal of Geographical Information Science* 32 (7): 1523–1540. DOI: https://doi.org/10.1080/13658816.2018.1424856.

Lybbert, Travis J, Christopher B Barrett, Solomon Desta, and D Layne Coppock. 2004. Stochastic wealth dynamics and risk management among a poor population. *Economic Journal* 114 (498): 750–777. DOI: https://doi.org/10.1111/j.1468-0297.2004.00242.x.

Matsuda, Ayako, Kazushi Takahashi, and Munenobu Ikegami. 2019. Direct and indirect impact of index-based livestock insurance in southern ethiopia. *Geneva Papers on Risk and Insurance-Issues and Practice* 44 (3): 481–502. DOI: https://doi.org/10.1057/s41288-019-00132-y.

McCarthy, Nancy, Brent M Swallow, Michael Kirk, and Peter BR Hazell. 1999. *Property Rights, Risk, and Livestock Development in Africa*. International Food Policy Research Institute. DOI: https://hdl.handle.net/10568/161459.

McPeak, John G. 2003. Analyzing and addressing localized degradation in the commons. *Land Economics* 79 (4): 515–536. DOI: 10.2307/3147297.

McPeak, John G., and Christopher B. Barrett. 2001. Differential risk exposure and stochastic poverty traps among east african pastoralists. *American Journal of Agricultural Economics* 83 (3): 674–679. DOI: 10.1111/0002-9092.00189.

McPeak, John G, Peter D Little, and Cheryl R Doss. 2011. *Risk and Social Change in an African Rural Economy: Livelihoods in Pastoralist Communities*. Routledge. DOI: https://doi.org/10.4324/9780203805824.

Mu, Jianhong E., Bruce A. McCarl, and Anne M. Wein. 2013. Adaptation to climate change: Changes in farmland use and stocking rate in the us. *Mitigation and Adaptation Strategies for Global Change* 18 (6): 713–730. DOI: 10.1007/s11027-012-9397-4.

Müller, Birgit, Martin F. Quaas, Karin Frank, and Stefan Baumgärtner. 2011. Pitfalls and potential of institutional change: Rain-index insurance and the sustainability of rangeland management. *Ecological Economics* 70 (11): 2137–2144. DOI: 10.1016/j.ecolecon.2011.07.009.

Muñoz-Sabater, Joaquín, Emanuel Dutra, Anna Agustí-Panareda, Clément Albergel, Gabriele Arduini, Gianpaolo Balsamo, Souhail Boussetta, et al. 2021. Era5-land: A state-of-the-art global reanalysis dataset for land applications. *Earth System Science Data* 13 (9): 4349–4383. DOI: https://doi.org/10.24381/cds.68d2bb30.

Noack, Frederik, and Christopher Costello. 2024. Credit markets, property rights, and the commons. *Journal of Political Economy* 132 (7): 2396–2450. DOI: https://doi.org/10.1086/729065.

Openshaw, Stan, and P. J. Taylor. 1979. A million or so correlation coefficients: Three experiments on the modifiable areal unit problem. In *Statistical Applications in the Spatial Sciences*, ed. N. Wrigley. London: Pion, 127–144.

Pellant, Mike, Patrick L. Shaver, David A. Pyke, Jeffrey E. Herrick, Nika Lepak, Gregg Riegel, Emily Kachergis, et al. 2020. Interpreting indicators of rangeland health, version 5: Technical reference 1734-6. U.S. Department of the Interior, Bureau of Land Management. Available at: https://pubs.er.usgs.gov/publication/70215720.

Pelletier, Johanne, Hambulo Ngoma, Nicole M. Mason, and Christopher B. Barrett. 2020. Does smallholder maize intensification reduce deforestation? evidence from zambia. *Global Environmental Change* 63: 102127. DOI: 10.1016/j.gloenvcha.2020.102127.

Poitras, Travis B, Miguel L Villarreal, Eric K Waller, Travis W Nauman, Mark E Miller,

and Michael C Duniway. 2018. Identifying optimal remotely-sensed variables for ecosystem monitoring in colorado plateau drylands. *Journal of Arid Environments* 153: 76–87. DOI: https://doi.org/10.1016/j.jaridenv.2017.12.008.

Purevjav, Avralt-Od, Tumenkhusel Avirmed, Steven W. Wilcox, and Christopher B Barrett. 2025. Climate rather than overgrazing explains most rangeland primary productivity change in mongolia. *Science* 389 (6766): 1229–1233. DOI: https://www.science.org/doi/abs/10.1126/science.adn0005.

Rambachan, Ashesh, and Jonathan Roth. 2023. A more credible approach to parallel trends. *Review of Economic Studies* 90 (5): 2555–2591. DOI: https://doi.org/10.1093/restud/rdad056.

Reeves, Matthew, Robert A. Washington-Allen, Jay Angerer, E. Raymond Hunt, Ranjani Wasantha Kulawardhana, Lalit Kumar, Tatiana Loboda, et al. 2015. Global view of remote sensing of rangelands: Evolution, applications, future pathways. In *Remote Sensing Handbook*, ed. Prasad S. Thenkabail. Boca Raton, FL: CRC Press, 237–275. Available at: https://pubs.usgs.gov/publication/70111380.

Reeves, Matthew C, and L Scott Baggett. 2014. A remote sensing protocol for identifying rangelands with degraded productive capacity. *Ecological Indicators* 43: 172–182. DOI: https://doi.org/10.1016/j.ecolind.2014.02.009.

Retallack, Angus, Graeme Finlayson, Bertram Ostendorf, Kenneth Clarke, and Megan Lewis. 2023. Remote sensing for monitoring rangeland condition: current status and development of methods. *Environmental and Sustainability Indicators* : 100285DOI: https://doi.org/10.1016/j.indic.2023.100285.

Rigge, Matthew, Collin Homer, Bruce Wylie, Yingxin Gu, Hua Shi, George Xian, Debra K Meyer, et al. 2019. Using remote sensing to quantify ecosystem site potential community structure and deviation in the great basin, united states. *Ecological Indicators* 96: 516–531. DOI: https://doi.org/10.1016/j.ecolind.2018.09.037.

Rigge, Matthew, Deb Meyer, and Brett Bunde. 2021. Ecological potential fractional component cover based on long-term satellite observations across the western united states. *Ecological Indicators* 133: 108447. DOI: https://doi.org/10.1016/j.ecolind.2021.108447.

Robinson, Marguerite S. 2001. *The Microfinance Revolution: Sustainable Finance for the Poor*. Washington, DC: World Bank Publications. DOI: 10.1596/0-8213-4524-9.

Roth, Jonathan, Pedro HC Sant'Anna, Alyssa Bilinski, and John Poe. 2023. What's trending in difference-in-differences? a synthesis of the recent econometrics literature. *Journal of*

Econometrics 235 (2): 2218–2244. DOI: https://doi.org/10.1016/j.jeconom.2023.03.008.

Sakketa, Tekalign Gutu, Dan Maggio, and John McPeak. 2025. The protective role of index insurance in the experience of violent conflict: Evidence from ethiopia. *Journal of Development Economics* 174: 103445. DOI: https://doi.org/10.1016/j.jdeveco.2024.103445.

Santos, Paulo, and Christopher B Barrett. 2011. Persistent poverty and informal credit. *Journal of Development Economics* 96 (2): 337–347. DOI: https://doi.org/10.1016/j.jdeveco.2010.08.017.

Santos, Paulo, and Christopher B. Barrett. 2019. Heterogeneous wealth dynamics: On the roles of risk and ability. In *The Economics of Poverty Traps*, eds. Christopher B. Barrett, Michael R. Carter, and Jean-Paul Chavas. Chicago, IL: University of Chicago Press, 265–290. DOI: 10.7208/chicago/9780226574448.003.0011.

Shi, Hua, Matthew Rigge, Kory Postma, and Brett Bunde. 2022. Trends analysis of rangeland condition monitoring assessment and projection (rcmap) fractional component time series (1985–2020). *GIScience & Remote Sensing* 59 (1): 1243–1265. DOI: https://doi.org/10.1080/15481603.2022.2104786.

Smith, Vincent H, and Barry K Goodwin. 2013. The environmental consequences of subsidized risk management and disaster assistance programs. *Annu. Rev. Resour. Econ.* 5 (1): 35–60. DOI: https://doi.org/10.1146/annurev-resource-110811-114505.

Son, Hyuk Harry. 2025. Ibli and child labor: Evidence from pastoral communities. Working paper. Available at: `https://hyukhson.github.io/files/ibli_childlabor.pdf`.

Soto, Gerardo E, Steven W. Wilcox, Patrick E Clark, Francesco P Fava, Nathaniel D Jensen, Njoki Kahiu, Chuan Liao, et al. 2024. Mapping rangeland health indicators in eastern africa from 2000 to 2022. *Earth System Science Data* 16 (11): 5375–5404. DOI: https://doi.org/10.5281/zenodo.7106166.

Standiford, Richard B., and Richard E. Howitt. 1992. Solving empirical bioeconomic models: A rangeland management application. *American Journal of Agricultural Economics* 74 (2): 421–433. DOI: 10.2307/1242496.

Stevenson, James R., Nelson Villoria, Derek Byerlee, Timothy Kelley, and Mywish Maredia. 2013. Green revolution research saved an estimated 18 to 27 million hectares from being brought into agricultural production. *Proceedings of the National Academy of Sciences* 110 (21): 8363–8368. DOI: 10.1073/pnas.1208065110.

Stoeffler, Quentin, Michael Carter, Catherine Guirkinger, and Wouter Gelade. 2022. The spillover impact of index insurance on agricultural investment by cotton farm-

ers in burkina faso. *The World Bank Economic Review* 36 (1): 114–140. DOI: https://doi.org/10.1093/wber/lhab011.

Tafere, Kibrom, Christopher B Barrett, and Erin Lentz. 2019. Insuring well-being? buyer's remorse and peace of mind effects from insurance. *American Journal of Agricultural Economics* 101 (3): 627–650. DOI: https://doi.org/10.1093/ajae/aay087.

Toth, Russell. 2015. Traps and thresholds in pastoralist mobility. *American Journal of Agricultural Economics* 97 (1): 315–332. DOI: https://doi.org/10.1093/ajae/aau064.

Toth, Russell, Christopher B. Barrett, Richard Bernstein, Patrick Clark, Carla Gomes, Shibia Mohamed, Andrew Mude, et al. 2020. Behavioral substitution of formal risk mitigation: Index insurance in east africa. Working paper.

Van Rooyen, Carina, Ruth Stewart, and Thea De Wet. 2012. The impact of microfinance in sub-saharan africa: A systematic review of the evidence. *World development* 40 (11): 2249–2262. DOI: https://doi.org/10.1016/j.worlddev.2012.03.012.

Villoria, Nelson. 2019a. Consequences of agricultural total factor productivity growth for the sustainability of global farming: Accounting for direct and indirect land use effects. *Environmental Research Letters* 14 (12): 125002. DOI: 10.1088/1748-9326/ab570e.

Villoria, Nelson B. 2019b. Technology spillovers and land use change: Empirical evidence from global agriculture. *American Journal of Agricultural Economics* 101 (3): 870–893. DOI: 10.1093/ajae/aay088.

Wang, Cong, Jason Beringer, Lindsay B Hutley, James Cleverly, Jing Li, Qinhuo Liu, and Ying Sun. 2019. Phenology dynamics of dryland ecosystems along the north australian tropical transect revealed by satellite solar-induced chlorophyll fluorescence. *Geophysical Research Letters* 46 (10): 5294–5302. DOI: https://doi.org/10.1029/2019GL082716.

Wilcox, Steven W., David R Just, and Ariel Ortiz-Bobea. 2025. The role of staple food prices in deforestation: Evidence from cambodia. *Land Economics* 101 (1): 89–118. DOI: https://doi.org/10.3368/le.101.1.100423-0097R.

Supplementary Appendix for:

The Environmental Impacts of Scaling a Microfinancial Product: Index-Based Livestock Insurance and East African Rangelands

Steven W. Wilcox, Christopher B. Barrett, Nathaniel Jensen, Patrick E. Clark, Francesco Pietro Fava, Gerardo E. Soto, Njoki Kahiu, Ying Sun

July 2026

A Supplementary Figures and Tables: IBLI roll-out, study area and units of Observation, and IBLI exposure

A.1 Trends in IBLI roll-out and adoption at the index unit level.

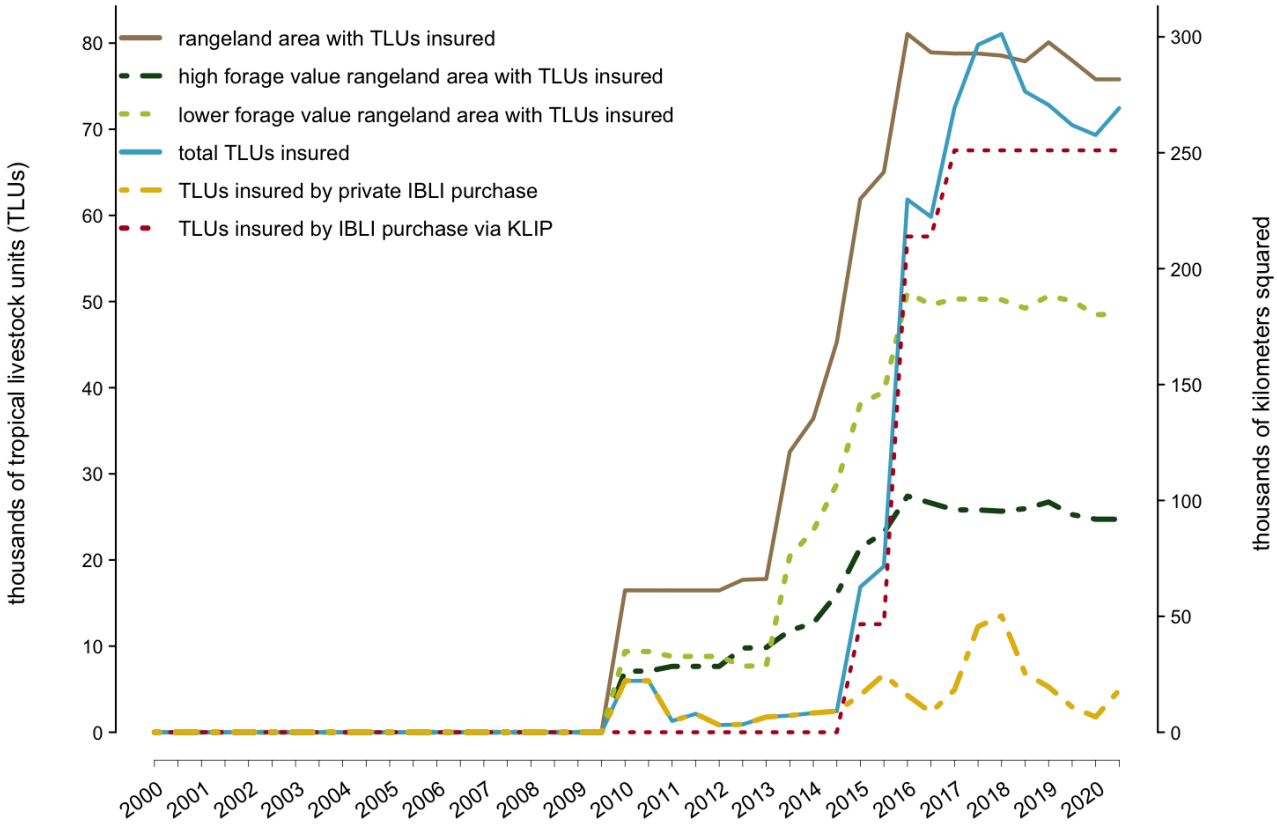


Figure A.1.1: IBLI expansion in thousands of TLUs insured and area of rangelands exposed in thousands km^2 in terms of total rangeland area, as well as rangeland area exposed by 'low' and 'high' forage quality rangelands. Higher exposure to low forage quality rangelands reflects that these rangeland types are dominant in the region. Definitions of 'low' and 'high' forage quality rangeland types are detailed in Section 3.3.

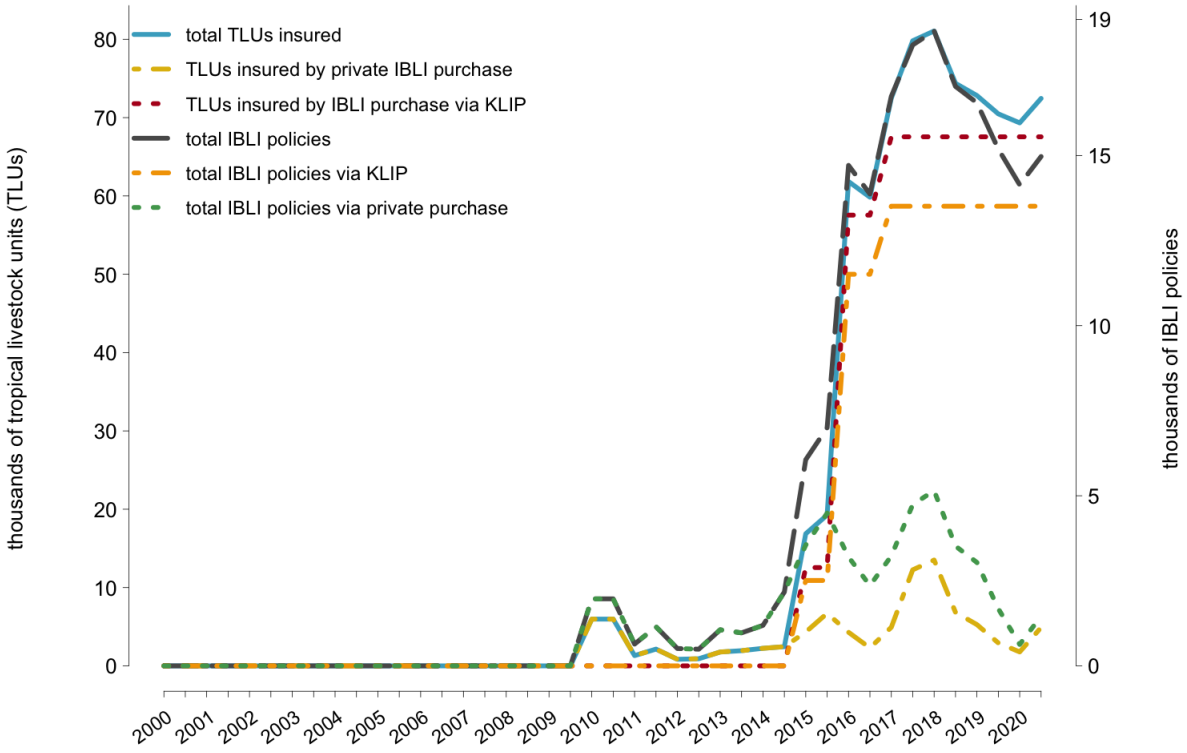


Figure A.1.2: Trends for the number of TLUs insured and number of policies.

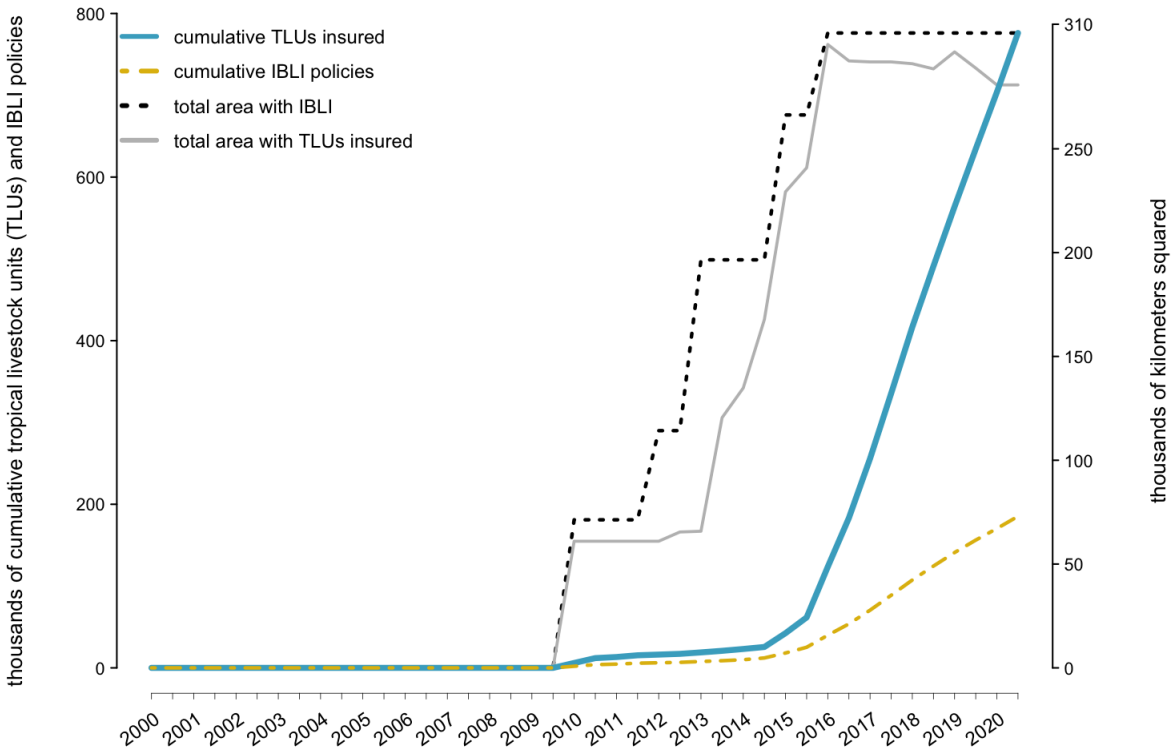


Figure A.1.3: Trends for the cumulative number of TLUs insured and cumulative number of policies, along with the corresponding rangeland area exposed.

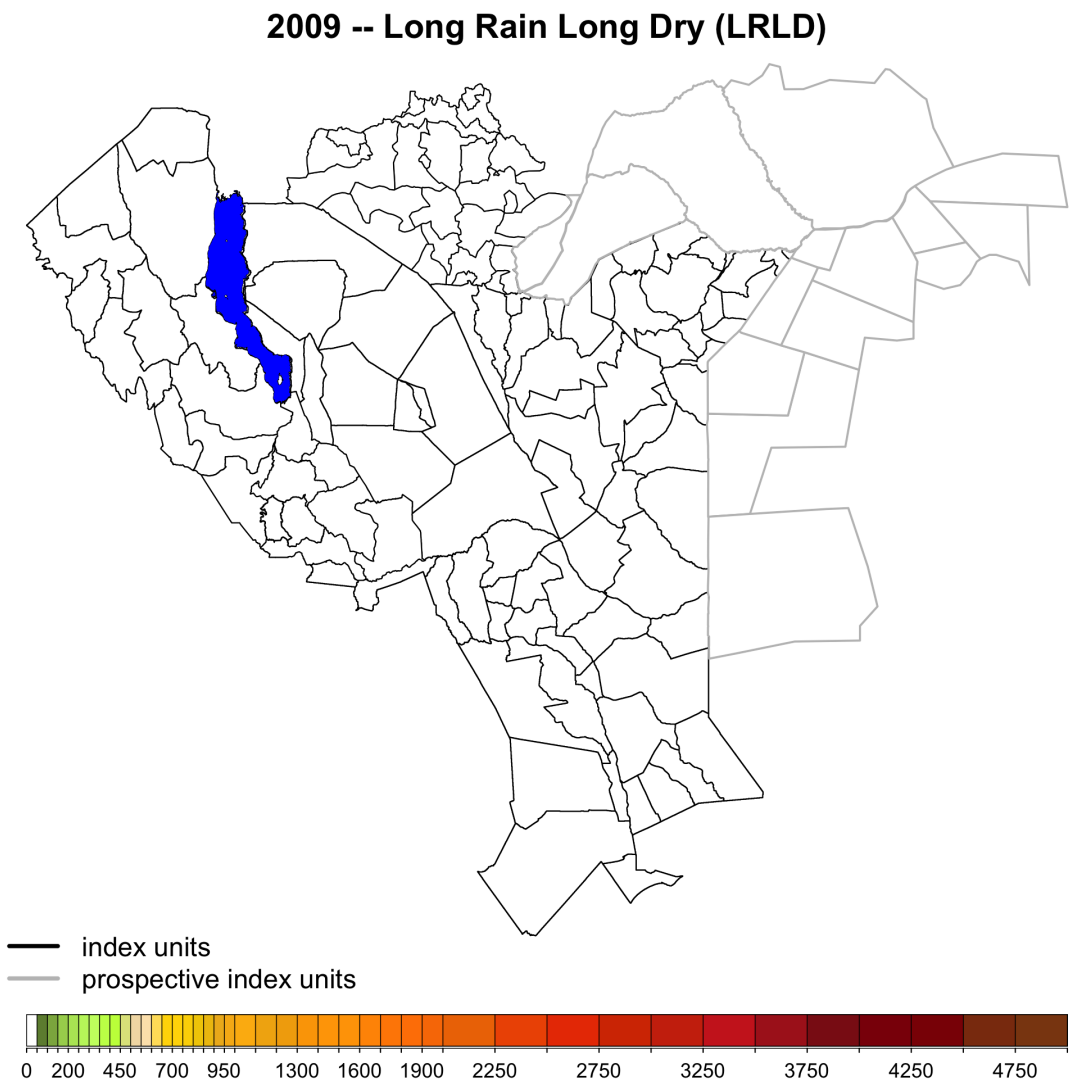


Figure A.1.4: Animation of observed, *contemporaneous* TLUs insured by index unit, year, and season over 2009-2020. Note that Adobe Acrobat reader may be required to view the full animation as intended.

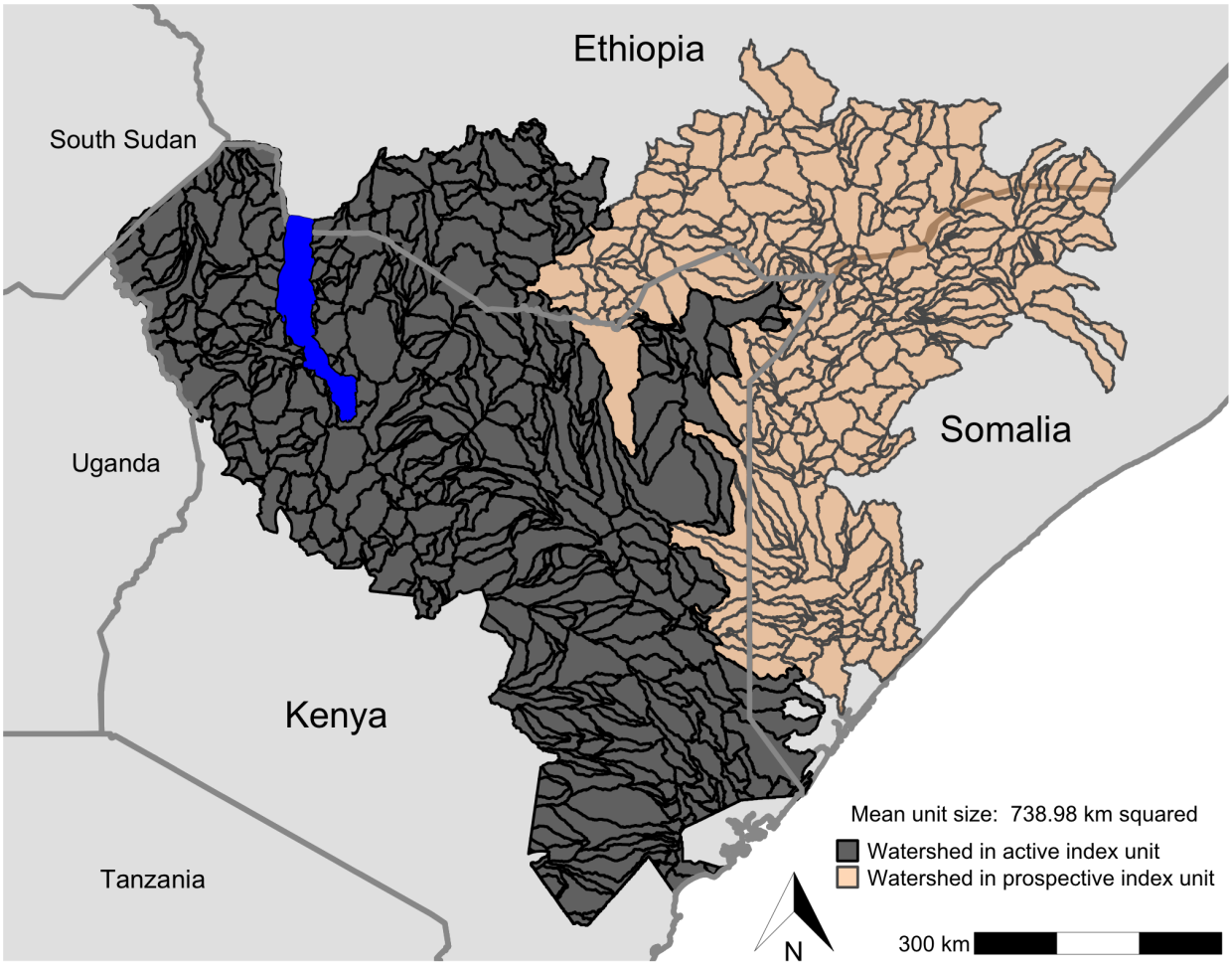


Figure A.1.5: Map of study area and intersecting HUC-8 units from Lehner and Grill (2013).

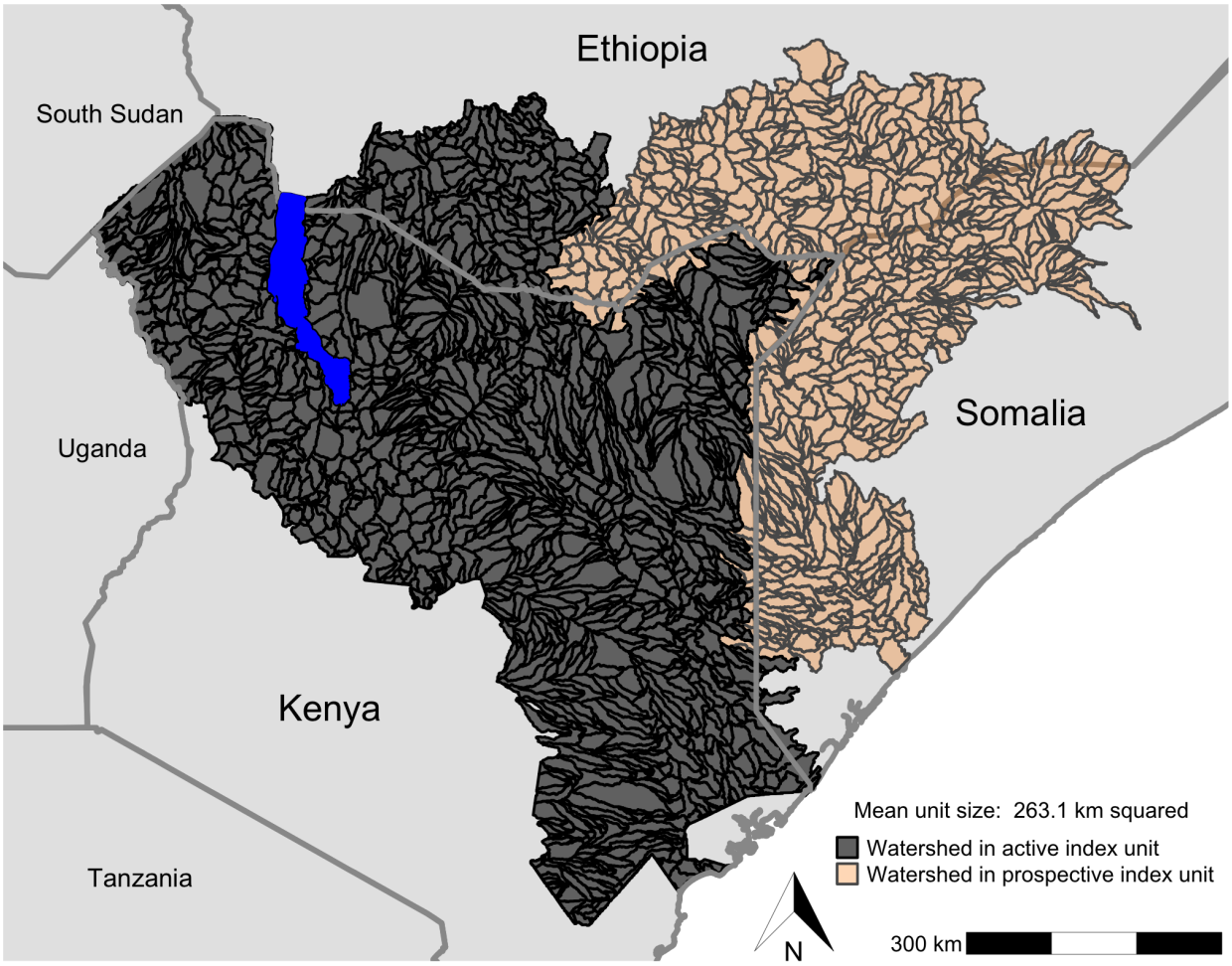


Figure A.1.6: Map of study area and intersecting HUC-9 units from Lehner and Grill (2013).

A.2 IBLI exposure via inverse distance weighting

Equation (A.2.1) defines the IBLI exposure variable of interest at the unit level that accounts for herder movement:

$$WIBE_i = IBE_i + \sum_{j^{-i}} \frac{(\mathbb{1}_j \; w_{ij})}{\sum\limits_{j-i} \mathbb{1}_j \; w_{ij}} IBE_j \tag{A.2.1}$$

$WIBE_i$ represents the estimated weighted total IBLI exposure of unit i (i.e., IUs, HUCs) for a given time period (time and pixel-level summations are omitted for simplicity). IBE_i is the total rangeland-area weighted exposure (in TLUs insured) observed within spatial unit i for some year and season, w_{ij} is a weighting function that scales the observed rangeland-area weighted exposure within another unit $j \neq i$, and the indicator function $\mathbb{1}_j$ is a binary variable equal to 1 if unit j is within the pre-defined neighborhood of unit i. Weights are normalized such that $\sum_{j^{-i}} \frac{\mathbb{1}_j \; w_{ij}}{\sum_{j^{-i}} \; \mathbb{1}_j \; w_{ij}} = 1$.

We operationalize equation (A.2.1) using inverse distance weighting (IDW) for w_{ij} and we use referenced GPS livestock collar data (Section 3.2) to define a neighborhood distance for each unit for each of our four levels of aggregation (Clark et al. 2006; Liao et al. 2017, 2018). Specifically, we apply a neighborhood distance of 63 km, which reflects the sum of the mean and standard deviation of observed herding distances during each SRSD season over 2011-2015. This is a conservative distance as herding distances tend to be a bit larger in the SRSD (see boxplots below in Figure A.2.1). To weight adjacent exposure within this neighborhood for units $j \neq i$ we use a series of 9 evenly spaced (7 km) concentric buffers b_j emanating from the border of each unit i. To accomplish this, we down-scale IBLI exposure from IUs to Landsat-scale (30m) pixels via an 'all' rangelands mask (described in Section 3.3) since movement is likely to occur through all land types. Intersecting rangeland-area weighted IBLI exposure within each buffer is therefore weighted by the inverse of distance $b_j - (7 \; km/2)$, which is the midway distance in meters between each buffer's inner and outer boundaries.[1]

To study IBLI exposure we focus on cumulative TLUs insured at the extensive and intensive margins and we study exposure as an irreversible state. Specifically, we consider a unit to be exposed to IBLI in the first period when cumulative $WIBE_i \geq 1$, so once one cumulative TLU is insured within a unit. Cumulative exposure accounts for the fact that any effects on rangelands are likely to be a function of the livestock units insured over time and the aggregate effects of herders' exposure to IBLI. Treating exposure as an irreversible state also accounts for the fact that there have been no disruptions to IBLI exposure during our study period.

Below we detail each of the steps in our algorithm for implementing our IDW approach to account for spill-overs in IBLI exposure.

[1]For example, for any unit i the outside border of the farthest buffer b_9, is 63 km away from the border of unit i. Hence the sum of IBLI exposure within the intersecting pixels of the farthest buffer is weighted by the inverse of, 63 km - (7 km /2) = 59.5 km.

- Step 1: For each year, season, index unit (IU) and control area (CA) (i.e., prospective index unit) convert IBLI exposure into a raster grid using the respective 'all' rangelands mask derived from Landsat scale (i.e., 30 m^2) land cover data from Soto et al. (2024) (see further details in Section 3.3).

- Step 2: For each year, season, IU and CA, count the number of pixels that result within each IU and CA from Step 1 and store the data.

- Step 3: For each year, season, IU and CA, divide the IBLI exposure variable of interest (i.e., cumulative TLUs insured) by the number of pixels from Step 2 and store the data. Step 3 produces rangeland area weighted IBLI exposure per pixel within IUs and CAs per year and season.

- Step 4: For each year, season, IU and CA, convert the rangeland area weighted data from Step 3 into a raster grid using the respective 'all' rangelands mask derived from Landsat scale (i.e., 30 m^2) land cover data from Soto et al. (2024), to produce a raster of rangeland area weighted IBLI exposure and store the data.

- Step 5: Using data from Step 4, for each unit, in each year and season, apply equation (A.2.1) by summing across all pixels within each unit, summing across pixels within each unit's respective concentric buffers and weight by the inverse distance, then add the two sums, and store the data for each unit (IUs and CAs (n = 130), HUC-8 (n = 870), HUC-9 (n = 2339), HUC-12 (n = 4753)).

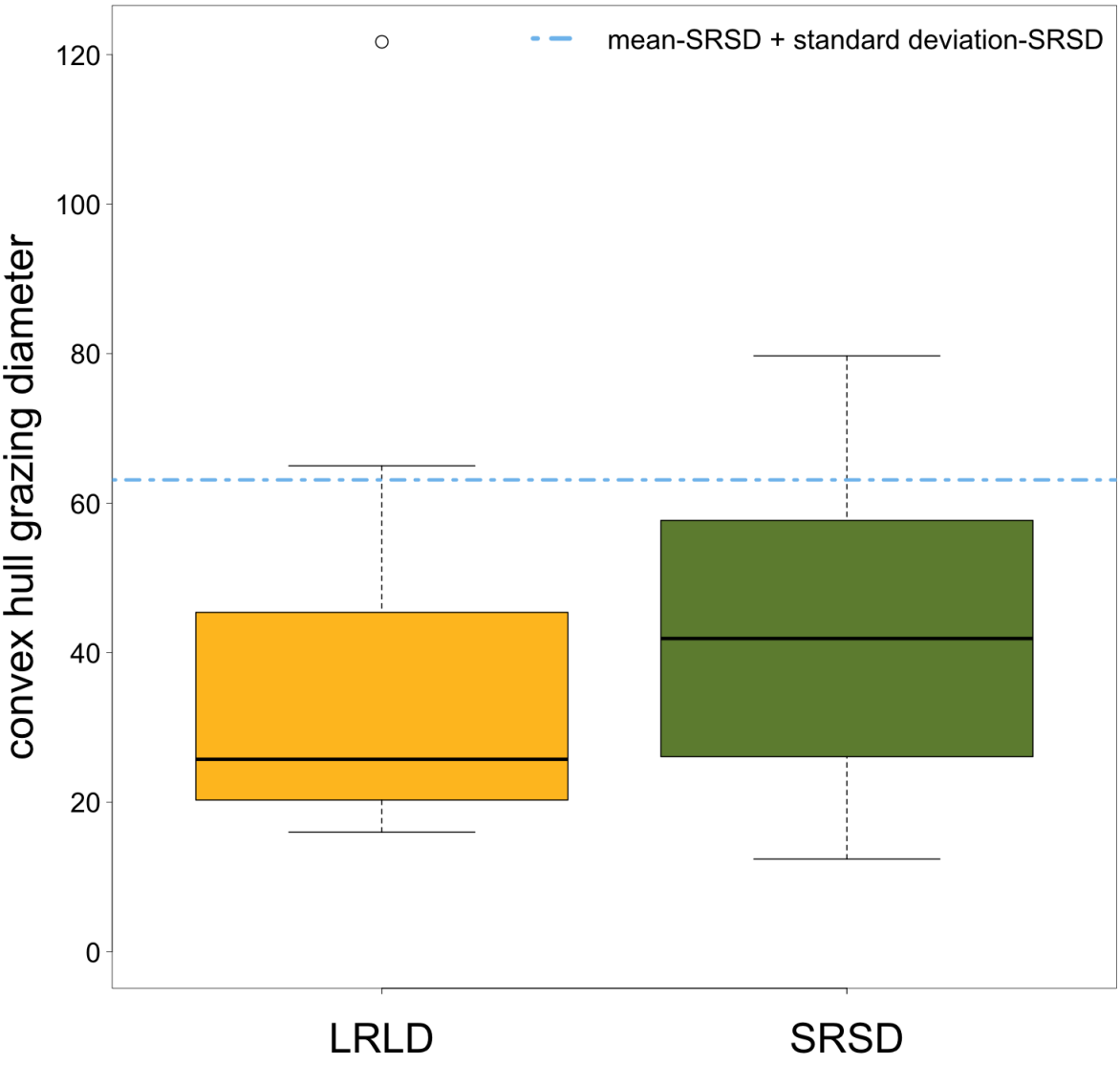


Figure A.2.1: Distribution of convex hull diameters across the LRLD and SRSD. To bound neighborhoods for inverse distance weighting we apply the mean diameter from the SRSD plus one standard deviation from the SRSD, which comes to 63 kilometers. (Author's calculations using GPS livestock collar data from Clark et al. 2006).

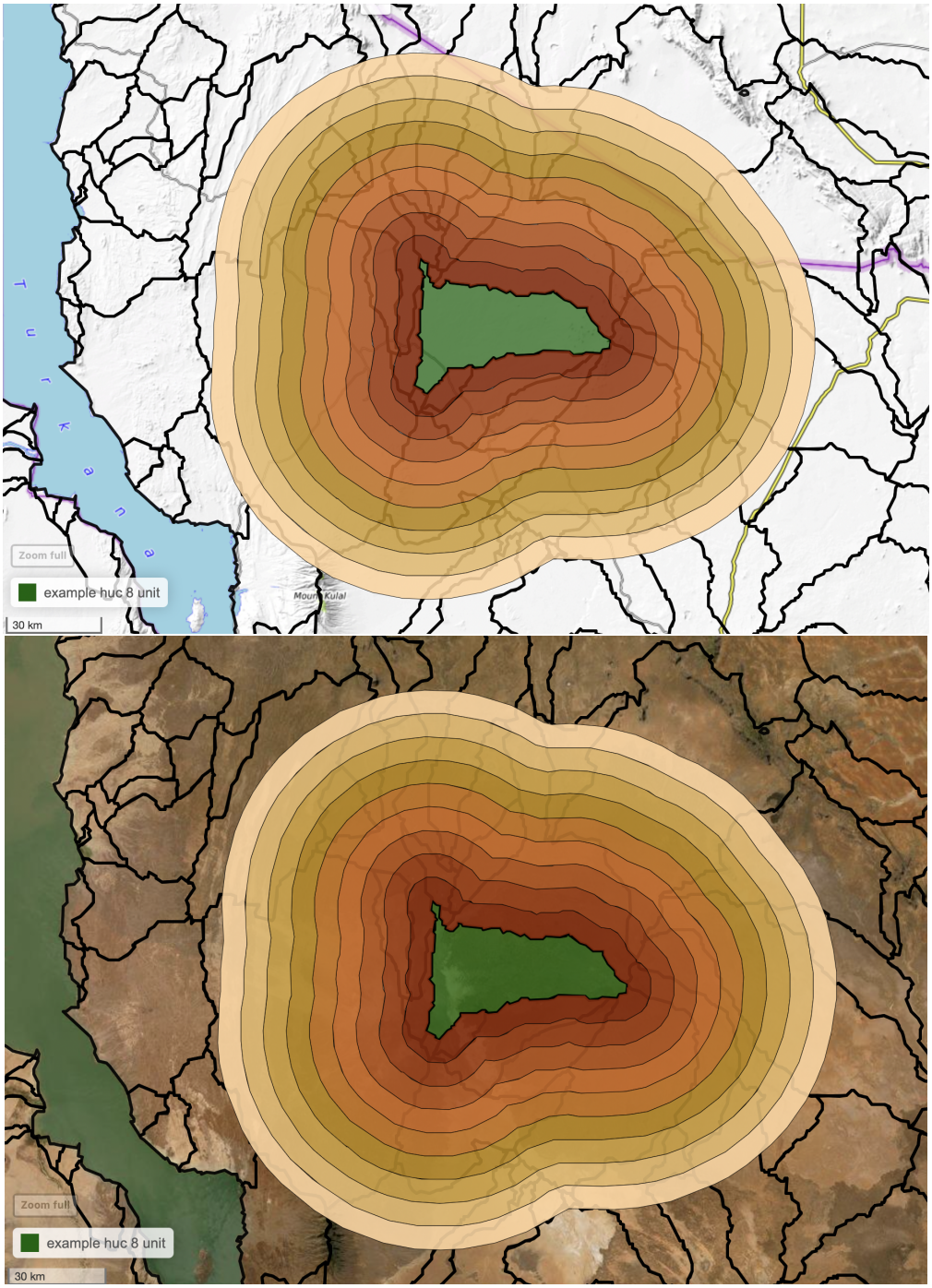


Figure A.2.2: Example neighborhood and concentric buffers for a HUC-8 watershed unit east of Lake Turkana.

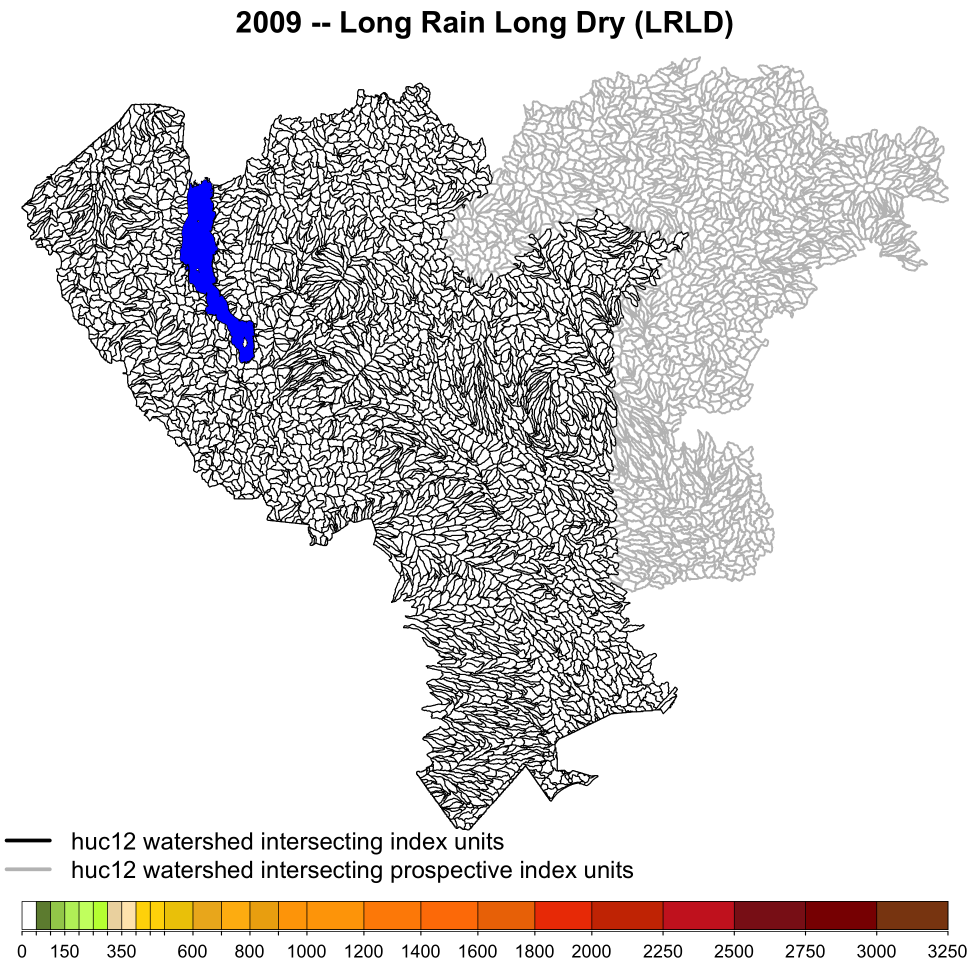


Figure A.2.3: Animation of inverse distance weighted *contemporaneous* (i.e., non-cumulative) TLUs insured by HUC-12 unit, year, and season. This figure shows the results of applying equation (A.2.1) using index-unit level IBLI sales data and the 'all' rangeland mask (see Section 3.3). Note that Adobe acrobat reader may be required to view the full animation as intended.

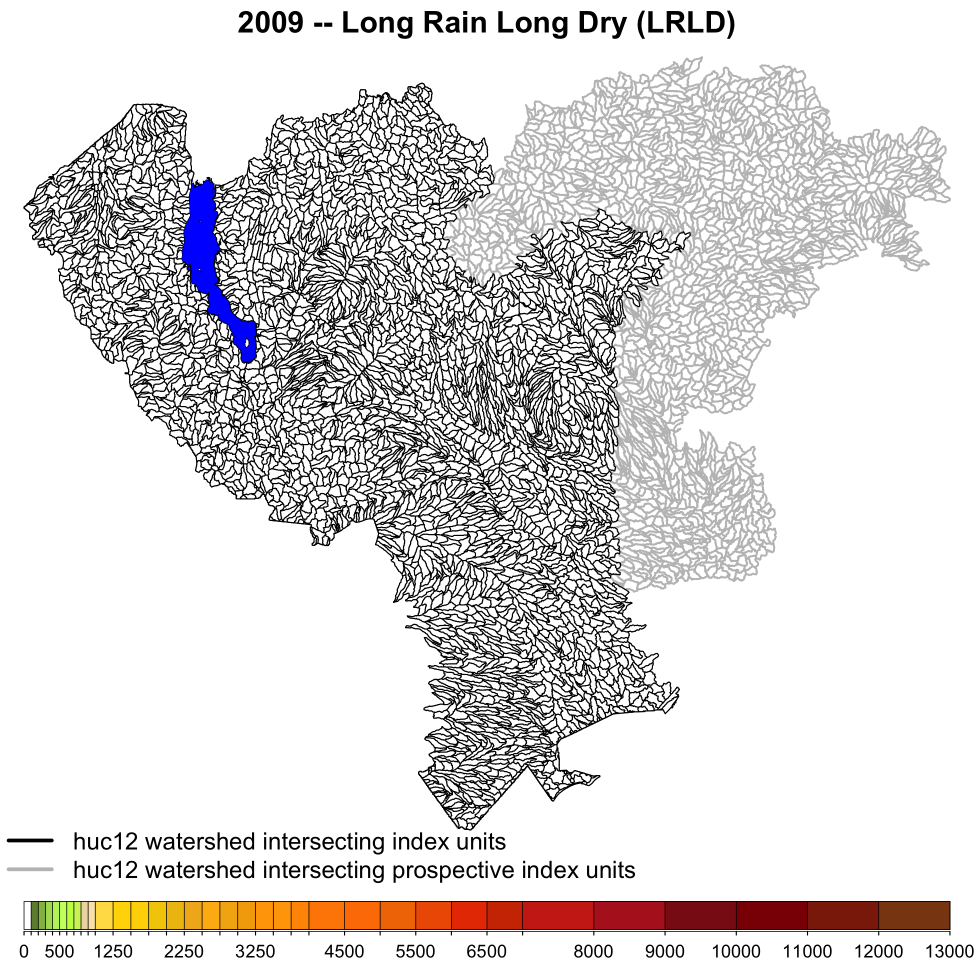


Figure A.2.4: Animation of inverse distance weighted *cumulative* TLUs insured by HUC-12, year, and season. This figure shows the results of applying equation (A.2.1) using index-unit level IBLI sales data and the 'all' rangeland mask (see Section 3). Note that Adobe acrobat reader may be required to view the full animation as intended.

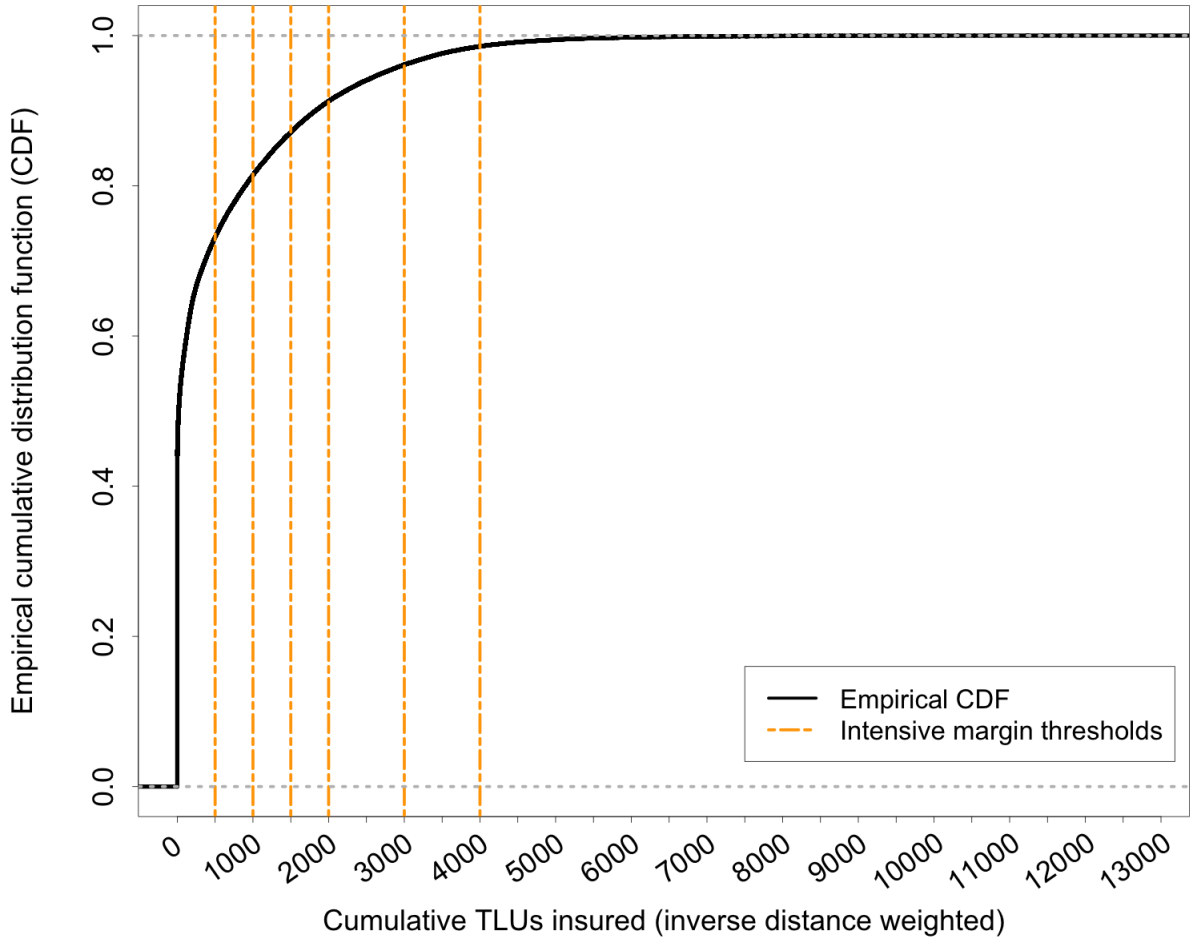


Figure A.2.5: Cumulative distribution function of inverse distance weighted cumulative IBLI exposure in TLUs insured over 2010 - 2020.

Table A.2.1: Summary statistics for tropical livestock units (TLUs) insured at each level of aggregation over 2010-2020 by differing exposure definitions.

Variable	Index Unit	HUC-8	HUC-9	HUC-12
TLUs insured	352.36	52.55	19.55	9.62
	(650.07)	(165.78)	(56.49)	(23.6)
	[2860]	[19140]	[51458]	[104566]
TLUs insured (IDW)	596.64	155.78	102.98	85.98
	(921.37)	(331.39)	(194.29)	(147.9)
	[2860]	[19140]	[51458]	[104566]
Cumulative TLUs insured	2133.33	318.17	118.35	58.24
	(4384.54)	(1092.54)	(366.98)	(151.88)
	[2860]	[19140]	[51458]	[104566]
Cumulative TLUs insured (IDW)	3587.36	945.74	625.29	521.33
	(6276.66)	(2219.14)	(1298.73)	(990.92)
	[2860]	[19140]	[51458]	[104566]

Note: Each column presents the mean, standard deviation (parenthesis), and sample size (square brackets) for each measure of IBLI exposure. Variables denoted with '(IDW)' reflect inverse distance weighted exposure as described in Section 3.2 and Appendix A.2. The first year with semi-annual IBLI coverage was 2010 (see Section 2 for further details). Variable names reflect the following specific definitions of IBLI coverage/exposure: contemporaneous without IDW ('TLUs insured'); contemporaneous with IDW ('TLUs insured (IDW)'); cumulative without IDW ('Cumulative TLUs insured'); and cumulative with IDW ('Cumulative TLUs insured (IDW)').

B Supplementary Figures and Tables: Rangeland Health Measures and Covariates

B.1 Rangeland condition measures within the rangeland health framework, summary statistics, and rangeland masks.

Table B.1.1: Remotely sensed (RS) indicators of rangeland health (RH) used in this study arranged by their relationship to the RH framework detailed by Pellant et al. (2020).

RH Attributes	**RH Assessment Indicators (RHAI)**	**RS-based Estimates of RHAI**	**Sources & Methods**
Biotic Integrity	dead or dying plants	non-photosynthetic vegetation	30m fractional cover Soto et al. (2024)
	functional / structural group canopy cover	photosynthetic vegetation	30m fractional cover Soto et al. (2024)
	functional/ structural groups, plant mortality and vigor	vegetation indices (e.g., EVI)$^{++}$	250m MODIS vegetation indices Didan et al. (2021)
Hydrologic Function	bare ground	bare ground	30m fractional cover Soto et al. (2024)
Soil / Site Stability			

$^{++}$Denotes indirect estimates of RHAI. Ground-based measurement protocols outlined by Pellant et al. (2020) recommend a variety of RHAI to capture each RH attribute. We rely on RS-based estimates of RHAI that are either direct or indirect estimates of standard ground-based measures of RHAI.

Table B.1.2: Summary statistics for rangland health attribute indicator measures at HUC-12 level over 2000-2020.

Variable	All	High	Low	CCW	SS	SV
BG share	0.28	0.13	0.33	0.04	0.28	0.59
	(0.24)	(0.14)	(0.25)	(0.11)	(0.32)	(0.28)
	[99510]	[98532]	[99444]	[72094]	[20570]	[85615]
PV share	0.21	0.26	0.21	0.45	0.19	0.11
	(0.14)	(0.12)	(0.15)	(0.16)	(0.15)	(0.11)
	[99510]	[98532]	[99444]	[72094]	[20570]	[85615]
NPV share	0.51	0.6	0.47	0.51	0.53	0.3
	(0.19)	(0.15)	(0.19)	(0.15)	(0.24)	(0.21)
	[99510]	[98532]	[99444]	[72094]	[20570]	[85615]
EVI	0.18	0.18	0.17	0.22	0.21	0.15
	(0.07)	(0.07)	(0.07)	(0.08)	(0.06)	(0.05)
	[199584]	[196642]	[199448]	[134850]	[35855]	[167792]

Note: Each column presents the mean, standard deviation (parenthesis), and sample size (square brackets) for each rangeland health measure at the HUC-12 level. Acronyms in this table are as follows: BG = bare ground; PV = photosynthetic vegetation; NPV = non-photosynthetic vegetation; and EVI = enhance vegetation index; all = all rangeland types; high = high forage quality rangeland types (including open canopy woodland (OCW), grassland (GR), sparse scrubland (SS), and cultivated land (CL)); low = low forage quality rangeland types (including sparse vegetation (SV), bushland (BU), dense scrubland (DS), and close canopy woodland (CCW)).

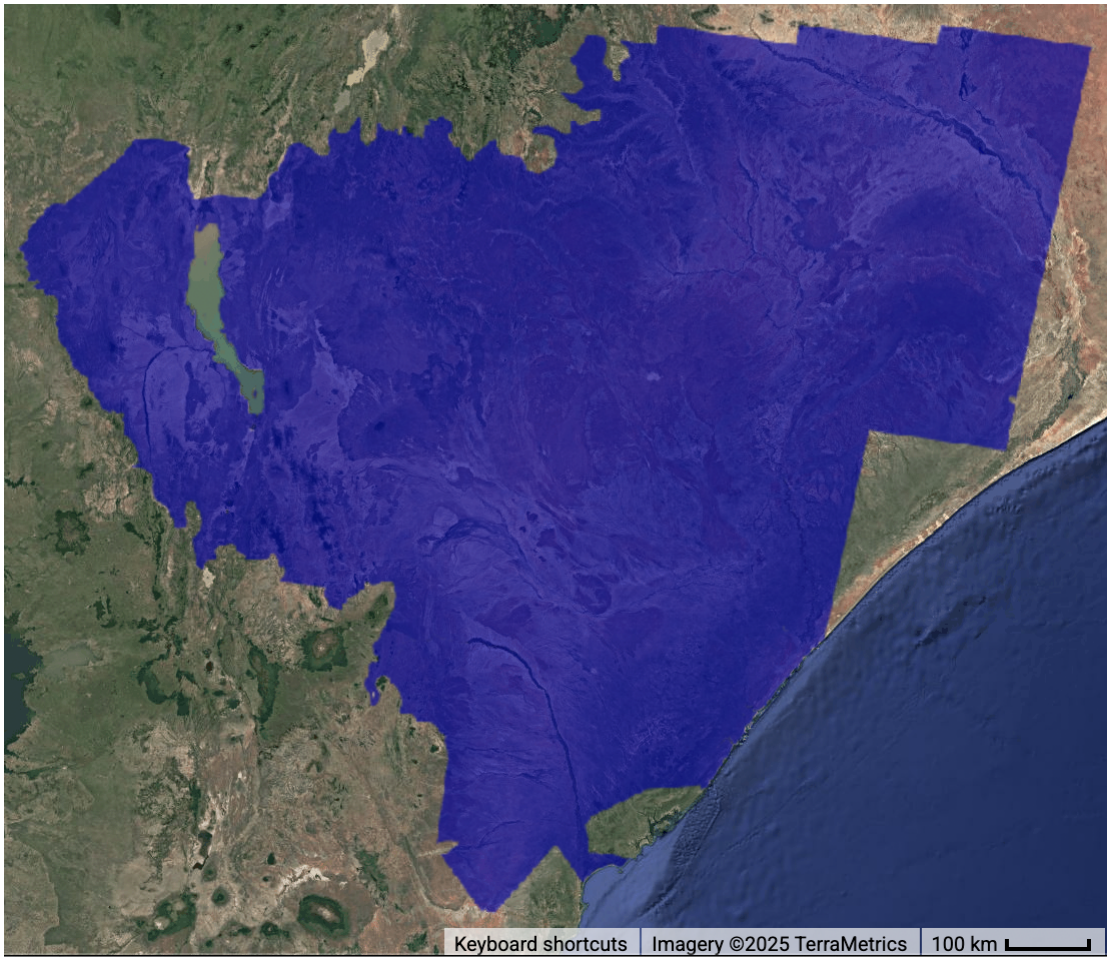


Figure B.1.1: Land cover mask for the ‘all’ rangelands over 2006-2010.

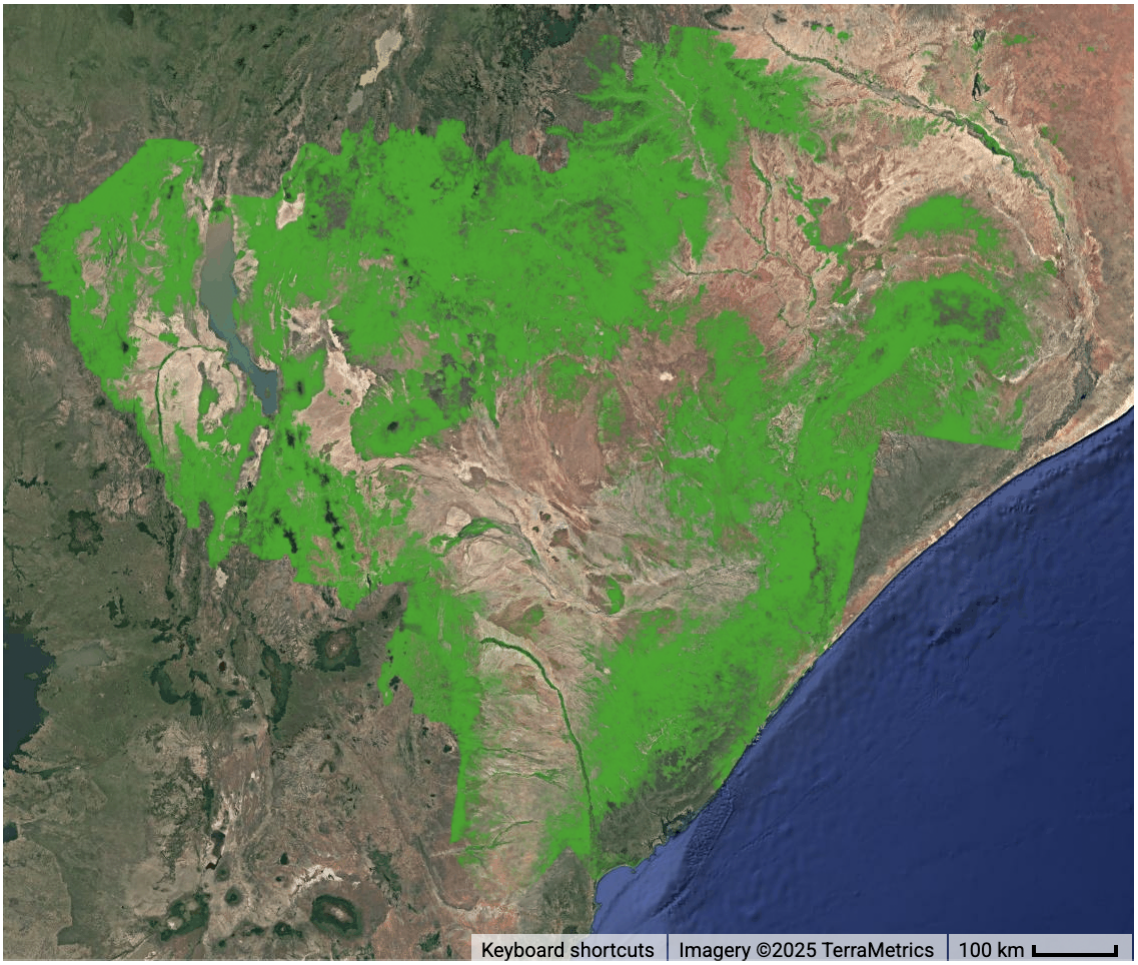


Figure B.1.2: Land cover mask for 'high' forage quality rangelands over 2006-2010.

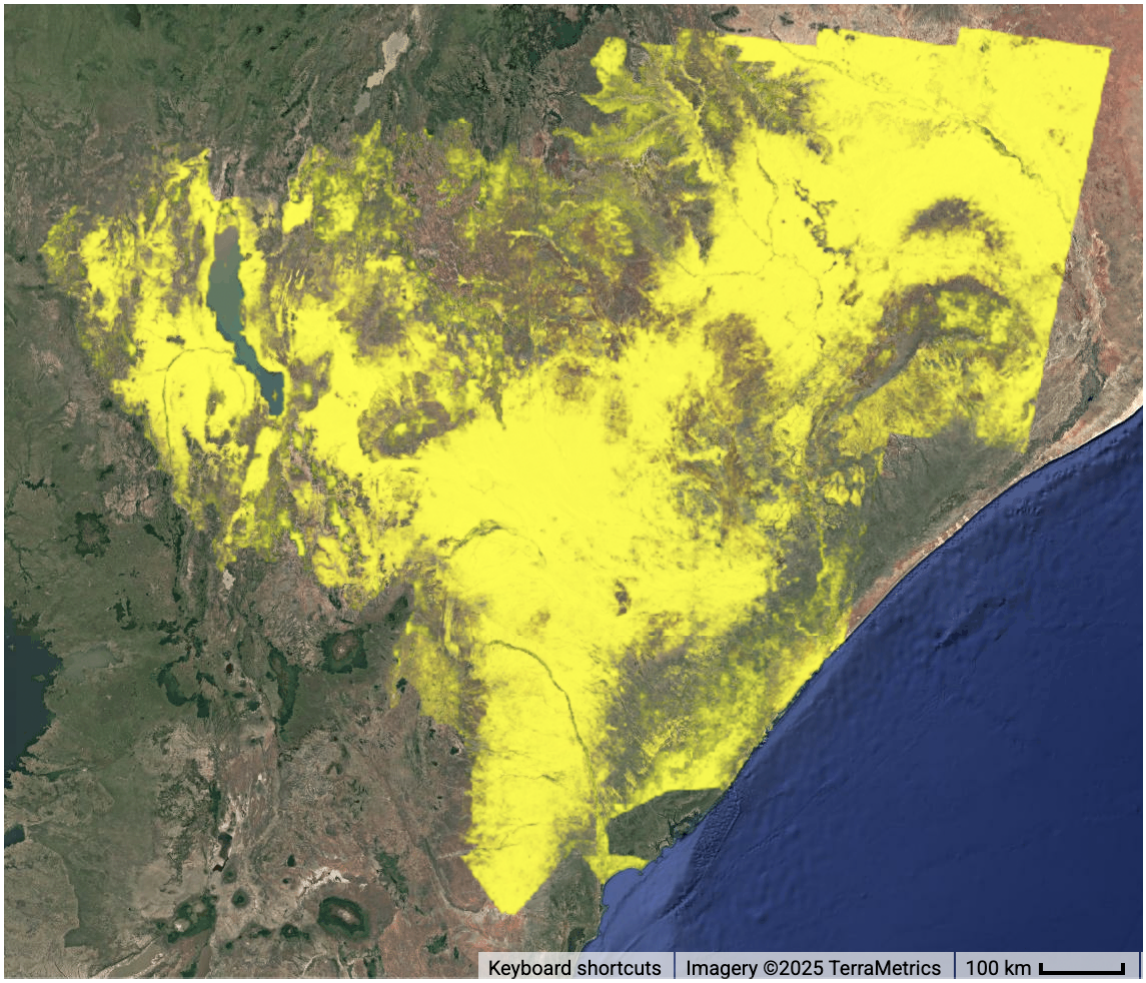


Figure B.1.3: Land cover mask for 'low' forage quality rangelands over 2006-2010.

Table B.1.3: Summary statistics for weather covariates at each level of aggregation over 2000-2020.

Variable	Index Unit	HUC-8	HUC-9	HUC-12
GDD 5-10 C	0.003	0.002	0.001	0.001
	(0.04)	(0.05)	(0.03)	(0.05)
	[5460]	[36540]	[98238]	[199626]
GDD 10-15 C	1.111	0.456	0.388	0.378
	(4.18)	(3.11)	(2.77)	(2.91)
	[5460]	[36540]	[98238]	[199626]
GDD 15-20 C	17.202	8.136	8.644	8.355
	(28.35)	(19.53)	(20.51)	(20.25)
	[5460]	[36540]	[98238]	[199626]
GDD 20-25 C	64.538	70.592	69.853	70.193
	(22.29)	(20.75)	(20.44)	(20.49)
	[5460]	[36540]	[98238]	[199626]
GDD 25-30 C	35.029	42.819	42.002	42.271
	(20.75)	(19.46)	(19.62)	(19.88)
	[5460]	[36540]	[98238]	[199626]
GDD 30-35 C	4.725	7.001	6.779	6.69
	(5.4)	(6.93)	(6.89)	(6.96)
	[5460]	[36540]	[98238]	[199626]
GDD 35-40 C	0.005	0.012	0.011	0.011
	(0.05)	(0.09)	(0.09)	(0.09)
	[5460]	[36540]	[98238]	[199626]
Precipitation mean (mm)	230.232	212.234	214.353	211.126
	(143.24)	(136.8)	(136.02)	(136.03)
	[5460]	[36498]	[98196]	[199542]
Precipitation standard deviation (mm)	42.786	28.073	21.049	17.471
	(32.88)	(28.42)	(22.43)	(19.21)
	[5460]	[36498]	[98196]	[199542]

Note: Each column presents the mean, standard deviation (parenthesis), and sample size (square brackets) for each measure. Temperature in degrees celsius (C) is captured by growing degree days (GDD) in 5 degree bins, defined as the average total number of hours in a unit divided by 24. Average precipitation is measured in millimeters (mm). No exposure to temperatures below 5° C or above 40° C was observed within the study area.

B.2 Unconditional and conditional trends in rangeland health measures.

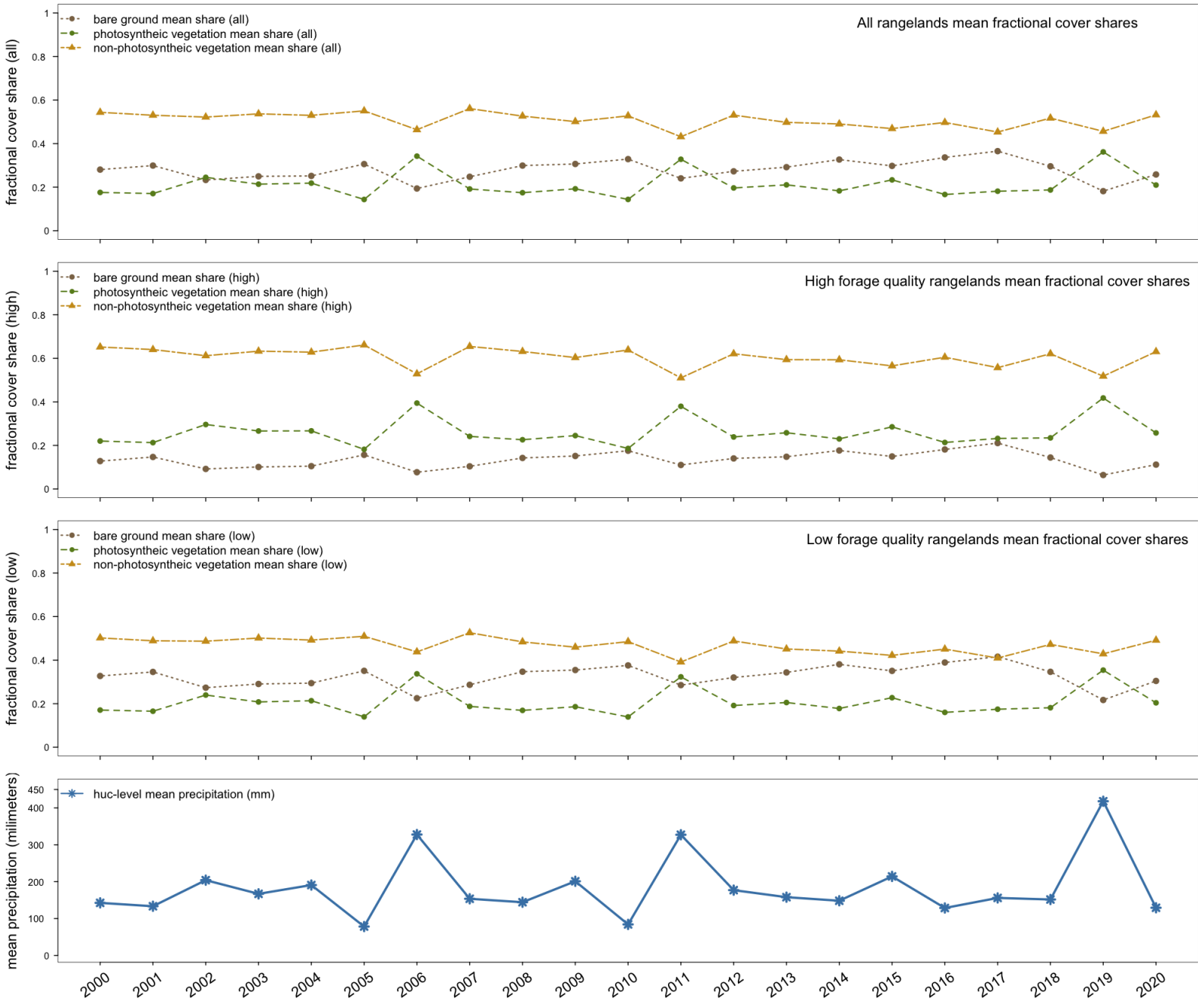


Figure B.2.1: Trends in the average fractional cover share of BG, PV, and NPV for all rangelands (top), high quality (second from top) and low quality (second from bottom) rangelands during the SRSD in each IBLI year, 2000-2020, with contemporaneous average precipitation at the HUC-12 level (bottom panel).



Figure B.2.2: Trends in seasonal mean EVI for all rangelands (top), high quality (second from top) and low quality (second from bottom) rangelands during the SRSD in each IBLI year, 2000-2020, with contemporaneous average precipitation at the HUC-12 level (bottom panel).

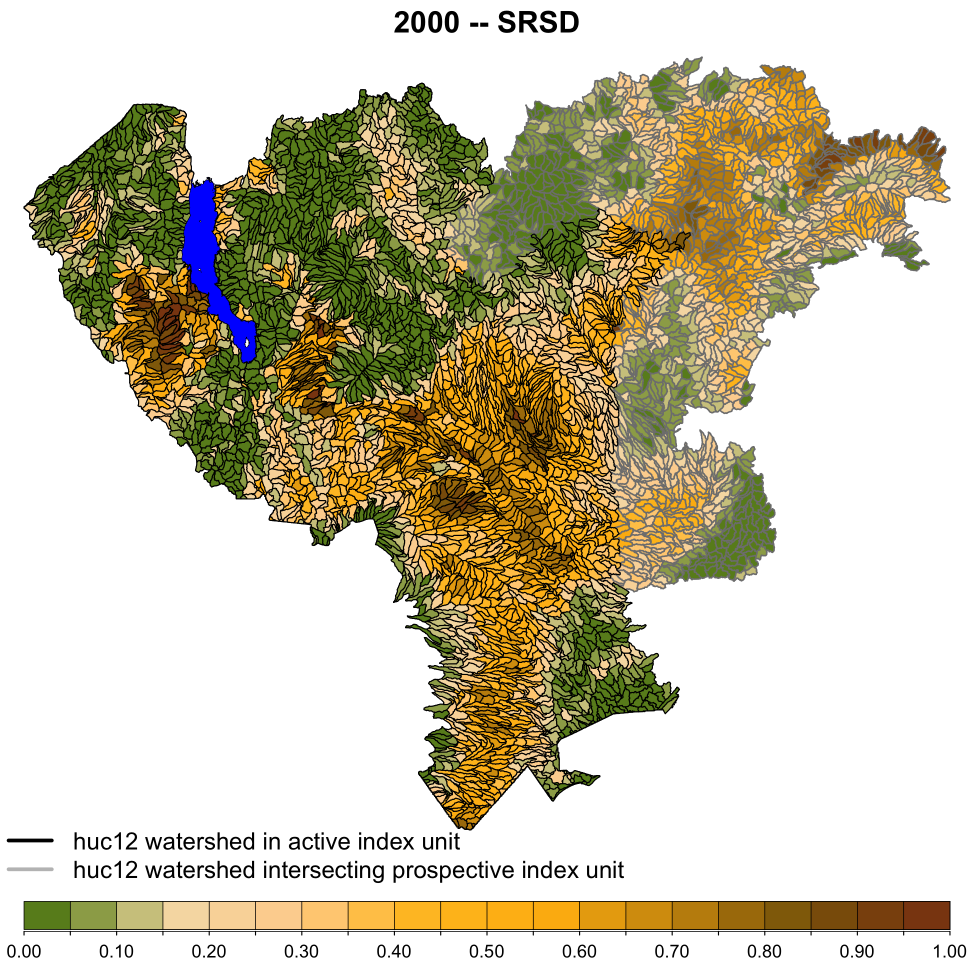


Figure B.2.3: Animation of the share of bare ground (BG) fractional cover at the HUC-12 level during the SRSD of each year for 'all' rangelands over 2000 - 2020. Note that Adobe acrobat reader may be required to view the full animation as intended.

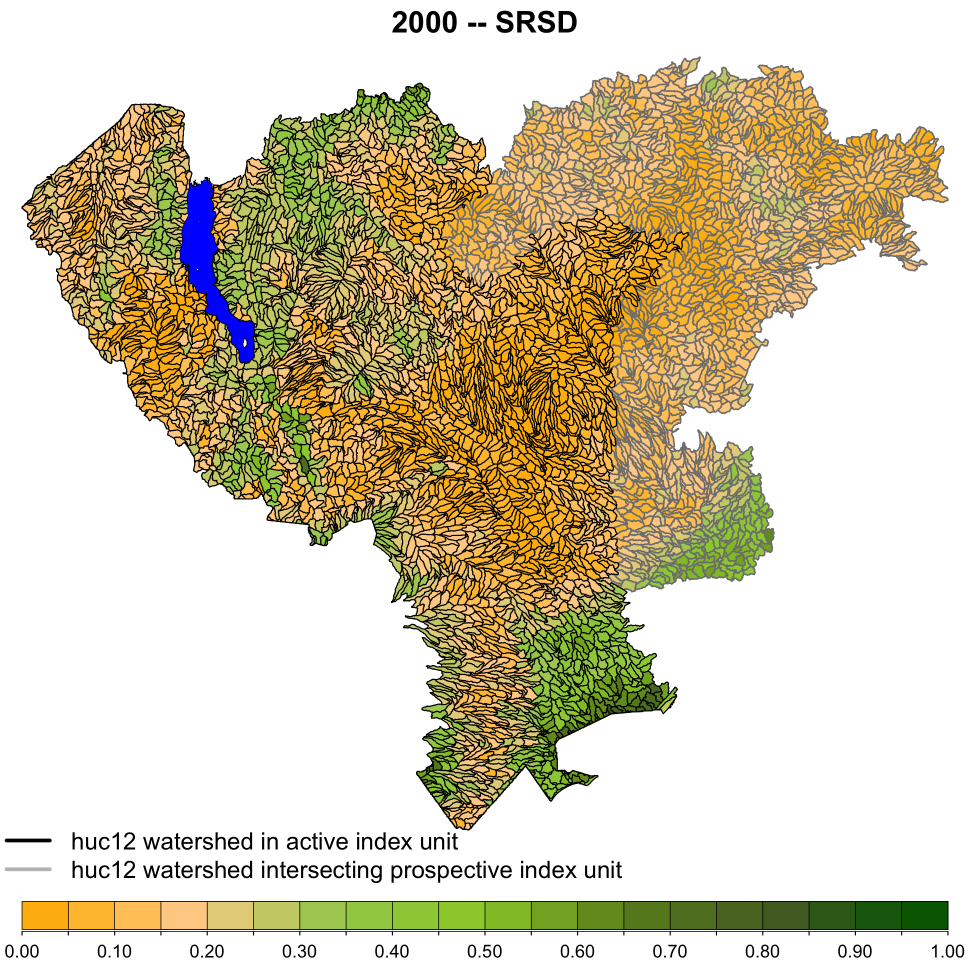


Figure B.2.4: Animation of the share of photosynthetic vegetation (PV) fractional cover at the HUC-12 level during the SRSD of each year for 'all' rangelands over 2000 - 2020. Note that Adobe acrobat reader may be required to view the full animation as intended.

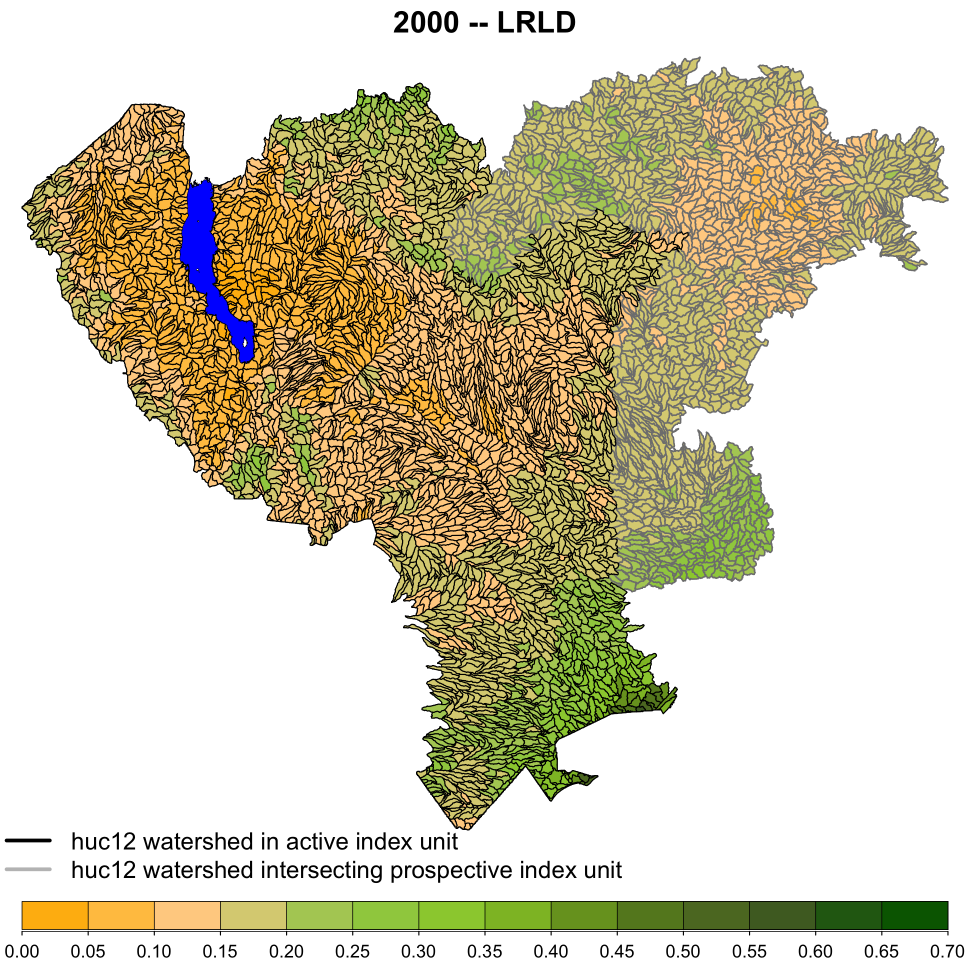


Figure B.2.5: Animation of average enhanced vegetation index (EVI) at the HUC-12 level by season and year for 'all' rangelands over 2000 - 2020. Note that Adobe acrobat reader may be required to view the full animation as intended.

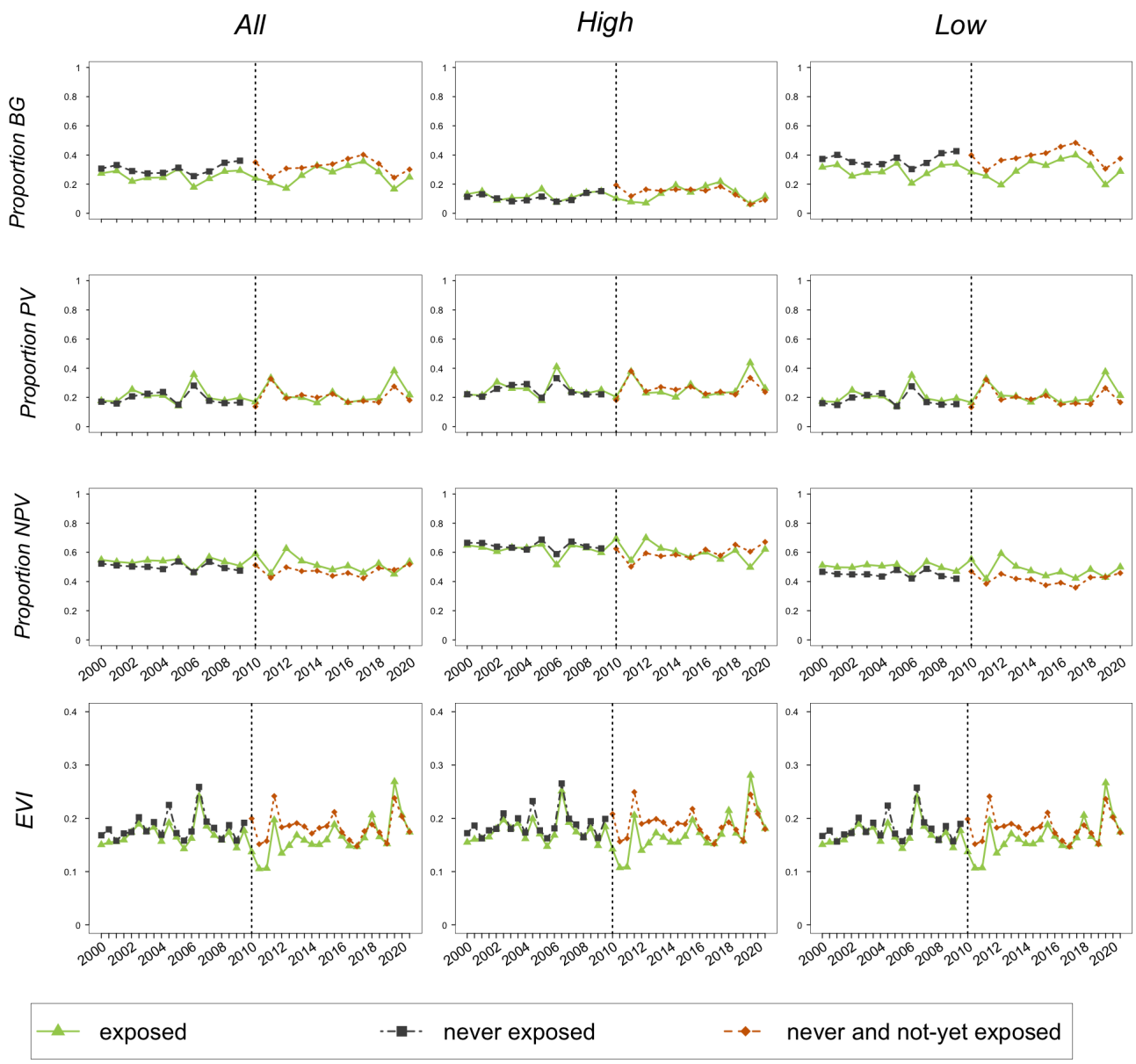


Figure B.2.6: Extensive margin conditional trends in RH indicator measures at the HUC-12 level; exposure is defined as having ≥ 1 cumulative TLU insured. Vertical dashed lines indicate when IBLI launched in 2010. RH indicators and values are captured on the vertical axes and time and variation by rangeland mask are featured along the horizontal axes (BG = bare ground, PV = photosynthetic vegetation, NPV = non-photosynthetic vegetation, EVI = enhanced vegetation index). Prior to exposure, comparison groups are fixed: the 'exposed' group includes any unit that is ever exposed; the 'never exposed' group includes never treated units only. For time periods including and following the vertical line, comparison groups vary each period per staggered exposure: the 'exposed' group is updated each period; and the 'never and not-yet exposed' group includes units in the 'never exposed' group and units that aren't yet exposed.

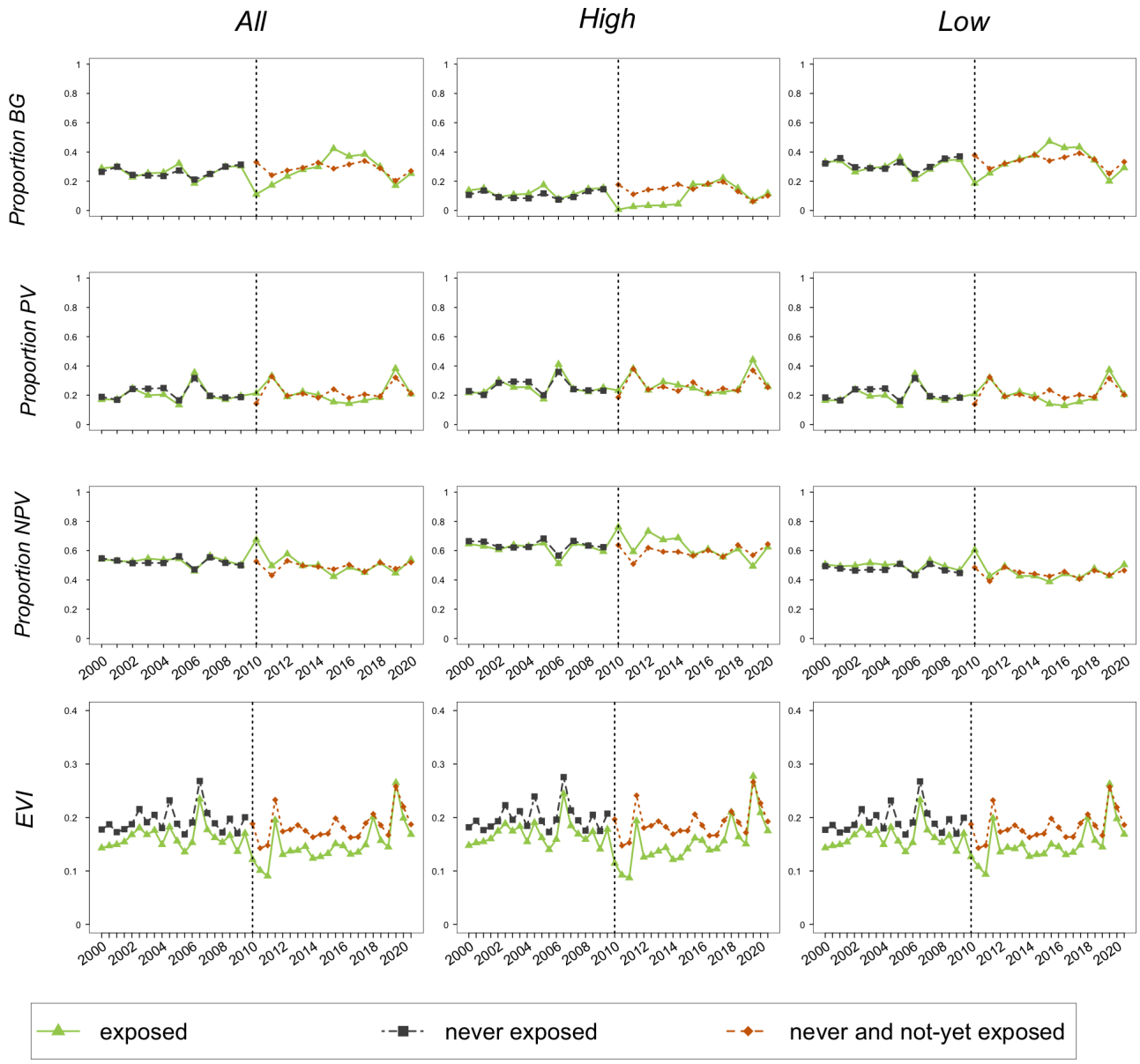


Figure B.2.7: Intensive margin conditional trends in RH indicator measures at the HUC-12 level; exposure is defined as having $\geq$ 500 cumulative TLU insured. Vertical dashed lines indicate when the first HUC-12 units were exposed to $\geq$ 500 cumulative TLUs insured in 2010. RH indicators and values are captured on the vertical axes and time and variation by rangeland mask are featured along the horizontal axes (BG = bare ground, PV = photosynthetic vegetation, NPV = non-photosynthetic vegetation, EVI = enhanced vegetation index). Prior to exposure, comparison groups are fixed: the 'exposed' group includes any unit that is ever exposed; the 'never exposed' group includes never treated units only. For time periods including and following the vertical line, comparison groups vary each period per staggered exposure: the 'exposed' group is updated each period; and the 'never and not-yet exposed' group includes units in the 'never exposed' group and units that aren't yet exposed.

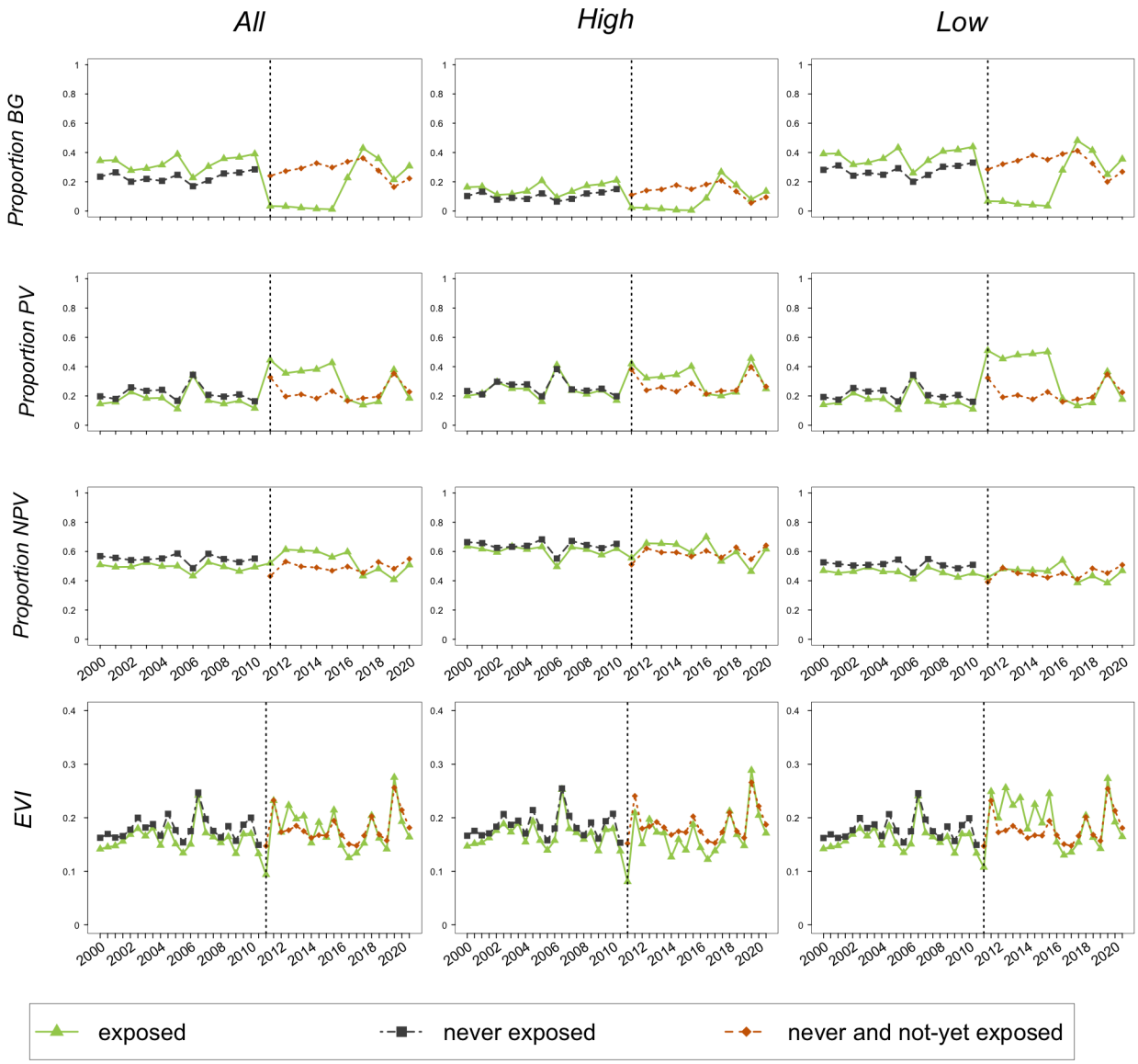


Figure B.2.8: Intensive margin conditional trends in RH indicator measures at the HUC-12 level; exposure is defined as having $\geq$ 2000 cumulative TLU insured. Vertical dashed lines indicate when the first HUC-12 units were exposed to $\geq$ 2000 cumulative TLUs insured in 2011. RH indicators and values are captured on the vertical axes and time and variation by rangeland mask are featured along the horizontal axes (BG = bare ground, PV = photosynthetic vegetation, NPV = non-photosynthetic vegetation, EVI = enhanced vegetation index). Prior to exposure, comparison groups are fixed: the 'exposed' group includes any unit that is ever exposed; the 'never exposed' group includes never treated units only. For time periods including and following the vertical line, comparison groups vary each period per staggered exposure: the 'exposed' group is updated each period; and the 'never and not-yet exposed' group includes units in the 'never exposed' group and units that aren't yet exposed.

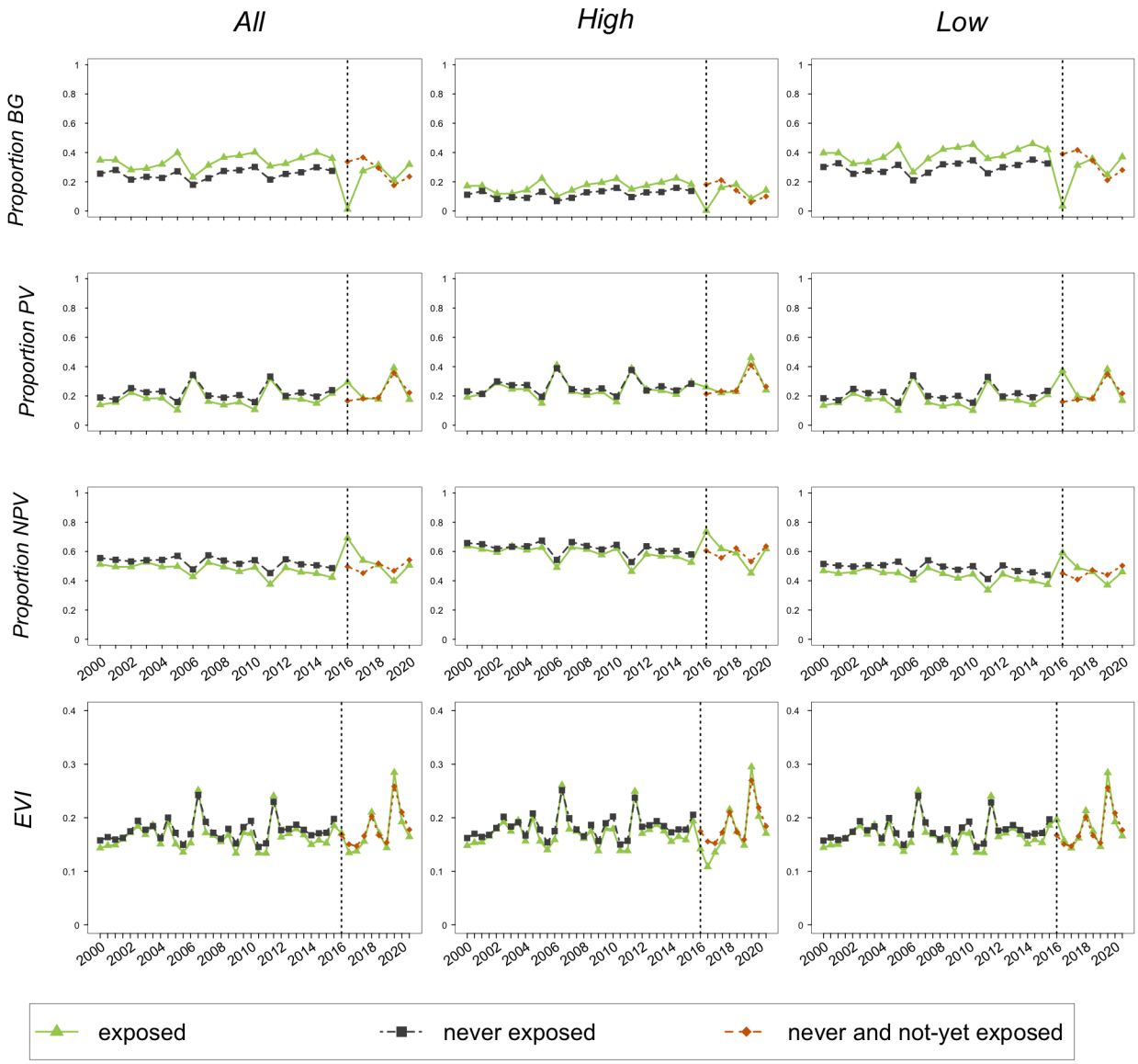


Figure B.2.9: Intensive margin conditional trends in RH indicator measures at the HUC-12 level; exposure is defined as having $\geq$ 3000 cumulative TLU insured. Vertical dashed lines indicate when the first HUC-12 units were exposed to $\geq$ 3000 cumulative TLUs insured in 2016. RH indicators and values are captured on the vertical axes and time and variation by rangeland mask are featured along the horizontal axes (BG = bare ground, PV = photosynthetic vegetation, NPV = non-photosynthetic vegetation, EVI = enhanced vegetation index). Prior to exposure, comparison groups are fixed: the 'exposed' group includes any unit that is ever exposed; the 'never exposed' group includes never treated units only. For time periods including and following the vertical line, comparison groups vary each period per staggered exposure: the 'exposed' group is updated each period; and the 'never and not-yet exposed' group includes units in the 'never exposed' group and units that aren't yet exposed.

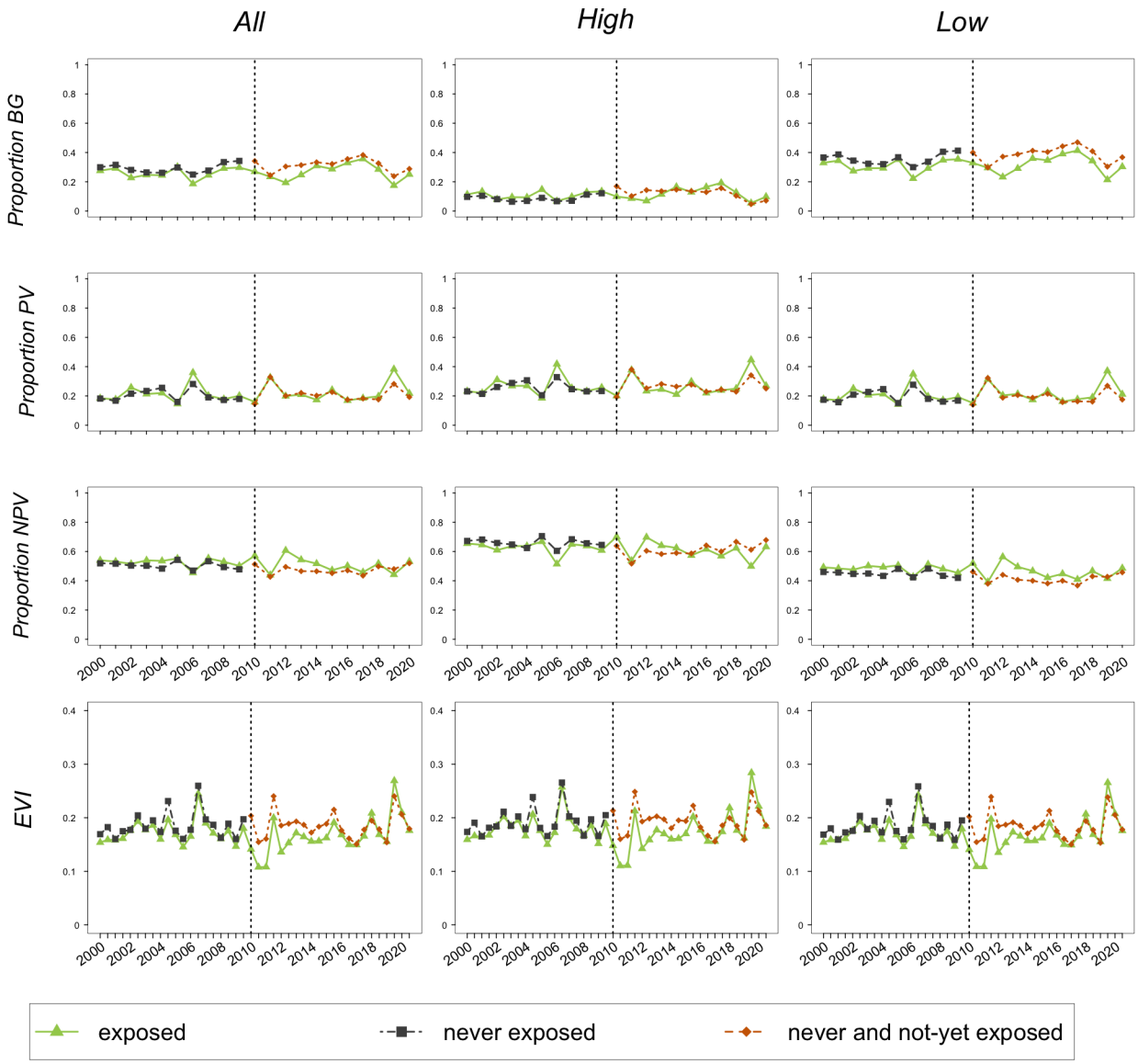


Figure B.2.10: Extensive margin conditional trends in RH indicator measures at the HUC-8 level; exposure is defined as having ≥ 1 cumulative TLU insured. Vertical dashed lines indicate when IBLI launched in 2010. RH indicators and values are captured on the vertical axes and time and variation by rangeland mask are featured along the horizontal axes (BG = bare ground, PV = photosynthetic vegetation, NPV = non-photosynthetic vegetation, EVI = enhanced vegetation index). Prior to exposure, comparison groups are fixed: the 'exposed' group includes any unit that is ever exposed; the 'never exposed' group includes never treated units only. For time periods including and following the vertical line, comparison groups vary each period per staggered exposure: the 'exposed' group is updated each period; and the 'never and not-yet exposed' group includes units in the 'never exposed' group and units that aren't yet exposed.

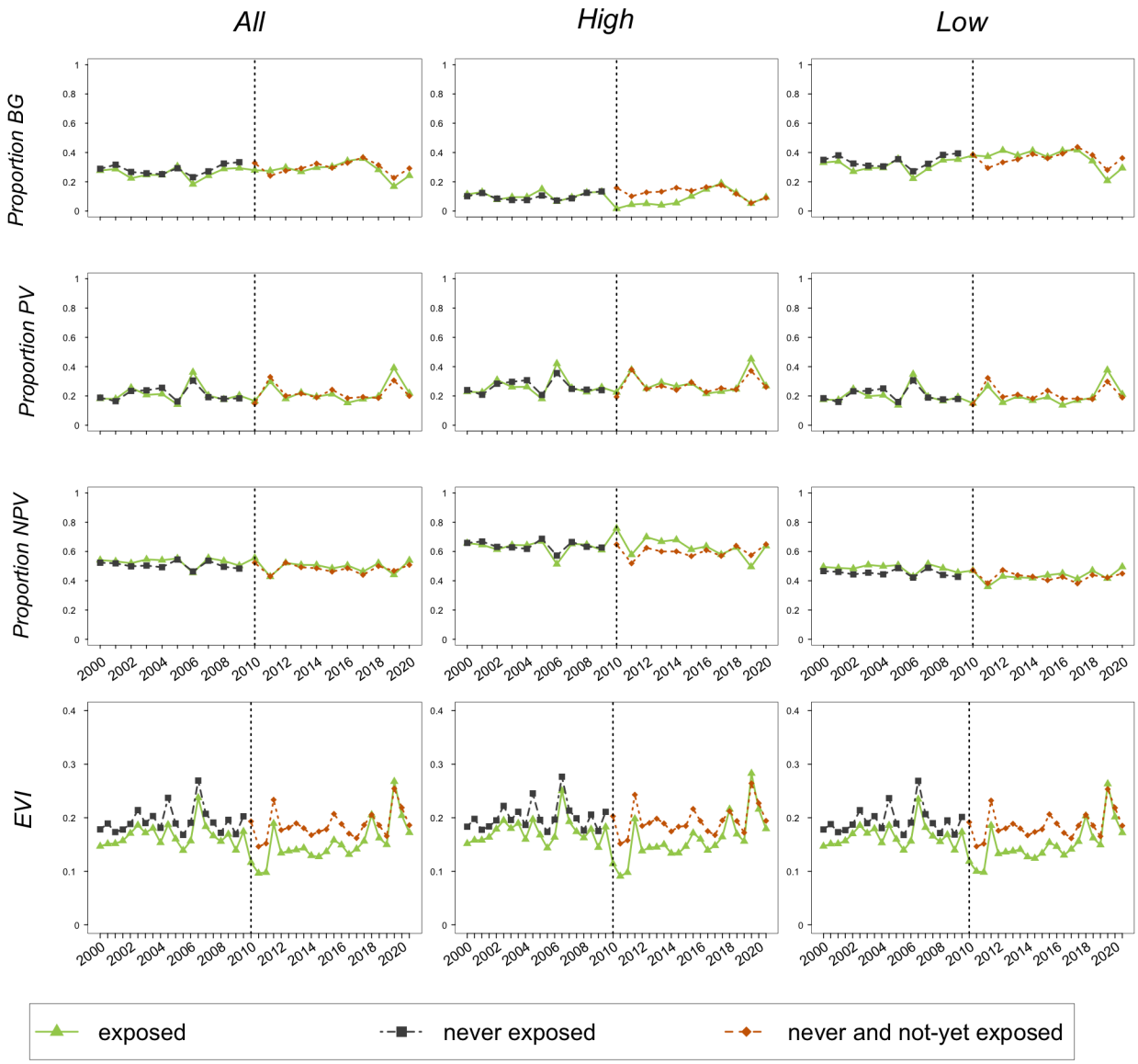


Figure B.2.11: Intensive margin conditional trends in RH indicator measures at the HUC-8 level; exposure is defined as having $\geq$ 500 cumulative TLU insured. Vertical dashed lines indicate when the first HUC-8 units were exposed to $\geq$ 500 cumulative TLUs insured in 2010. RH indicators and values are captured on the vertical axes and time and variation by rangeland mask are featured along the horizontal axes (BG = bare ground, PV = photosynthetic vegetation, NPV = non-photosynthetic vegetation, EVI = enhanced vegetation index). Prior to exposure, comparison groups are fixed: the 'exposed' group includes any unit that is ever exposed; the 'never exposed' group includes never treated units only. For time periods including and following the vertical line, comparison groups vary each period per staggered exposure: the 'exposed' group is updated each period; and the 'never and not-yet exposed' group includes units in the 'never exposed' group and units that aren't yet exposed.

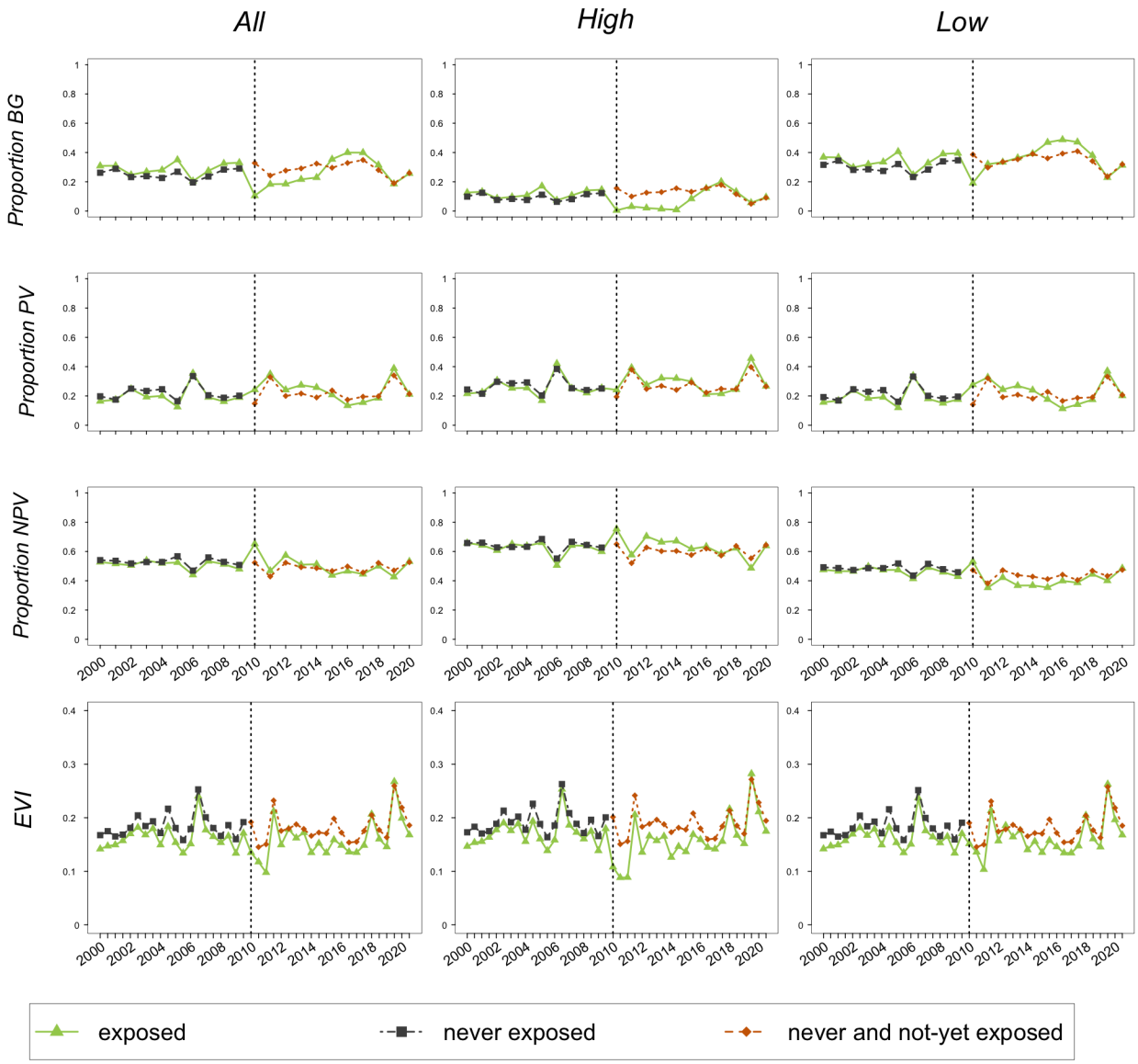


Figure B.2.12: Intensive margin conditional trends in RH indicator measures at the HUC-8 level; exposure is defined as having $\geq$ 2000 cumulative TLU insured. Vertical dashed lines indicate when the first HUC-8 units were exposed to $\geq$ 2000 cumulative TLUs insured in 2010. RH indicators and values are captured on the vertical axes and time and variation by rangeland mask are featured along the horizontal axes (BG = bare ground, PV = photosynthetic vegetation, NPV = non-photosynthetic vegetation, EVI = enhanced vegetation index). Prior to exposure, comparison groups are fixed: the 'exposed' group includes any unit that is ever exposed; the 'never exposed' group includes never treated units only. For time periods including and following the vertical line, comparison groups vary each period per staggered exposure: the 'exposed' group is updated each period; and the 'never and not-yet exposed' group includes units in the 'never exposed' group and units that aren't yet exposed.

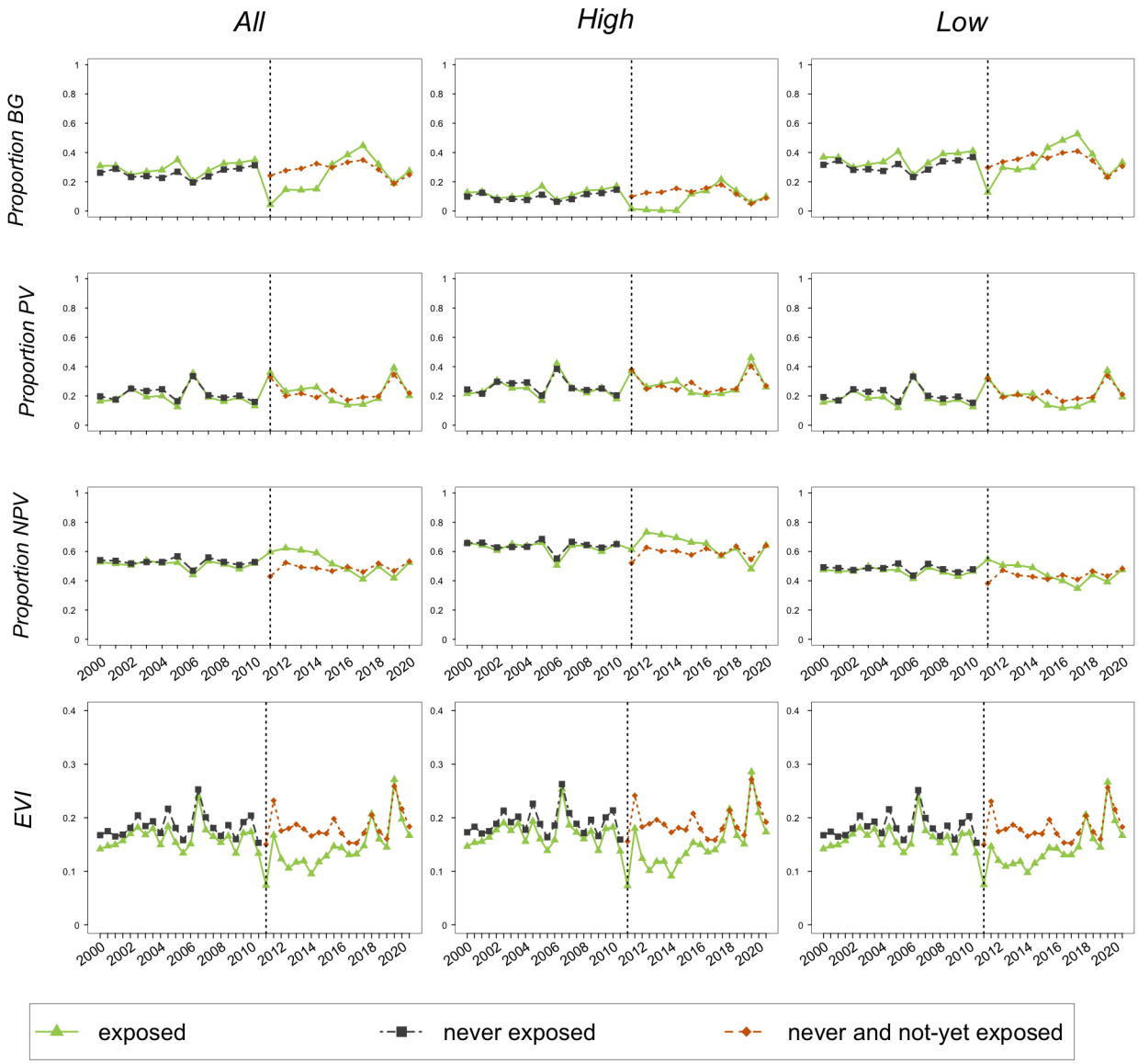


Figure B.2.13: Intensive margin conditional trends in RH indicator measures at the HUC-8 level; exposure is defined as having $\geq$ 3000 cumulative TLU insured. Vertical dashed lines indicate when the first HUC-8 units were exposed to $\geq$ 3000 cumulative TLUs insured in 2011. RH indicators and values are captured on the vertical axes and time and variation by rangeland mask are featured along the horizontal axes (BG = bare ground, PV = photosynthetic vegetation, NPV = non-photosynthetic vegetation, EVI = enhanced vegetation index). Prior to exposure, comparison groups are fixed: the 'exposed' group includes any unit that is ever exposed; the 'never exposed' group includes never treated units only. For time periods including and following the vertical line, comparison groups vary each period per staggered exposure: the 'exposed' group is updated each period; and the 'never and not-yet exposed' group includes units in the 'never exposed' group and units that aren't yet exposed.

C Two-Way Fixed Effects DiD and DiD Diagnostics

Although we will ultimately use more sophisticated staggered DiD estimators, we illustrate the problem initially with a standard two-way fixed effects (TWFE) specification:

$$Y_{i,r,s,t} = D_{ist}\delta + \mathbf{X}'_{\mathbf{i,s,t}}\alpha + \gamma_i + \sigma_t + \nu_{i,r,s,t} \tag{C.1}$$

where δ captures the average effect of the IBLI exposure dummy variable D_{ist} for areal unit i in rangeland type r in season s and IBLI-year t on RH indicator Y.[2] The vector $\mathbf{X}'$ includes measures of average precipitation or precipitation variability and binned hours of temperature exposure, and γ_i and σ_t represent unit and time fixed effects, respectively. Our construction of D_{ist} assumes regular movement of herders across rangeland types such that once a spatial unit is exposed to IBLI, all rangeland types within that unit are exposed. Construction of D_{ist} also assumes herders' movements across unit boundaries as modeled using IDW (see Section 2.3 and Appendix 2). Since weather processes are more smooth over space than rangeland type variation r we rely on weather realizations summarized across the entirety of each unit i in periods s and t.

We implement two sets of tests for the appropriateness of TWFE for DiD estimation suggested by Jakiela (2021). First, we residualize D_{ist} by regressing it on time and location fixed effects. We then study the distributions of residualized D_{ist} by exposed and comparison (not-yet or never exposed) groups, to check for negative weights among the exposed group. Second, we employ optimal binscatter methods from Cattaneo et al. (2024b) to semi-parametrically regress residualized outcomes Y against residualized D and apply formal tests of the null hypothesis for treatment effect homogeneity, which implies a linear relationship between residualized Y and D.

A set of example TWFE results using equation (C.1) are provided in Table C.1 below. These results should be interpreted cautiously because the aforementioned tests suggest TWFE is in appropriate in this setting. Specifically, Figures C.1 and C.2 present evidence for the presence of negative weights and the aforementioned optimal binscatter tests reject the assumption of treatment effect homogeneity(see Figures C.3 - C.5 and Table C.2). For these reasons, we rely on the staggered DiD estimator from Gardner et al. (2025).

[2] An 'IBLI-year' begins March 1. Thus our year 2010 reflects the first year of IBLI exposure, from March 1, 2010, through February 28, 2011.

Table C.1: Example two-way fixed effects DiD specifications studying variation from all rangelands at the HUC-12 level and extensive margin IBLI exposure.

	Dependent variable: Bare ground (BG) share all rangelands				
Post-IBLI extensive margin (dummy)	-0.024^{***}	0.020^{***}	0.004^{***}	0.016^{***}	0.016^{***}
	(0.002)	(0.001)	(0.001)	(0.001)	(0.003)
Adjusted R^2	0.167	0.923	0.933	0.943	0.943
	Dependent variable: Photosynthetic vegetation (PV) share all rangelands				
Post-IBLI extensive margin (dummy)	-0.006^{***}	-0.005^{***}	-0.002^{***}	-0.016^{***}	-0.016^{***}
	(0.001)	(0.001)	(0.001)	(0.001)	(0.003)
Adjusted R^2	0.422	0.810	0.827	0.833	0.833
	Dependent variable: Non-photosynthetic vegetation (NPV) share all rangelands				
Post-IBLI extensive margin (dummy)	0.030^{***}	-0.015^{***}	-0.002^{**}	0.0002	0.0002
	(0.002)	(0.001)	(0.001)	(0.001)	(0.004)
Adjusted R^2	0.149	0.883	0.893	0.901	0.901
Fractional cover model parameters:					
Unit FEs	N	Y	Y	Y	Y
Year FEs	N	N	Y	Y	Y
Unit specific linear trends	N	N	N	Y	Y
Standard errors	HW	HW	HUC	HUC	IU
Observations	99,426	99,426	99,426	99,426	99,426
	Dependent variable: Mean enhanced vegetation index (EVI) all rangelands				
Post-IBLI extensive margin (dummy)	-0.017^{***}	-0.002^{***}	0.002^{***}	-0.003^{***}	-0.003^{**}
	(0.0003)	(0.0002)	(0.0003)	(0.0003)	(0.001)
Adjusted R^2	0.570	0.852	0.884	0.891	0.891
Vegetation index model parameters:					
Unit FEs	N	Y	Y	Y	Y
Period FEs	N	N	Y	Y	Y
Unit specific linear trends	N	N	N	Y	Y
Standard errors	HW	HW	HUC	HUC	IU
Observations	199,416	199,416	199,416	199,416	199,416

Note: Extensive margin exposure is defined as ≥ 1 cumulative TLU insured. Fractional cover models have SRSD variation and EVI models have semi-annual variation in the LRLD and SRSD seasons. All models include average precipitation, the standard deviation of precipitation, and 5° temperature bins, with the exception of 10° bins at the upper and lower ends due to limited exposure at the lowest and highest 5 degree bins (i.e., 5 -15° C, and 35-45° C). Standard errors vary from robust Huber-White to clustered at the HUC-level or index unit (IU) level. $^{*}p<0.1$; $^{**}p<0.05$; $^{***}p<0.01$.

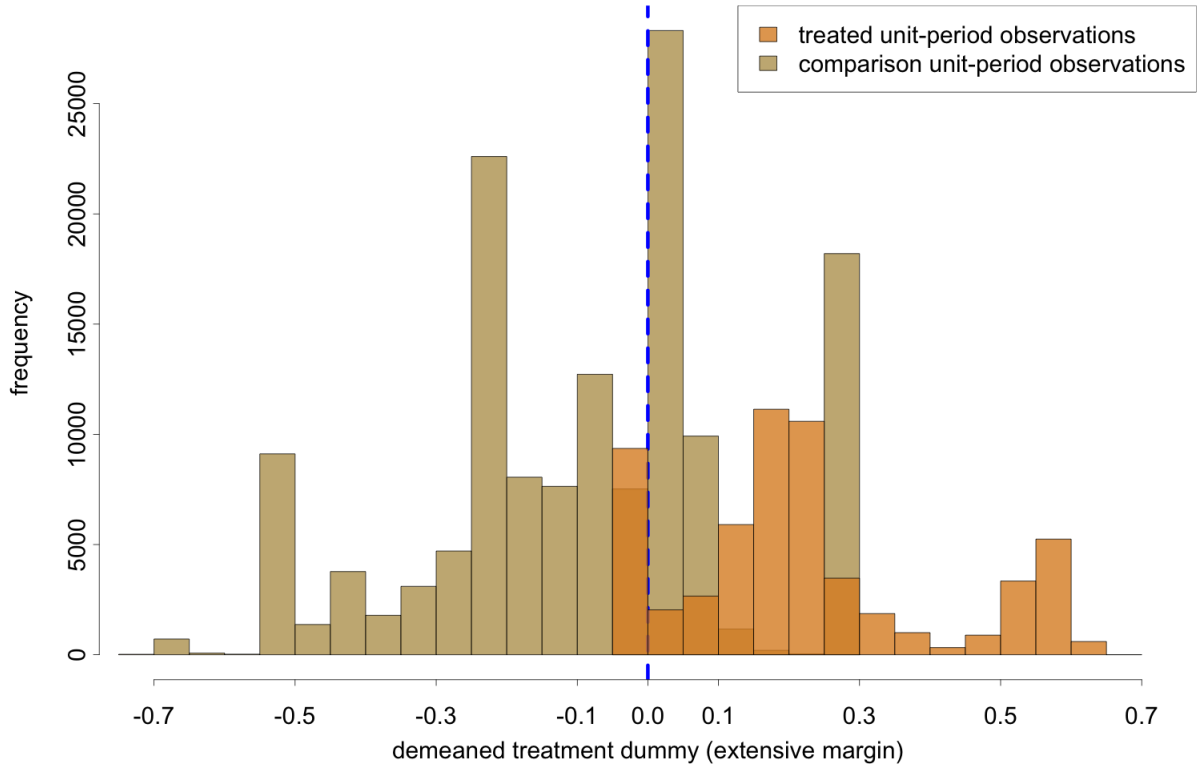


Figure C.1: Distribution of residualized treatment dummy D at the HUC-12 level from two-way fixed effects estimation focused on extensive margin exposure following Jakiela (2021). Extensive margin exposure is defined as ≥ 1 cumulative TLU insured by IBLI.

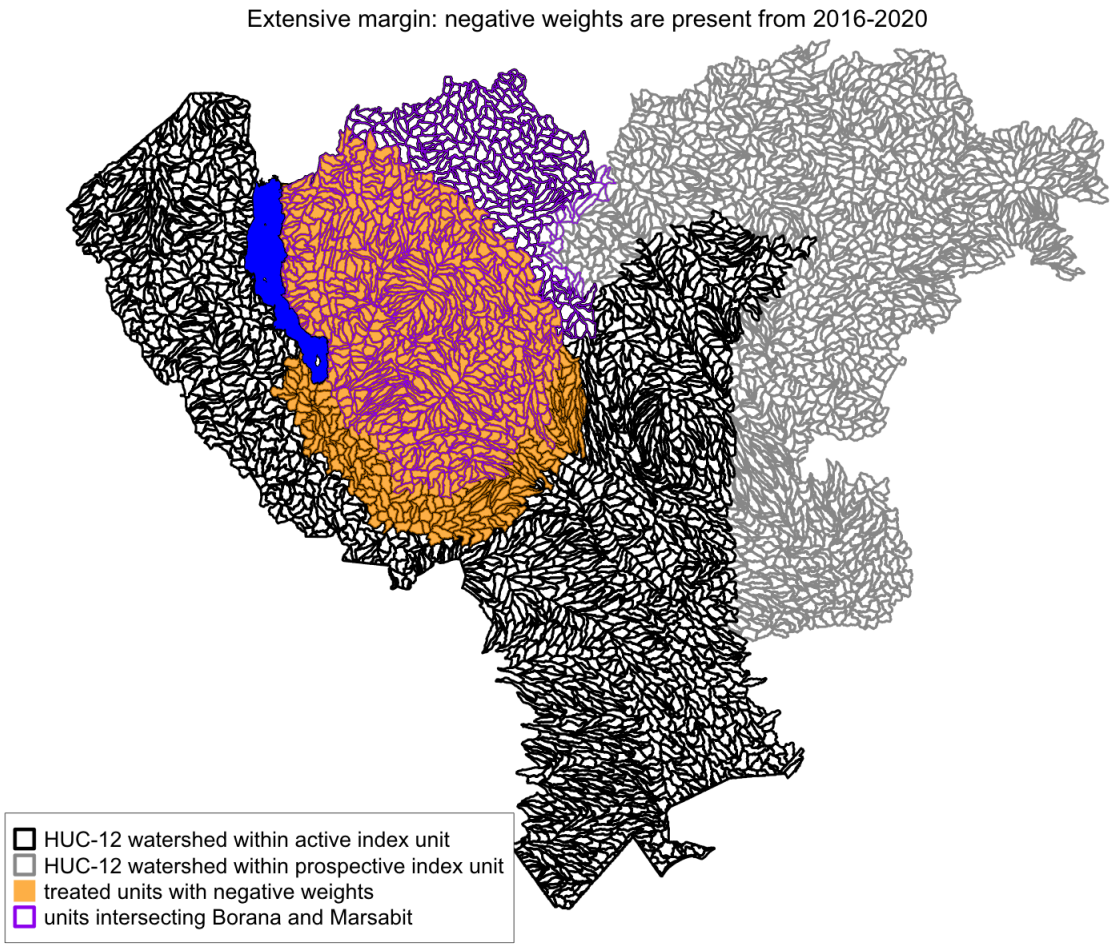


Figure C.2: Spatial distribution of negative weights present in later periods (2016-2020) at the HUC-12 level. Negative weights are identified from studying the distribution of residualized treatment dummy D at the HUC-12 level from two-way fixed effects estimation focused on extensive margin exposure following Jakiela (2021). Extensive margin exposure is defined as ≥ 1 cumulative TLU insured by IBLI.

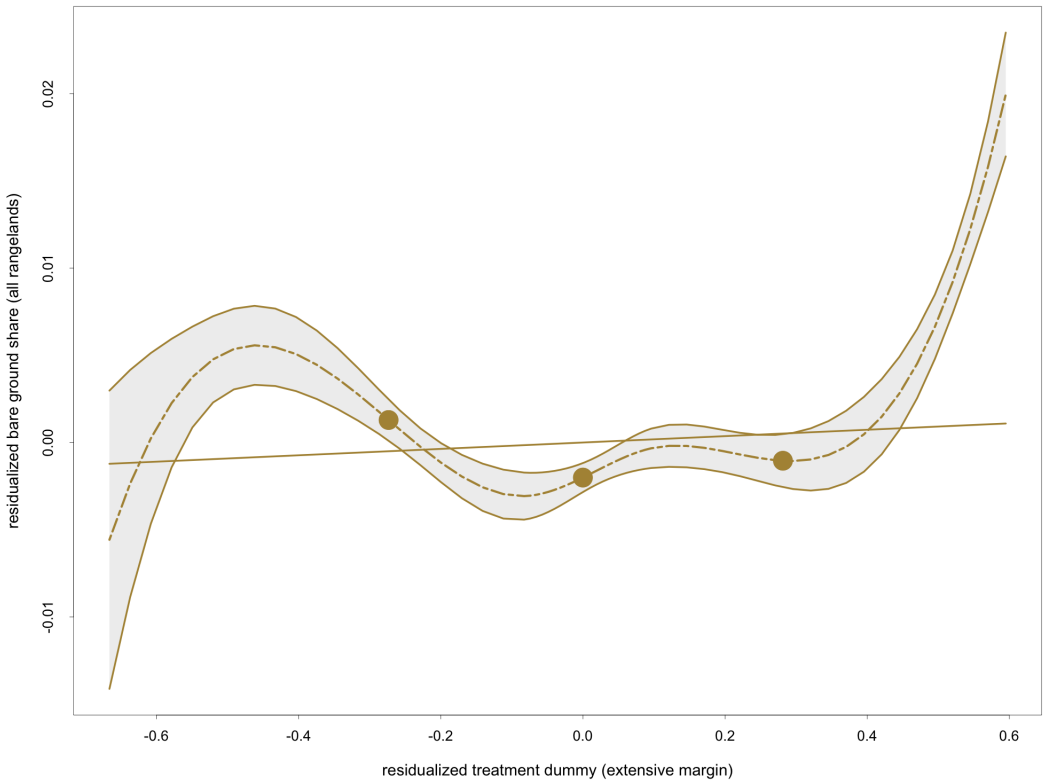


Figure C.3: Optimal binscatter of residualized bare ground (BG) share on the semi-parametric function $\mu(D)$, where D is a residualized treatment dummy reflecting extensive margin exposure defined as ≥ 1 cumulative TLU insured, with a contrasting linear fit. Estimation is motivated by tests suggested by Jakiela (2021) for the linearity of the treatment effect. Estimations employ the integrated mean squared error (IMSE)-optimal direct plug-in rule for bin selection and cubic B-splines within and between bins. Points reflect the mean within bins for unexposed and exposed units, which are quantile-spaced. Confidence bands are clustered at the index unit level. See Cattaneo et al. 2024b for details on optimal binscatter estimation.

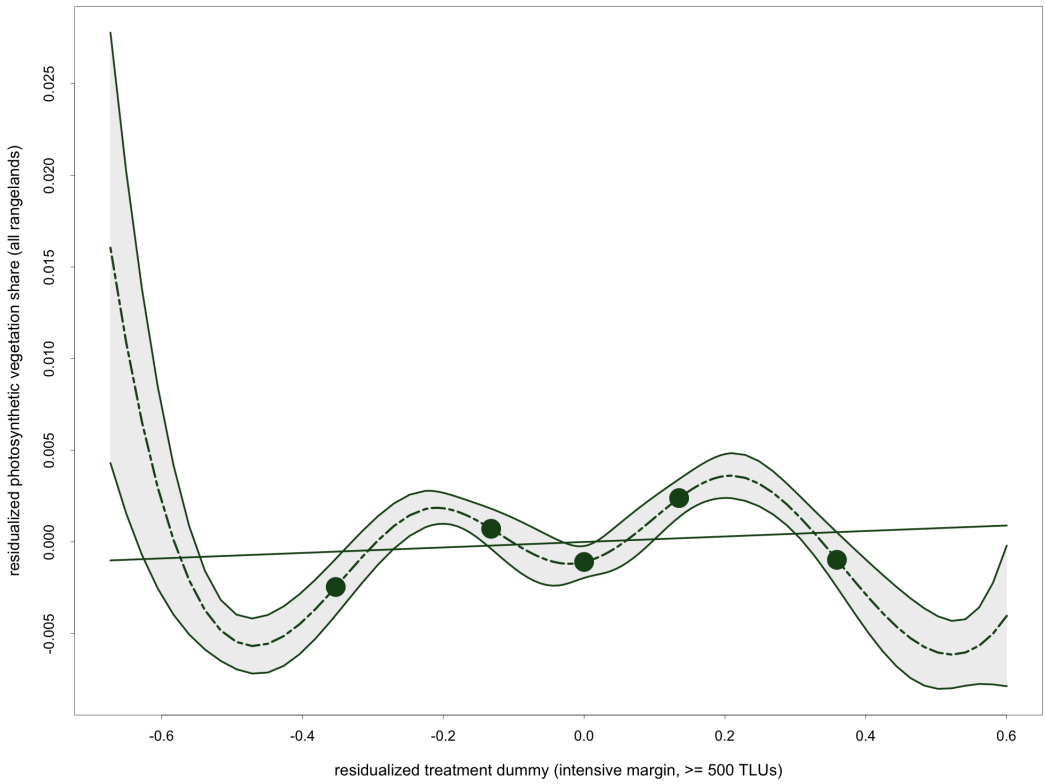


Figure C.4: Optimal binscatter of residualized photosynthetic vegetation (PV) share on the semi-parametric function $\mu(D)$, where D is a residualized treatment dummy reflecting extensive margin exposure defined as ≥ 1 cumulative TLU insured, with a contrasting linear fit. Estimation is motivated by tests suggested by Jakiela (2021) for the linearity of the treatment effect. Estimations employ the integrated mean squared error (IMSE)-optimal direct plug-in rule for bin selection and cubic B-splines within and between bins. Points reflect the mean within bins for unexposed and exposed units, which are quantile-spaced. Confidence bands are clustered at the index unit level. See Cattaneo et al. 2024b for details on optimal binscatter estimation.

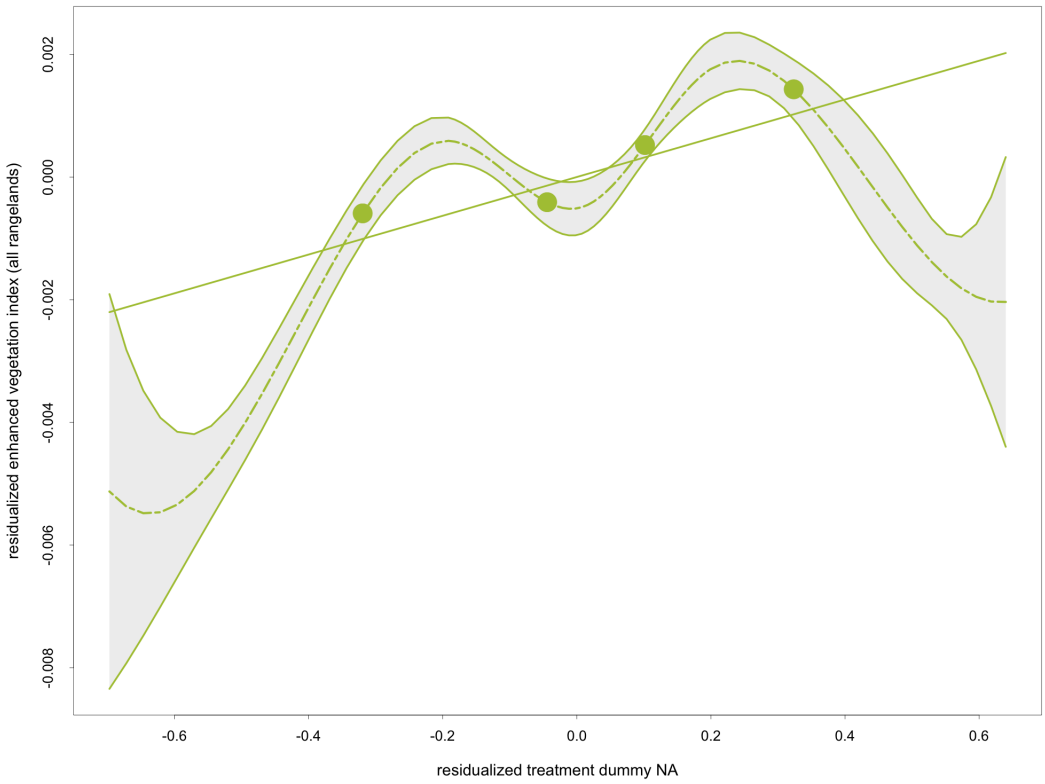


Figure C.5: Optimal binscatter of residualized average enhanced vegetation index (EVI) on the semi-parametric function $\mu(D)$, where D is a residualized treatment dummy reflecting extensive margin exposure defined as ≥ 1 cumulative TLU insured, with a contrasting linear fit. Estimation is motivated by tests suggested by Jakiela (2021) for the linearity of the treatment effect. Estimations employ the integrated mean squared error (IMSE)-optimal direct plug-in rule for bin selection and cubic B-splines within and between bins. Points reflect the mean within bins for unexposed and exposed units, which are quantile-spaced. Confidence bands are clustered at the index unit level. See Cattaneo et al. 2024b for details on optimal binscatter estimation.

Table C.2: Optimal binscatter pair-wise tests of the plausibility of the assumption of treatment effect homogeneity at the HUC-12 level following Cattaneo et al. (2024b).

	Dependent variables:		
	BG share	PV share	EVI
t-statistic from H0: $\mu(D)_{exposed} = \mu(D)_{un-exposed}$	3.302	3.544	3.239
	(0.014)	(0.004)	(0.007)
J-unexposed	4	4	4
J-exposed	6	5	4
N clusters - unexposed	130	130	130
N clusters - exposed	126	126	126
N observations - unexposed	69718	69718	141065
N observations - exposed	29750	29750	58435

Note: This test determines if $\mu(D)$ for a treated group is the same as $\mu(D)$ for a control group. Respective tests stem from optimal binscatter estimations between residualized dependent variables listed above and residualized extensive margin exposed dummy D defined as ≥ 1 cumulative TLU insured following Jakiela (2021) for exposed and un-exposed subsets. P-values are in parentheses below t-statistics. J is the number of bins. N clusters is the total number of clusters, and observations for exposed and unexposed groups. Standard errors are clustered at the index unit level. Tests are implemented using the *binspwc* function in the *binsreg* R package Cattaneo et al. (2024a). $^{***}p < 0.01$; $^{**}p < 0.05$; $^{*}p < 0.1$.

D Staggered Differences-in-Differences

D.1 Extensive Margin Results

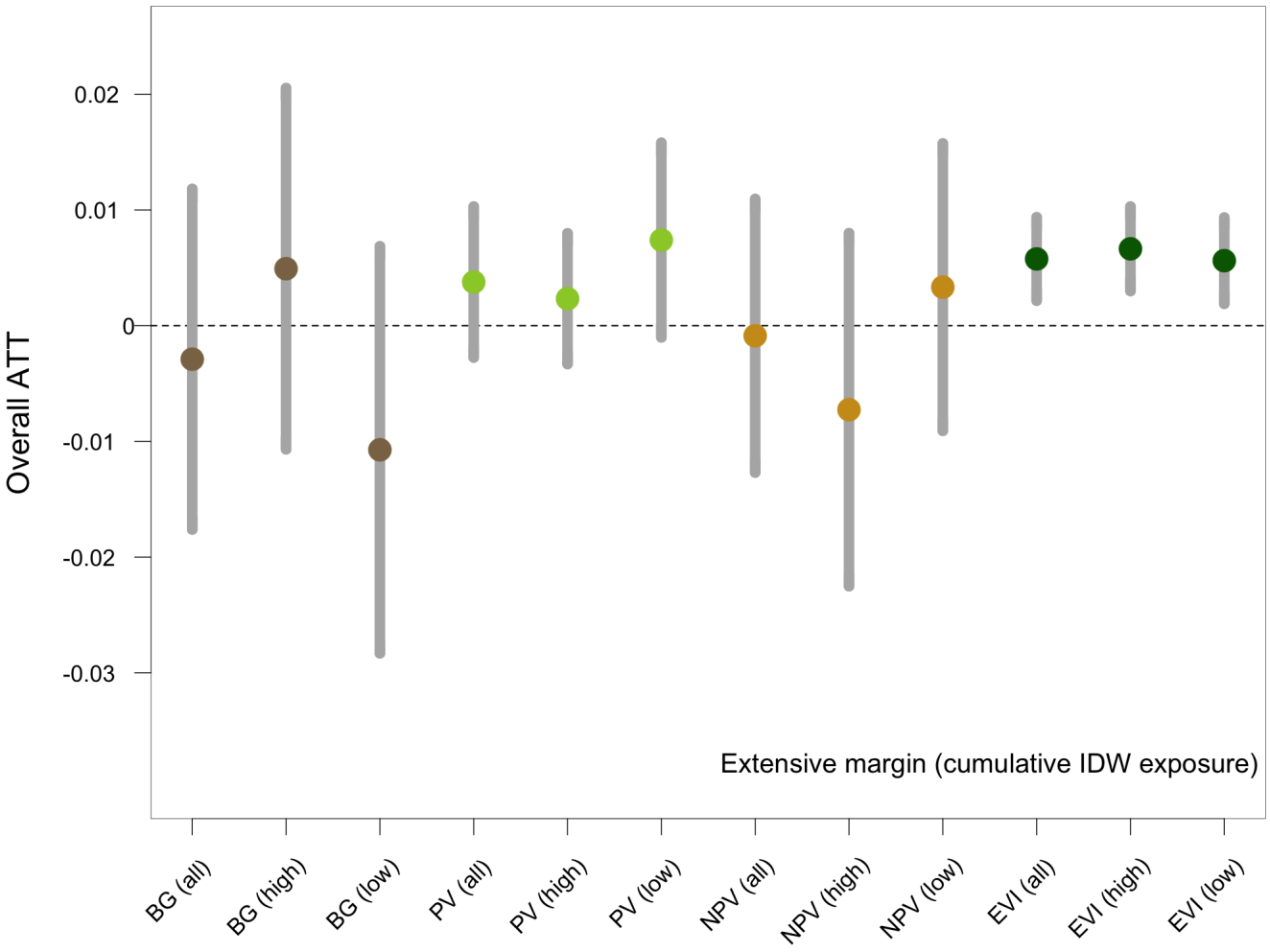


Figure D.1.1: Overall ATTs with 95% confidence intervals for tests of impacts at HUC-12 level from IBLI exposure at the extensive margin based on the sum of IDW exposure (≥ 1 TLU insured). ATTs reflect point estimates of β in equation (2) from Gardner et al. (2025). Standard errors are clustered at the index unit level. From left to right, estimated coefficients reflect IBLI's impacts on BG, PV, NPV and EVI within all, high, and low rangelands (see Section 3.3). The number of observations for respective estimations are: fractional cover all mask, $n = 99,426$; fractional cover high mask, $n = 98,373$; fractional cover low mask, $n = 99,361$; EVI all mask, $n = 199,416$; EVI high mask, $n = 196,474$; EVI low mask, $n = 199,280$. First stage covariates are the same across models and include: the mean and standard deviation of seasonal precipitation (mm), and mean GDD in 5° C bins with the exception of two 10° C bins from 5-10° C and 30-45° C due to limited exposure from 5-10° C and 35-40° C. Each model includes unit and period fixed effects.

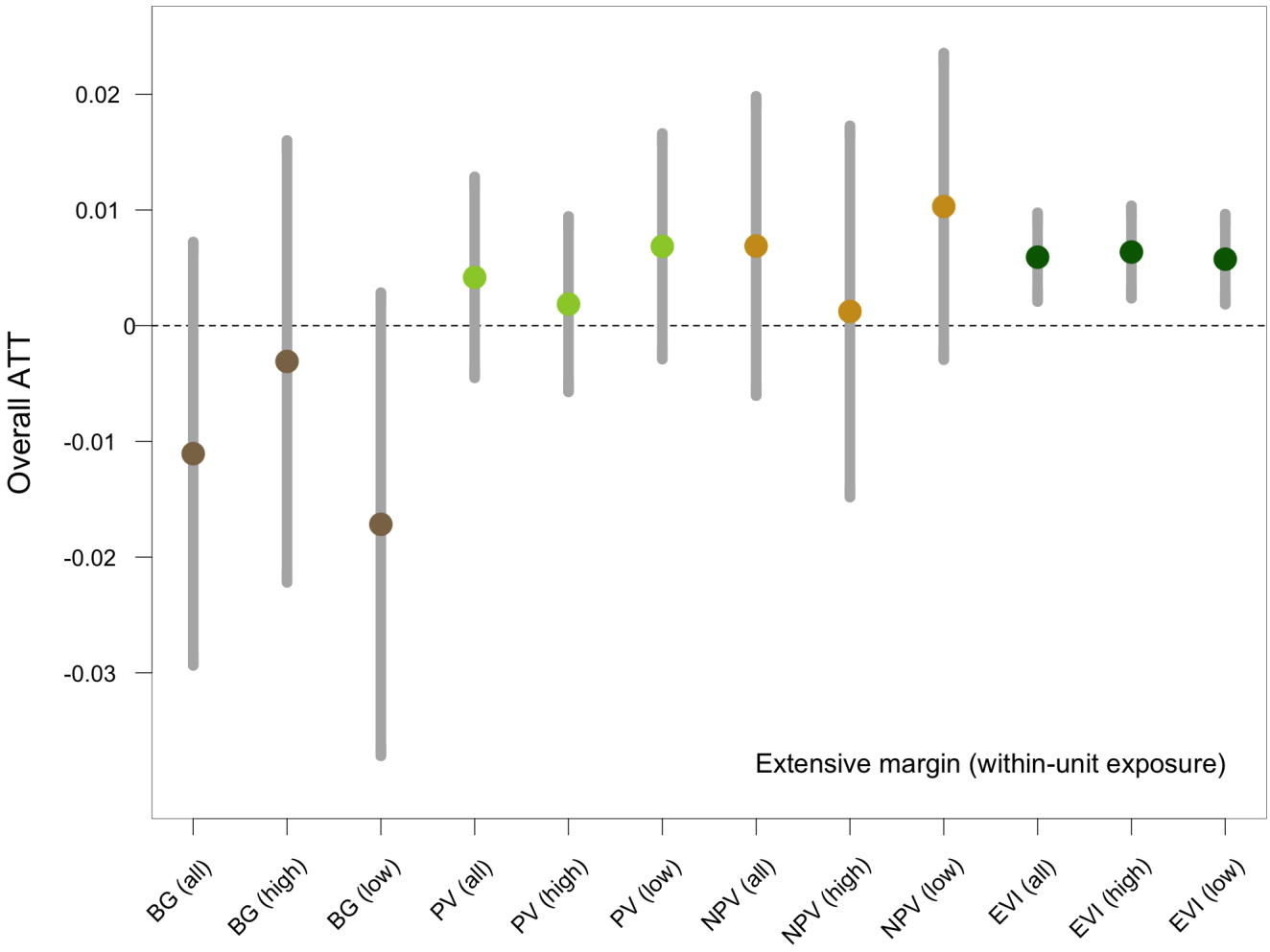


Figure D.1.2: Overall ATTs with 95% confidence intervals for tests of impacts at HUC-12 level from IBLI exposure at the extensive margin based on the sum of within unit exposure without inverse distance weighting ($\geq$ 1 TLU insured). ATTs reflect point estimates of β in equation (2) from Gardner et al. (2025). Standard errors are clustered at the index unit level. From left to right, estimated coefficients reflect IBLI's impacts on BG, PV, NPV and EVI within all, high, and low rangelands (see Section 3.3). The number of observations for respective estimations are: fractional cover all mask, $n = 99,426$; fractional cover high mask, $n = 98,373$; fractional cover low mask, $n = 99,361$; EVI all mask, $n = 199,416$; EVI high mask, $n = 196,474$; EVI low mask, $n = 199,280$. First stage covariates are the same across models and include: the mean and standard deviation of seasonal precipitation (mm), and mean GDD in 5° C bins with the exception of two 10° C bins from 5-10° C and 30-45° C due to limited exposure from 5-10° C and 35-40° C. Each model includes unit and period fixed effects.

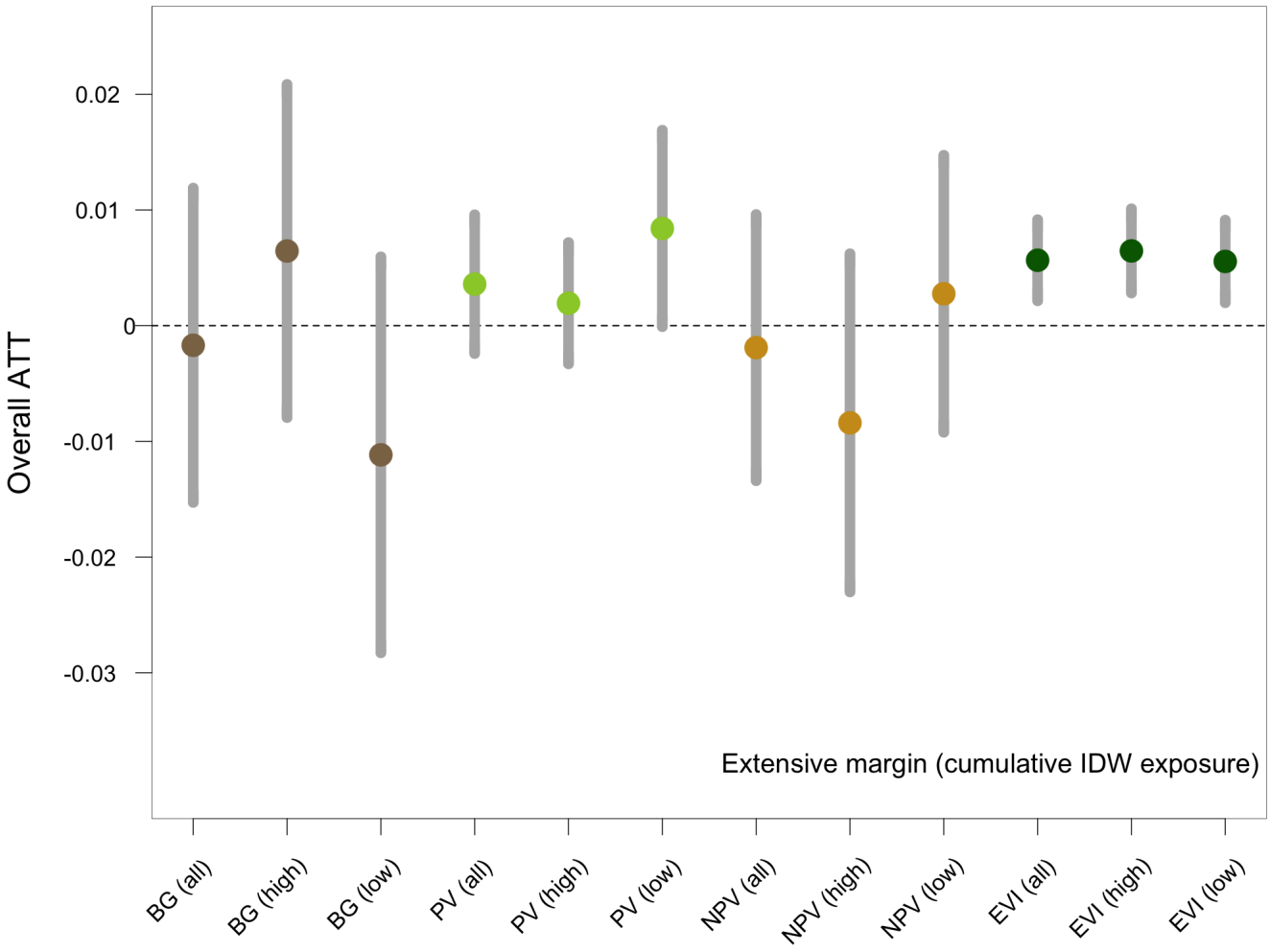


Figure D.1.3: Overall ATTs with 95% confidence intervals for tests of impacts at HUC-9 level from IBLI exposure at the extensive margin based on the sum of IDW exposure (≥ 1 TLU insured). ATTs reflect point estimates of β in equation (2) from Gardner et al. (2025). Standard errors are clustered at the index unit level. From left to right, estimated coefficients reflect IBLI's impacts on BG, PV, NPV and EVI within all, high, and low rangelands (see Section 3.3). The number of observations for respective estimations are: fractional cover all mask, $n = 48,953$; fractional cover high mask, $n = 48,520$; fractional cover low mask, $n = 48,922$; EVI all mask, $n = 98,154$; EVI high mask, $n = 97,012$; EVI low mask, $n = 98,102$. First stage covariates are the same across models and include: the mean and standard deviation of seasonal precipitation (mm), and mean GDD in 5° C bins with the exception of two 10° C bins from 5-10° C and 30-45° C due to limited exposure from 5-10° C and 35-40° C. Each model includes unit and period fixed effects.

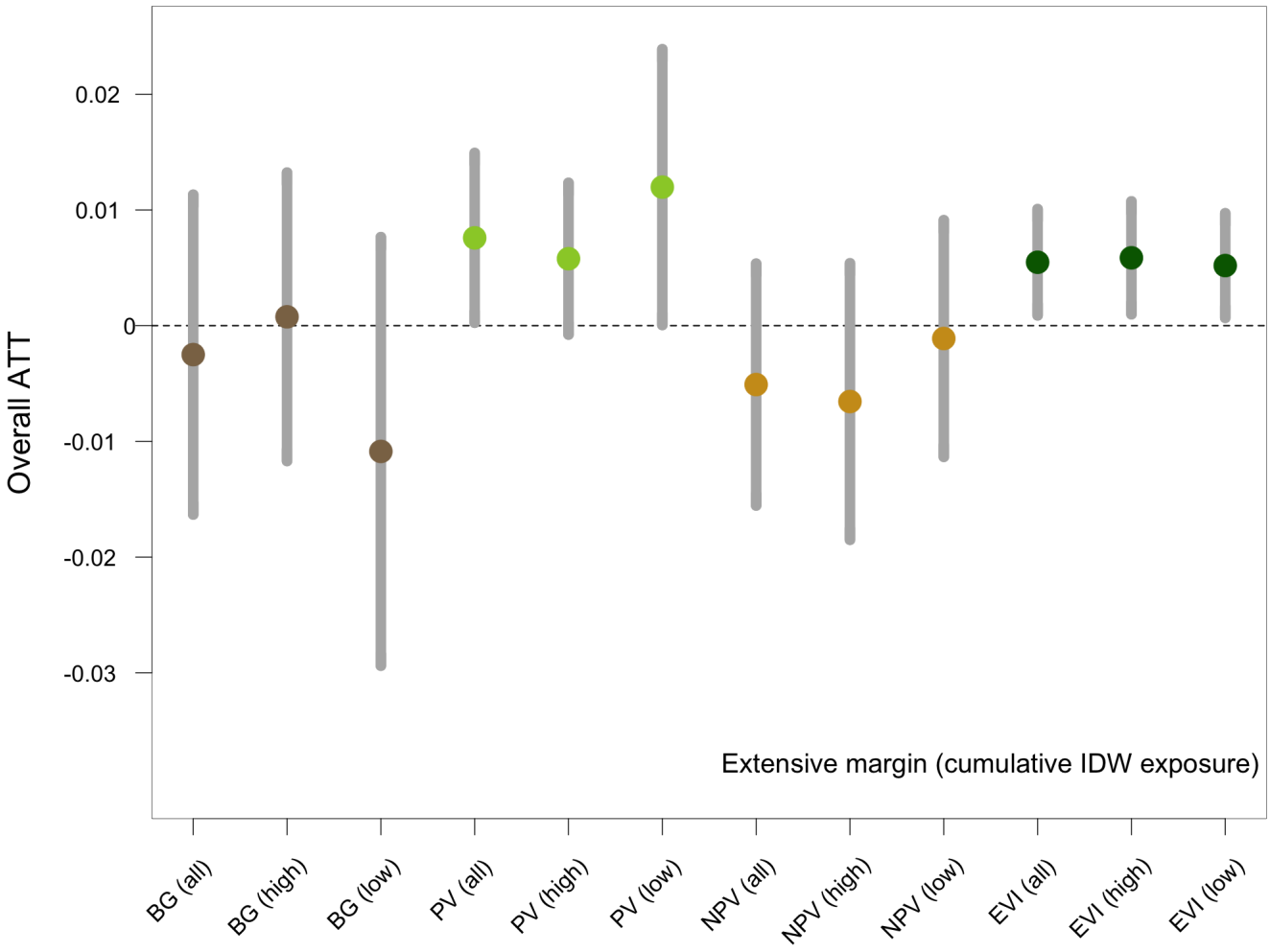


Figure D.1.4: Overall ATTs with 95% confidence intervals for tests of impacts at HUC-8 level from IBLI exposure at the extensive margin based on the sum of IDW exposure (≥ 1 TLU insured). ATTs reflect point estimates of β in equation (2) from Gardner et al. (2025). Standard errors are clustered at the index unit level. From left to right, estimated coefficients reflect IBLI's impacts on BG, PV, NPV and EVI within all, high, and low rangelands (see Section 3.3). The number of observations for respective estimations are: fractional cover all mask, $n = 18,221$; fractional cover high mask, $n = 18,095$; fractional cover low mask, $n = 18,215$; EVI all mask, $n = 36,498$; EVI high mask, $n = 36,246$; EVI low mask, $n = 36,488$. First stage covariates are the same across models and include: the mean and standard deviation of seasonal precipitation (mm), and mean GDD in 5° C bins with the exception of two 10° C bins from 5-10° C and 30-45° C due to limited exposure from 5-10° C and 35-40° C. Each model includes unit and period fixed effects.

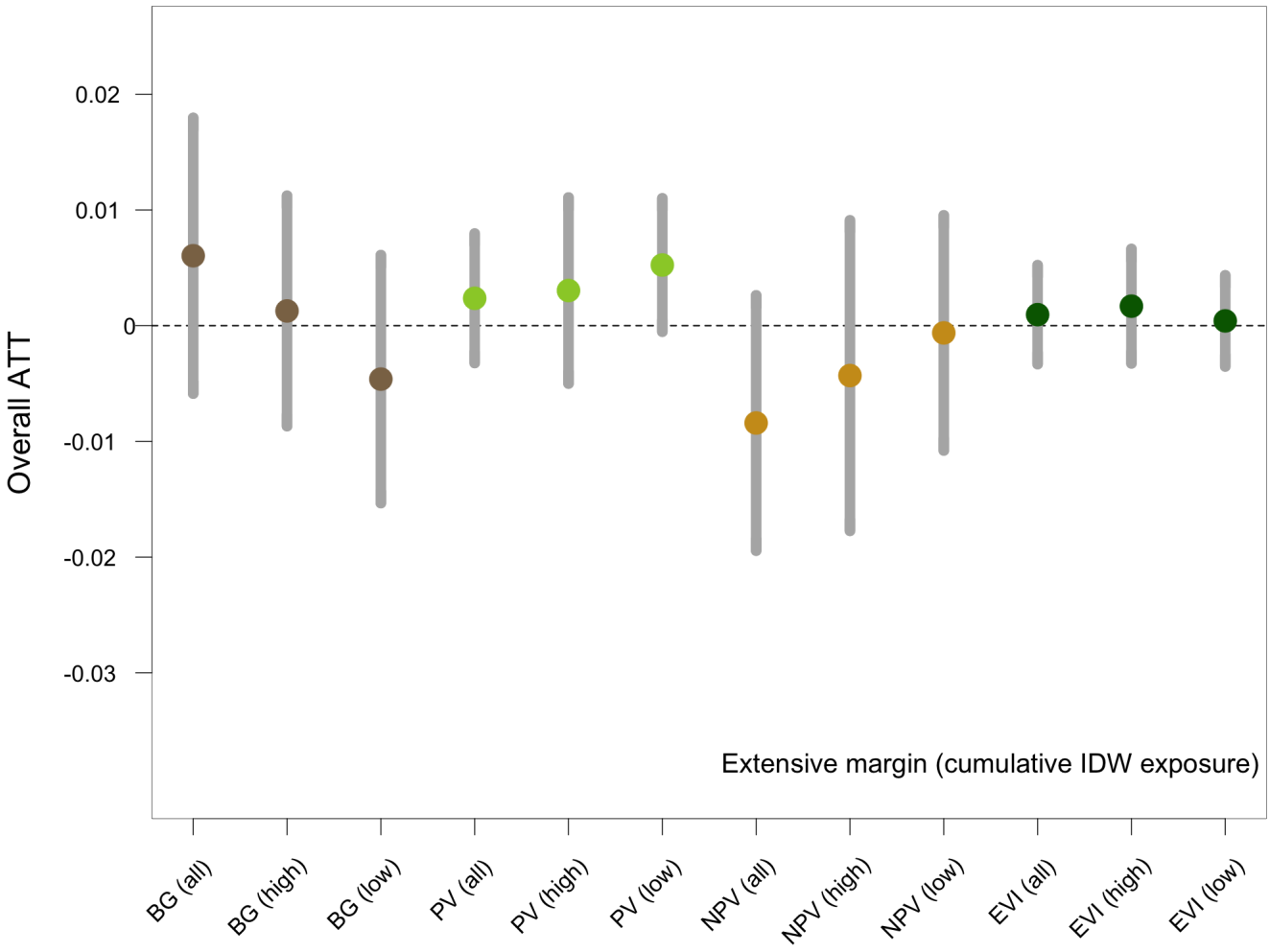


Figure D.1.5: Overall ATTs with 95% confidence intervals for tests of impacts at IU and CA level from IBLI exposure at the extensive margin based on the sum of IDW exposure ($\geq$ 1 TLU insured). ATTs reflect point estimates of β in equation (2) using from Gardner et al. (2025). Standard errors are clustered at the index unit level. From left to right, estimated coefficients reflect IBLI's impacts on BG, PV, NPV and EVI within all, high, and low rangelands (see Section 3.3). The number of observations for respective estimations are: fractional cover all mask, $n = 2,730$; fractional cover high mask, $n = 2,730$; fractional cover low mask, $n = 2,730$; EVI all mask, $n = 5,460$; EVI high mask, $n = 5,460$; EVI low mask, $n = 5,460$. First stage covariates are the same across models and include: the mean and standard deviation of seasonal precipitation (mm), and mean GDD in 5° C bins with the exception of two 10° C bins from 5-10° C and 30-45° C due to limited exposure from 5-10° C and 35-40° C. Each model includes unit and period fixed effects.

D.2 Intensive Margin Results

Table D.2.1: First stage results for the share of bare ground (BG) in all rangelands at the HUC-12 level (see corresponding second stage results in Table 1 of main text).

	Dependent variable: Bare ground (BG) share all rangelands			
Precipitation mean (mm)	-0.00026***	-0.00022***	-0.00024***	-0.00026***
	(0.00007)	(0.00003)	(0.00004)	(0.00004)
Precipitation stn. dev. (mm)	-0.00178***	0.00025*	0.00012	0.00037**
	(0.00068)	(0.00013)	(0.00013)	(0.00015)
GDD 5-15 C	0.00514***	-0.01179***	-0.01089***	-0.01103**
	(0.00194)	(0.00250)	(0.00412)	(0.00466)
GDD 15-20 C	-0.00082	-0.01161***	-0.01014**	-0.01010**
	(0.00098)	(0.00238)	(0.00410)	(0.00464)
GDD 20-25 C	0.00072	-0.01340***	-0.01285***	-0.01289***
	(0.00100)	(0.00258)	(0.00437)	(0.00483)
GDD 25-30 C	-0.00088	-0.01241***	-0.01118***	-0.01207**
	(0.00077)	(0.00253)	(0.00409)	(0.00464)
GDD 30-35 C	0.00627***	-0.00999***	-0.01037**	-0.01054**
	(0.00137)	(0.00277)	(0.00467)	(0.00500)
GDD 35-45 C	-0.00208	-0.00723**	-0.00884**	-0.01006**
	(0.00274)	(0.00304)	(0.00423)	(0.00496)
Constant	0.15815***			
	(0.02912)			
Unit FE	No	Yes	Yes	Yes
Period FE	No	No	Yes	Yes
Unit-specific linear trends	No	No	No	Yes
Observations	69,691	69,691	69,691	69,691
RMSE	0.219	0.062	0.058	0.053
R^2	0.171	0.934	0.941	0.951
AIC	-14,052.3	-180,589.0	-188,562.8	-191,979.2
BIC	-13,969.9	-137,063.0	-144,853.7	-104,817.2
Adjusted R^2	0.171	0.929	0.937	0.943

Note: Standard errors are clustered at the level of index unit level. *p<0.1; **p<0.05; ***p<0.01.

Table D.2.2: First stage results for the share of photosynthetic vegetation (PV) in all rangelands at the HUC-12 level (see corresponding second stage results in Table 1 of main text).

	Dependent variable: Photosynthetic vegetation (PV) share all rangelands			
Precipitation mean (mm)	0.00059***	0.00056***	0.00046***	0.00047***
	(0.00004)	(0.00004)	(0.00004)	(0.00004)
Precipitation stn. dev. (mm)	0.00118***	0.00009	0.00001	-0.00010
	(0.00022)	(0.00018)	(0.00018)	(0.00020)
GDD 5-15 C	0.00313***	0.00635**	-0.04691***	-0.04566***
	(0.00076)	(0.00256)	(0.01419)	(0.01483)
GDD 15-20 C	-0.00262***	0.00233	-0.05137***	-0.05079***
	(0.00054)	(0.00278)	(0.01426)	(0.01487)
GDD 20-25 C	-0.00351***	0.00164	-0.05192***	-0.05160***
	(0.00053)	(0.00262)	(0.01422)	(0.01484)
GDD 25-30 C	0.00121**	-0.00027	-0.05366***	-0.05290***
	(0.00046)	(0.00255)	(0.01421)	(0.01482)
GDD 30-35 C	-0.00457***	-0.00060	-0.05306***	-0.05294***
	(0.00077)	(0.00254)	(0.01420)	(0.01480)
GDD 35-45 C	-0.00327***	-0.00121	-0.05608***	-0.05543***
	(0.00104)	(0.00266)	(0.01418)	(0.01489)
Constant	0.37920***			
	(0.05603)			
Unit FEs	No	Yes	Yes	Yes
Period FEs	No	No	Yes	Yes
Unit-specific linear trends	No	No	No	Yes
Observations	69,691	69,691	69,691	69,691
RMSE	0.100	0.057	0.054	0.052
R^2	0.434	0.814	0.835	0.849
AIC	-122,655.6	-190,906.1	-198,913.6	-195,606.0
BIC	-122,573.2	-147,380.0	-155,204.5	-108,444.0
Adjusted R^2	0.434	0.801	0.822	0.825

Note: Standard errors are clustered at the level of index unit level. *p<0.1; **p<0.05; ***p<0.01.

Table D.2.3: First stage results for the share of non-photosynthetic vegetation (NPV) in all rangelands at the HUC-12 level (see corresponding second stage results in Table 1 of main text).

Dependent variable: Non-photosynthetic vegetation (NPV) share all rangelands				
Precipitation mean (mm)	-0.00033***	-0.00034***	-0.00022***	-0.00022***
	(0.00007)	(0.00003)	(0.00003)	(0.00003)
Precipitation stn. dev. (mm)	0.00060	-0.00034*	-0.00013	-0.00027
	(0.00056)	(0.00018)	(0.00018)	(0.00021)
GDD 5-15 C	-0.00827***	0.00544**	0.05780***	0.05669***
	(0.00174)	(0.00256)	(0.01451)	(0.01429)
GDD 15-20 C	0.00344***	0.00928***	0.06151***	0.06090***
	(0.00086)	(0.00241)	(0.01448)	(0.01427)
GDD 20-25 C	0.00279***	0.01175***	0.06477***	0.06449***
	(0.00088)	(0.00251)	(0.01448)	(0.01426)
GDD 25-30 C	-0.00032	0.01269***	0.06484***	0.06497***
	(0.00058)	(0.00256)	(0.01448)	(0.01426)
GDD 30-35 C	-0.00171	0.01059***	0.06343***	0.06348***
	(0.00118)	(0.00251)	(0.01444)	(0.01418)
GDD 35-45 C	0.00535**	0.00843**	0.06492***	0.06548***
	(0.00213)	(0.00341)	(0.01432)	(0.01415)
Constant	0.46265***			
	(0.04373)			
Unit FEs	No	Yes	Yes	Yes
Period FEs	No	No	Yes	Yes
Unit-specific linear trends	No	No	No	Yes
Observations	69,691	69,691	69,691	69,691
RMSE	0.177	0.062	0.058	0.055
R^2	0.148	0.896	0.908	0.919
AIC	-43,718.0	-180,585.5	-189,227.6	-188,395.2
BIC	-43,635.6	-137,059.4	-145,518.5	-101,233.2
Adjusted R^2	0.148	0.888	0.901	0.906

Note: Standard errors are clustered at the level of index unit level. *p<0.1; **p<0.05; ***p<0.01.

Table D.2.4: First stage results for mean enhanced vegetation index (EVI) in all rangelands at the HUC-12 level (see corresponding second stage results in Table 1 of main text).

	Dependent variable: Mean enhanced vegetation index (EVI) in all rangelands			
Precipitation mean (mm)	0.00032***	0.00021***	0.00014***	0.00014***
	(0.00002)	(0.00001)	(0.00001)	(0.00001)
Precipitation stn. dev. (mm)	-0.00025**	0.00007	0.00011***	0.00011**
	(0.00010)	(0.00005)	(0.00004)	(0.00004)
GDD 5-15 C	0.00205***	0.00023	0.00074***	0.00078**
	(0.00030)	(0.00021)	(0.00021)	(0.00031)
GDD 15-20 C	-0.00101***	-0.00068***	-0.00028***	-0.00024*
	(0.00011)	(0.00011)	(0.00010)	(0.00012)
GDD 20-25 C	-0.00067***	-0.00021**	0.00005	-0.000002
	(0.00025)	(0.00010)	(0.00011)	(0.00013)
GDD 25-30 C	0.00040	-0.00049***	-0.00033***	-0.00029***
	(0.00028)	(0.00009)	(0.00010)	(0.00010)
GDD 30-35 C	-0.00209***	-0.00061***	-0.00007	-0.00005
	(0.00038)	(0.00016)	(0.00013)	(0.00014)
GDD 35-45 C	-0.00005	-0.00036*	0.00019	0.00028
	(0.00036)	(0.00019)	(0.00025)	(0.00026)
Constant	0.22038***			
	(0.01532)			
Unit FE	No	Yes	Yes	Yes
Period FE	No	No	Yes	Yes
Unit-specific linear trends	No	No	No	Yes
Observations	141,010	141,010	141,010	141,010
RMSE	0.044	0.024	0.022	0.021
R^2	0.565	0.865	0.893	0.903
AIC	-481,678.9	-637,261.5	-670,386.5	-673,837.4
BIC	-481,590.2	-590,383.5	-623,104.5	-579,756.3
Adjusted R^2	0.565	0.860	0.890	0.896

Note: Standard errors are clustered at the level of index unit level. *p<0.1; **p<0.05; ***p<0.01.

D.3 Robustness Checks

Table D.3.1: Intensive margin tests (overall ATTs) for the effect of IBLI on rangelands using inverse distance weighted (IDW) continuous measures of the total cumulative TLUs insured at the HUC-9 level (see Gardner et al. (2025) pg. 17-18).

	Dependent variable: Bare ground (BG) share all rangelands			
Total cumulative TLUs insured (IDW)	0.000008***	-0.000004***	-0.000003	0.0000008
	(0.000003)	(0.000001)	(0.000003)	(0.000002)
BG second stage statistics				
Observations	48,953	48,953	48,953	48,953
Adjusted R^2	0.001	0.004	0.002	0.0001
	Dependent variable: Photosynthetic vegetation (PV) share all rangelands			
Total cumulative TLUs insured (IDW)	-0.000005***	0.000006***	0.000006***	-0.000002
	(0.000002)	(0.0000008)	(0.000001)	(0.000003)
PV second stage statistics				
Observations	48,953	48,953	48,953	48,953
Adjusted R^2	0.002	0.014	0.014	0.001
	Dependent variable: Non-photosynthetic vegetation (NPV) share all rangelands			
Total cumulative TLUs insured (IDW)	-0.000005*	-0.000002**	-0.000004	0.000001
	(0.000003)	(0.000001)	(0.000003)	(0.000003)
NPV second stage statistics				
Observations	48,953	48,953	48,953	48,953
Adjusted R^2	0.0008	0.001	0.004	0.0005
	Dependent variable: Mean enhanced vegetation index (EVI) all rangelands			
Total cumulative TLUs insured (IDW)	-0.0000006	0.000001***	0.000004***	0.000002**
	(0.0000009)	(0.0000004)	(0.0000008)	(0.0000009)
EVI second stage statistics				
Observations	98,154	98,154	98,154	98,154
Adjusted R^2	0.00008	0.003	0.022	0.009
First stage specifications (BG, PV, NPV, EVI)				
Unit fixed effects	No	Yes	Yes	Yes
Period fixed effects	No	No	Yes	Yes
Unit-specific trends	No	No	No	Yes

Note: First stage covariates are the same across models and include: the mean and standard deviation of seasonal precipitation (mm), and mean GDD in 5° C bins with the exception of two 10° C bins from 5-10° C and 30-45° C due to limited exposure from 5-10° C and 35-40° C. Standard errors are clustered at the level of index unit level. *p<0.1; **p<0.05; ***p<0.01.

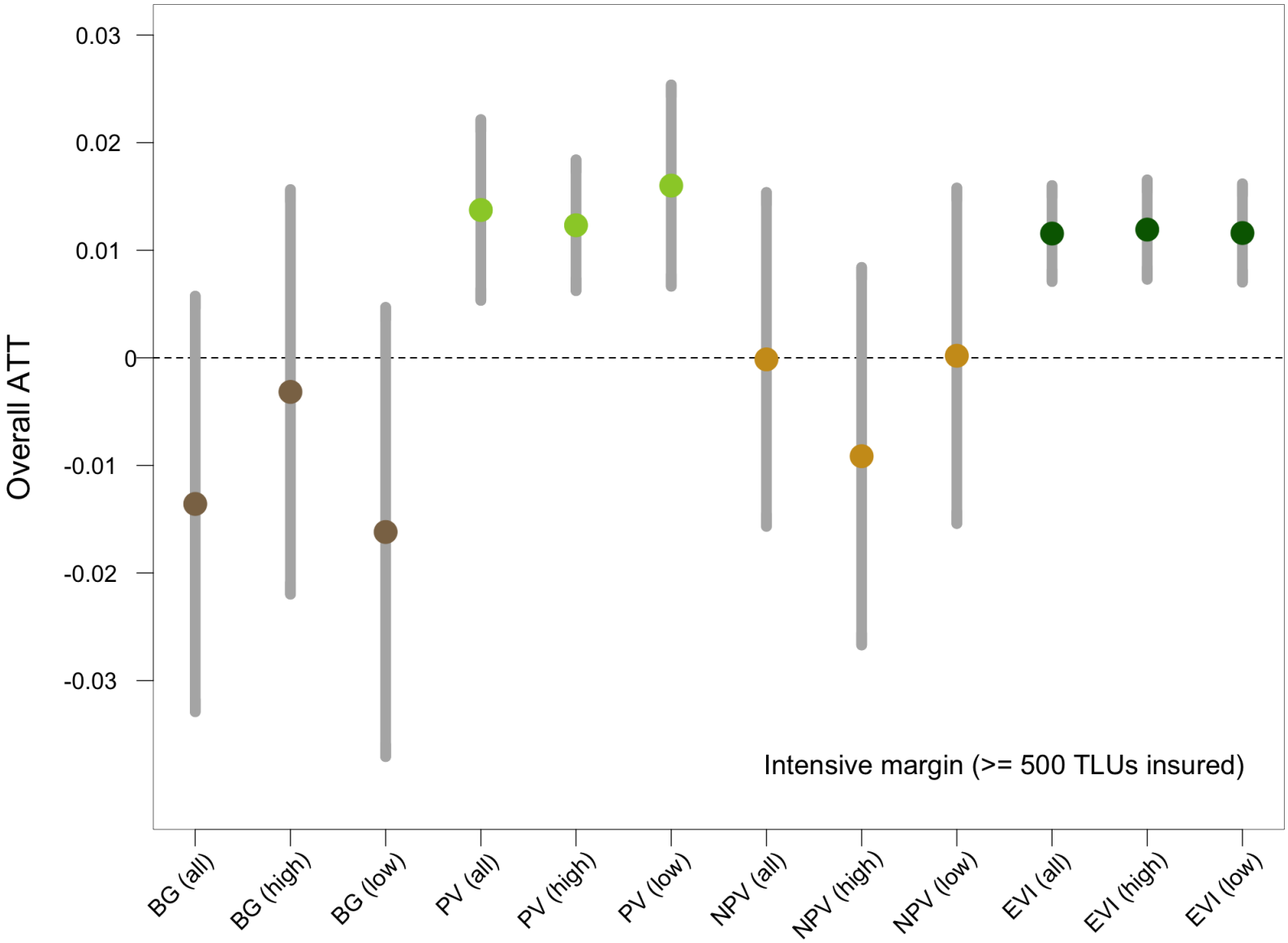


Figure D.3.1: Overall ATTs with 95% confidence intervals for tests of impacts at HUC-12 level from IBLI exposure at the intensive margin of $\geq$ 500 cumulative IDW TLUs insured. ATTs reflect point estimates of β in equation (2) from Gardner et al. (2025) (see Section 4). Standard errors are clustered at the index unit level. From left to right, estimated coefficients reflect IBLI's impacts on BG, PV, NPV and EVI within all, high, and low rangelands (see Section 3.3). The number of observations for respective estimations are: fractional cover all mask, $n = 99,426$; fractional cover high mask, $n = 98,373$; fractional cover low mask, $n = 99,361$; EVI all mask, $n = 199,416$; EVI high mask, $n = 196,416$; EVI low mask, $n = 199,416$. First stage covariates are the same across models and include: the mean and standard deviation of seasonal precipitation (mm), and mean GDD in 5° C bins with the exception of two 10° C bins from 5-10° C and 30-45° C due to limited exposure from 5-10° C and 35-40° C. Each model includes unit and period fixed effects.

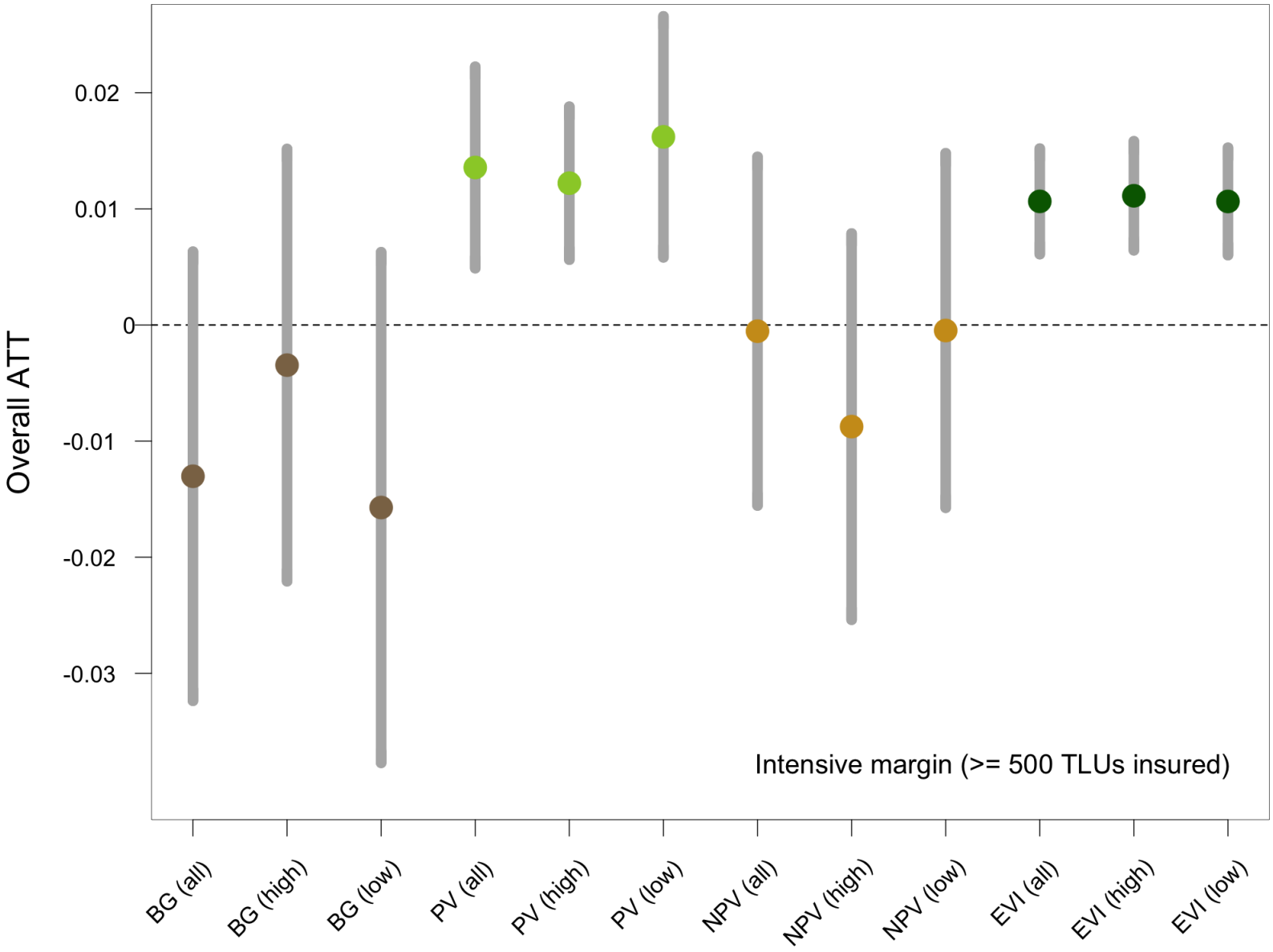


Figure D.3.2: Overall ATTs with 95% confidence intervals for tests of impacts at HUC-9 level from IBLI exposure at the intensive margin of $\geq$ 500 cumulative IDW TLUs insured. ATTs reflect point estimates of β in equation (2) from Gardner et al. (2025) (see Section 4). Standard errors are clustered at the index unit level. From left to right, estimated coefficients reflect IBLI's impacts on BG, PV, NPV and EVI within all, high, and low rangelands (see Section 3.3). The number of observations for respective estimations are: fractional cover all mask, $n = 48,953$; fractional cover high mask, $n = 48,520$; fractional cover low mask, $n = 48,922$; EVI all mask, $n = 98,154$; EVI high mask, $n = 97,012$; EVI low mask, $n = 98,102$. First stage covariates are the same across models and include: the mean and standard deviation of seasonal precipitation (mm), and mean GDD in 5° C bins with the exception of two 10° C bins from 5-10° C and 30-45° C due to limited exposure from 5-10° C and 35-40° C. Each model includes unit and period fixed effects.

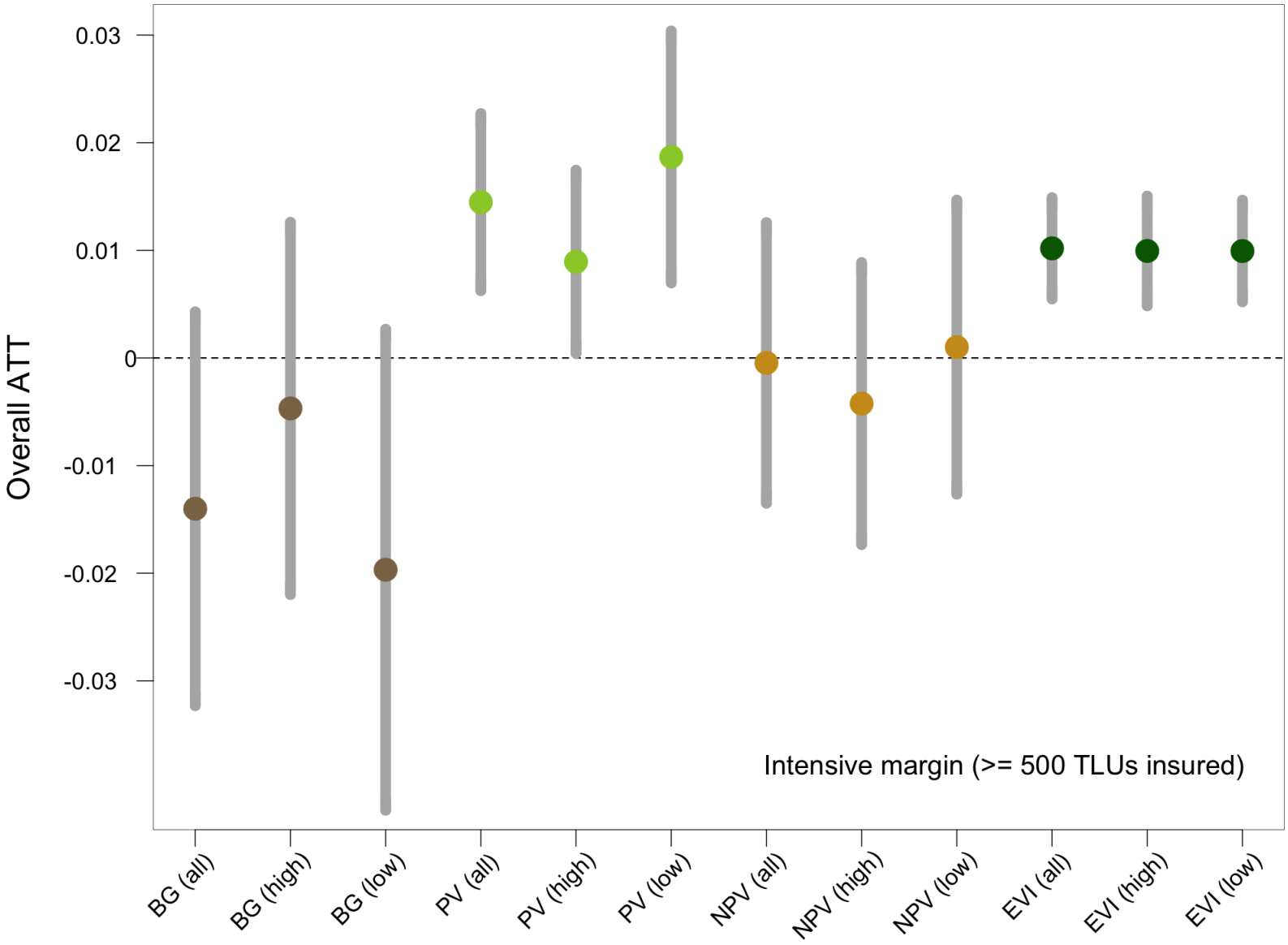


Figure D.3.3: Overall ATTs with 95% confidence intervals for tests of impacts at HUC-8 level from IBLI exposure at the intensive margin of $\geq$ 500 cumulative IDW TLUs insured. ATTs reflect point estimates of β in equation (2) from Gardner et al. (2025) (see Section 4). Standard errors are clustered at the index unit level. From left to right, estimated coefficients reflect IBLI's impacts on BG, PV, NPV and EVI within all, high, and low rangelands (see Section 3.3). The number of observations for respective estimations are: fractional cover all mask, $n = 18,215$; fractional cover high mask, $n = 18,095$; fractional cover low mask, $n = 18,215$; EVI all mask, $n = 36,488$; EVI high mask, $n = 36,246$; EVI low mask, $n = 36,488$. First stage covariates are the same across models and include: the mean and standard deviation of seasonal precipitation (mm), and mean GDD in 5° C bins with the exception of two 10° C bins from 5-10° C and 30-45° C due to limited exposure from 5-10° C and 35-40° C. Each model includes unit and period fixed effects.

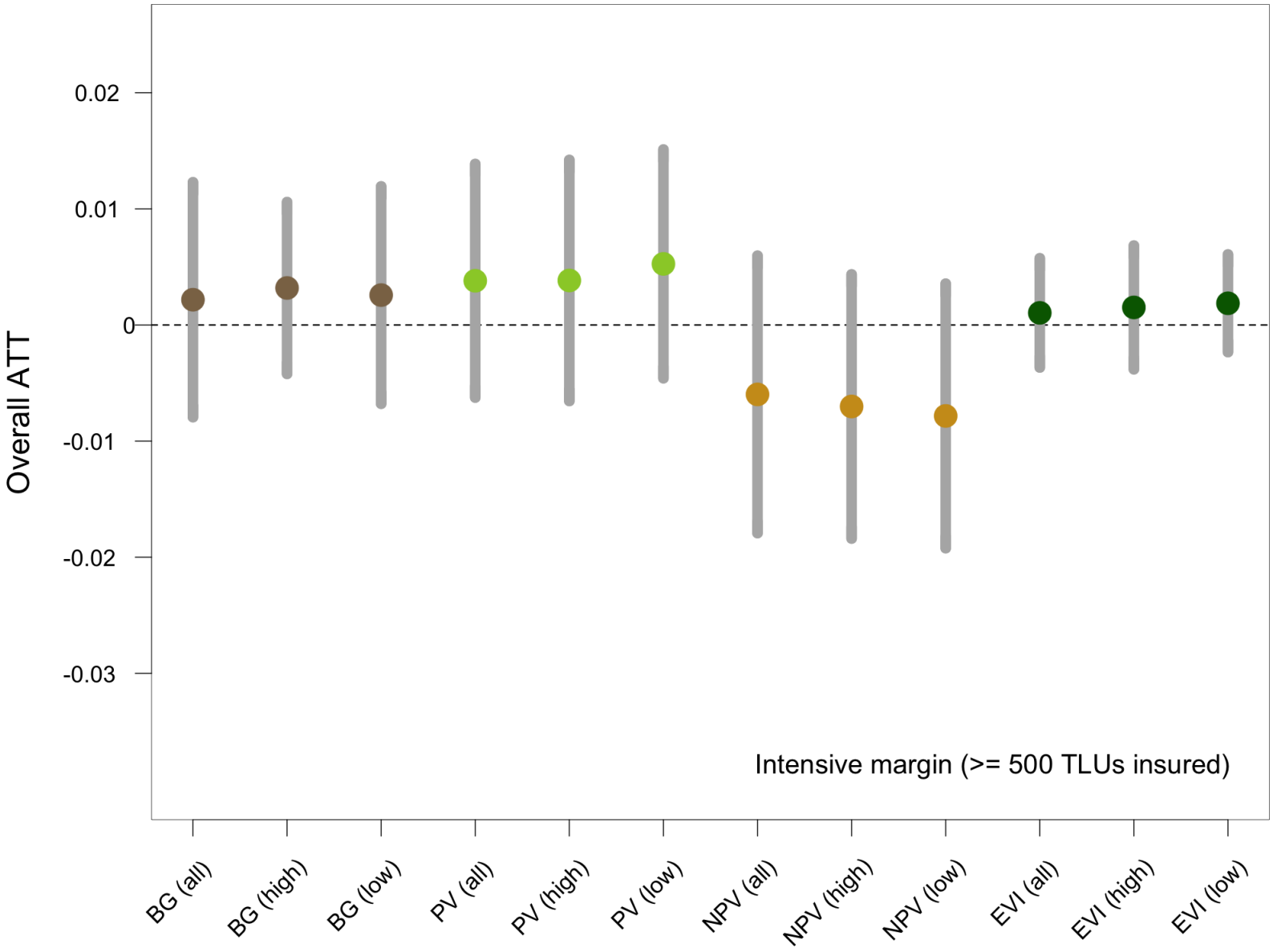


Figure D.3.4: Overall ATTs with 95% confidence intervals for tests of impacts at IU-CA level from IBLI exposure at the intensive margin of $\geq$ 500 cumulative IDW TLUs insured. ATTs reflect point estimates of β in equation (2) from Gardner et al. (2025) (see Section 4). Standard errors are clustered at the index unit level. From left to right, estimated coefficients reflect IBLI's impacts on BG, PV, NPV and EVI within all, high, and low rangelands (see Section 3.3). The number of observations for respective estimations are: fractional cover all mask, $n = 2,730$; fractional cover high mask, $n = 2,730$; fractional cover low mask, $n = 2,730$; EVI all mask, $n = 5,460$; EVI high mask, $n = 5,460$; EVI low mask, $n = 5,460$. First stage covariates are the same across models and include: the mean and standard deviation of seasonal precipitation (mm), and mean GDD in 5° C bins with the exception of two 10° C bins from 5-10° C and 30-45° C due to limited exposure from 5-10° C and 35-40° C. Each model includes unit and period fixed effects.

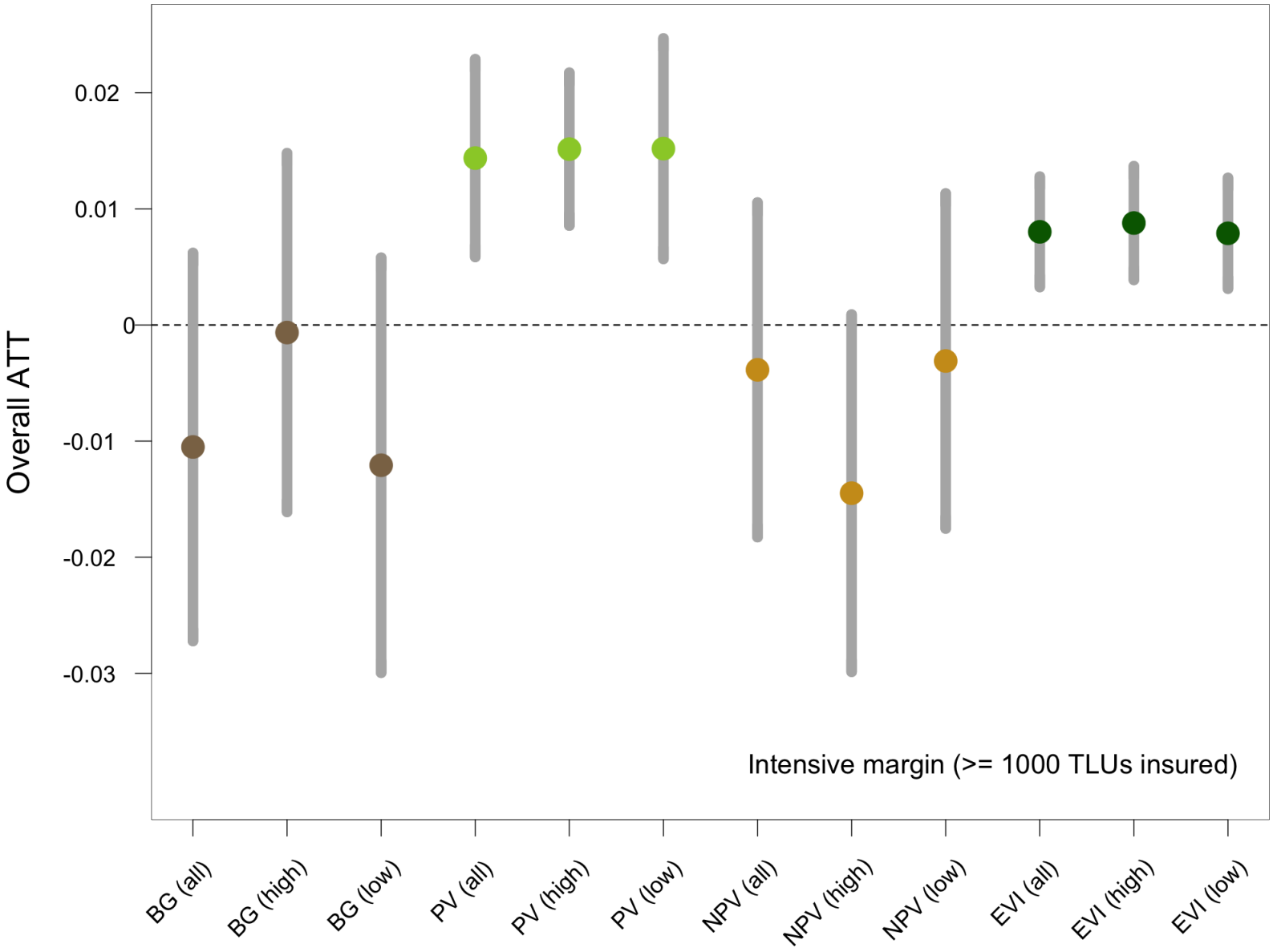


Figure D.3.5: Overall ATTs with 95% confidence intervals for tests of impacts at HUC-12 level from IBLI exposure at the intensive margin of $\geq$ 1000 cumulative IDW TLUs insured. ATTs reflect point estimates of β in equation (2) from Gardner et al. (2025) (see Section 4). Standard errors are clustered at the index unit level. From left to right, estimated coefficients reflect IBLI's impacts on BG, PV, NPV and EVI within all, high, and low rangelands (see Section 3.3). The number of observations for respective estimations are: fractional cover all mask, $n = 99,426$; fractional cover high mask, $n = 98,373$; fractional cover low mask, $n = 99,361$; EVI all mask, $n = 199,500$; EVI high mask, $n = 196,558$; EVI low mask, $n = 199,364$. First stage covariates are the same across models and include: the mean and standard deviation of seasonal precipitation (mm), and mean GDD in 5° C bins with the exception of two 10° C bins from 5-10° C and 30-45° C due to limited exposure from 5-10° C and 35-40° C. Each model includes unit and period fixed effects.

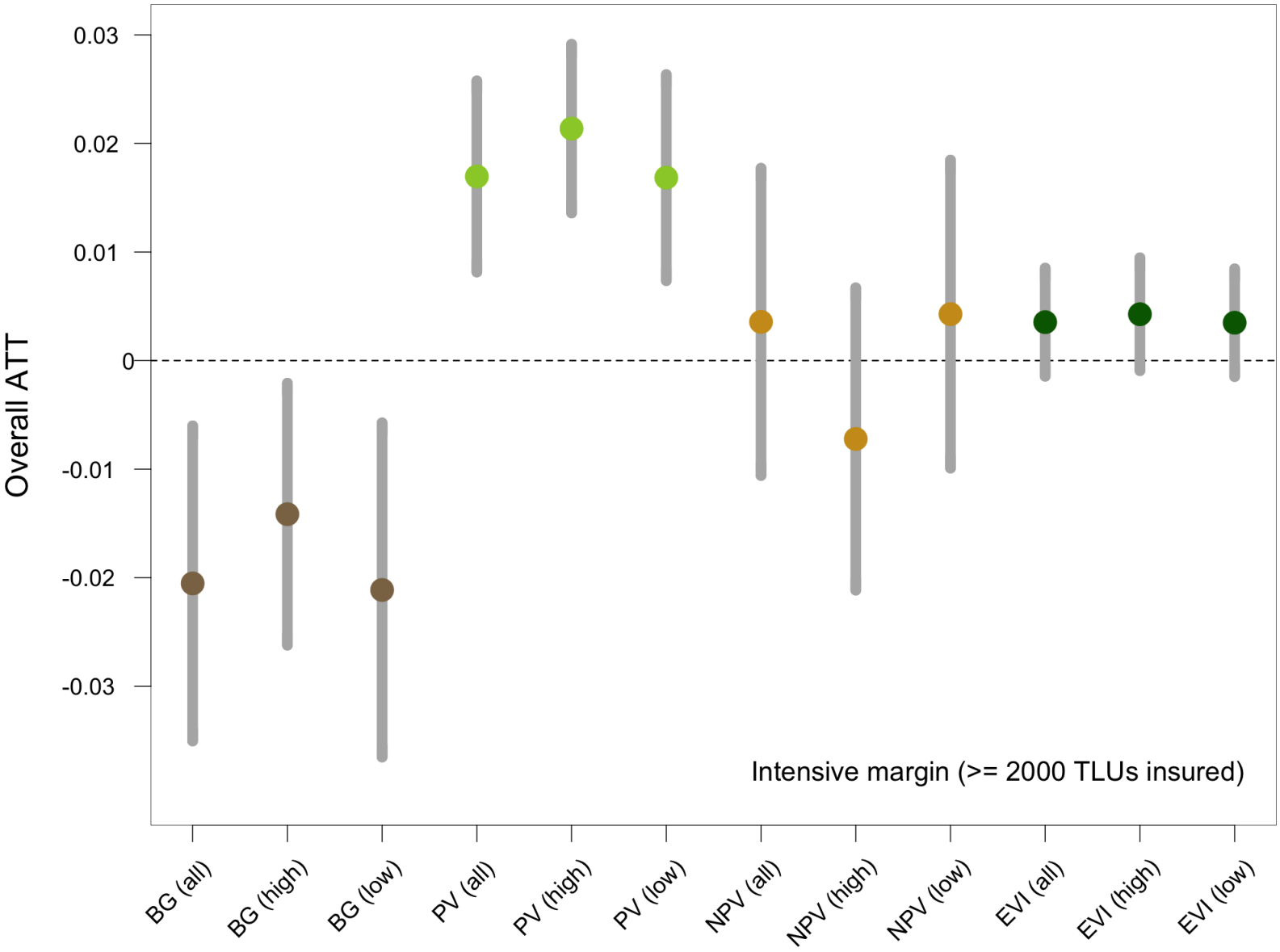


Figure D.3.6: Overall ATTs with 95% confidence intervals for tests of impacts at HUC-12 level from IBLI exposure at the intensive margin of $\geq$ 2000 cumulative IDW TLUs insured. ATTs reflect point estimates of β in equation (2) from Gardner et al. (2025) (see Section 4). Standard errors are clustered at the index unit level. From left to right, estimated coefficients reflect IBLI's impacts on BG, PV, NPV and EVI within all, high, and low rangelands (see Section 3.3). The number of observations for respective estimations are: fractional cover all mask, $n = 99,426$; fractional cover high mask, $n = 98,373$; fractional cover low mask, $n = 99,361$; EVI all mask, $n = 199,500$; EVI high mask, $n = 196,558$; EVI low mask, $n = 199,364$. First stage covariates are the same across models and include: the mean and standard deviation of seasonal precipitation (mm), and mean GDD in 5° C bins with the exception of two 10° C bins from 5-10° C and 30-45° C due to limited exposure from 5-10° C and 35-40° C. Each model includes unit and period fixed effects.

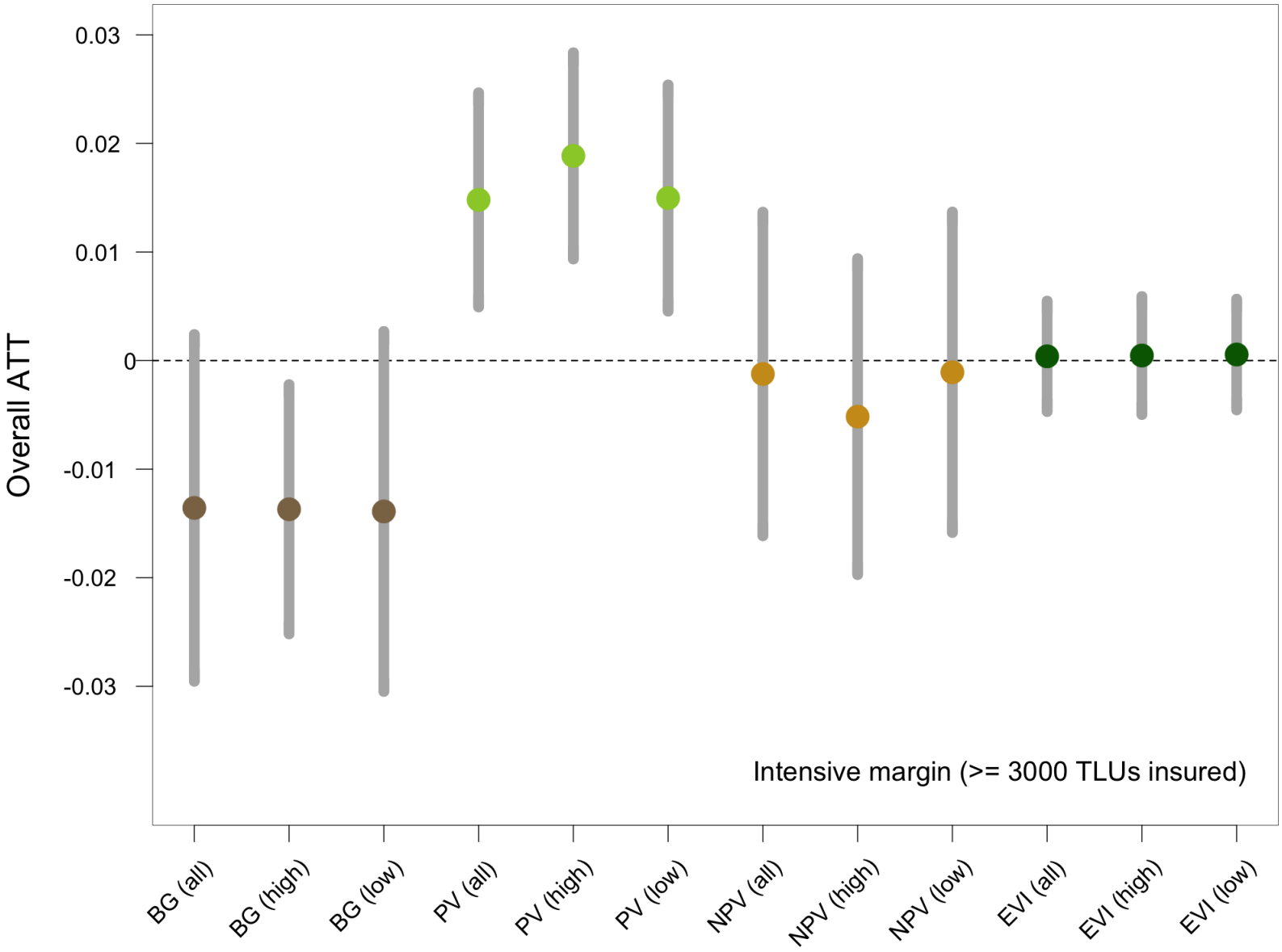


Figure D.3.7: Overall ATTs with 95% confidence intervals for tests of impacts at HUC-12 level from IBLI exposure at the intensive margin of $\geq$ 3000 cumulative IDW TLUs insured. ATTs reflect point estimates of β in equation (2) from Gardner et al. (2025) (see Section 4). Standard errors are clustered at the index unit level. From left to right, estimated coefficients reflect IBLI's impacts on BG, PV, NPV and EVI within all, high, and low rangelands (see Section 3.3). The number of observations for respective estimations are: fractional cover all mask, $n = 99,426$; fractional cover high mask, $n = 98,373$; fractional cover low mask, $n = 99,361$; EVI all mask, $n = 199,500$; EVI high mask, $n = 196,558$; EVI low mask, $n = 199,364$. First stage covariates are the same across models and include: the mean and standard deviation of seasonal precipitation (mm), and mean GDD in 5° C bins with the exception of two 10° C bins from 5-10° C and 30-45° C due to limited exposure from 5-10° C and 35-40° C. Each model includes unit and period fixed effects.

Table D.3.2: Overall ATT tests for seasonal differences in the effect of IBLI on average EVI.

	Extensive margin test for different effects by season		
	EVI-all	EVI-high	EVI-low
Post-IBLI extensive margin (dummy)	0.00369**	0.00462**	0.00359*
	(0.00186)	(0.00197)	(0.00190)
Post-IBLI extensive margin (dummy) ×	0.00423	0.00412	0.00414
LRLD season (dummy)	(0.00279)	(0.00281)	(0.00274)
Second stage statistics			
Observations	199,416	196,474	199,280
Adjusted R^2	0.014	0.015	0.013
	Intensive margin test for different effects by season (continuous exposure)		
	EVI-all	EVI-high	EVI-low
Total cumulative TLUs insured (IDW)	0.000005***	0.000005***	0.000005***
	(0.000001)	(0.000001)	(0.000001)
Total cumulative TLUs insured (IDW) ×	0.00000015	0.0000003	0.000000017
LRLD season (dummy)	(0.000002)	(0.000002)	(0.000002)
Second stage statistics			
Observations	199,416	196,474	199,280
Adjusted R^2	0.024	0.026	0.023
First stage specifications			
Unit fixed effects	Y	Y	Y
Period fixed effects	Y	Y	Y
Weather covariates	Y	Y	Y

Note: Estimated effects are from extensive margin and continuous intensive margin versions of the two-stage estimator from Gardner et al. (2025) (see Section 4). Respective second stage equations are augmented with an interaction term between respective IBLI exposure variables and a dummy variable capturing the LRLD season. First stage weather covariates are the same across models and include: the mean and standard deviation of seasonal precipitation (mm), and mean GDD in 5° C bins with the exception of two 10° C bins from 5-10° C and 30-45° C due to limited exposure from 5-10° C and 35-40° C. Standard errors are clustered at the index unit level. *p <0.1; **p <0.05; ***p <0.01.

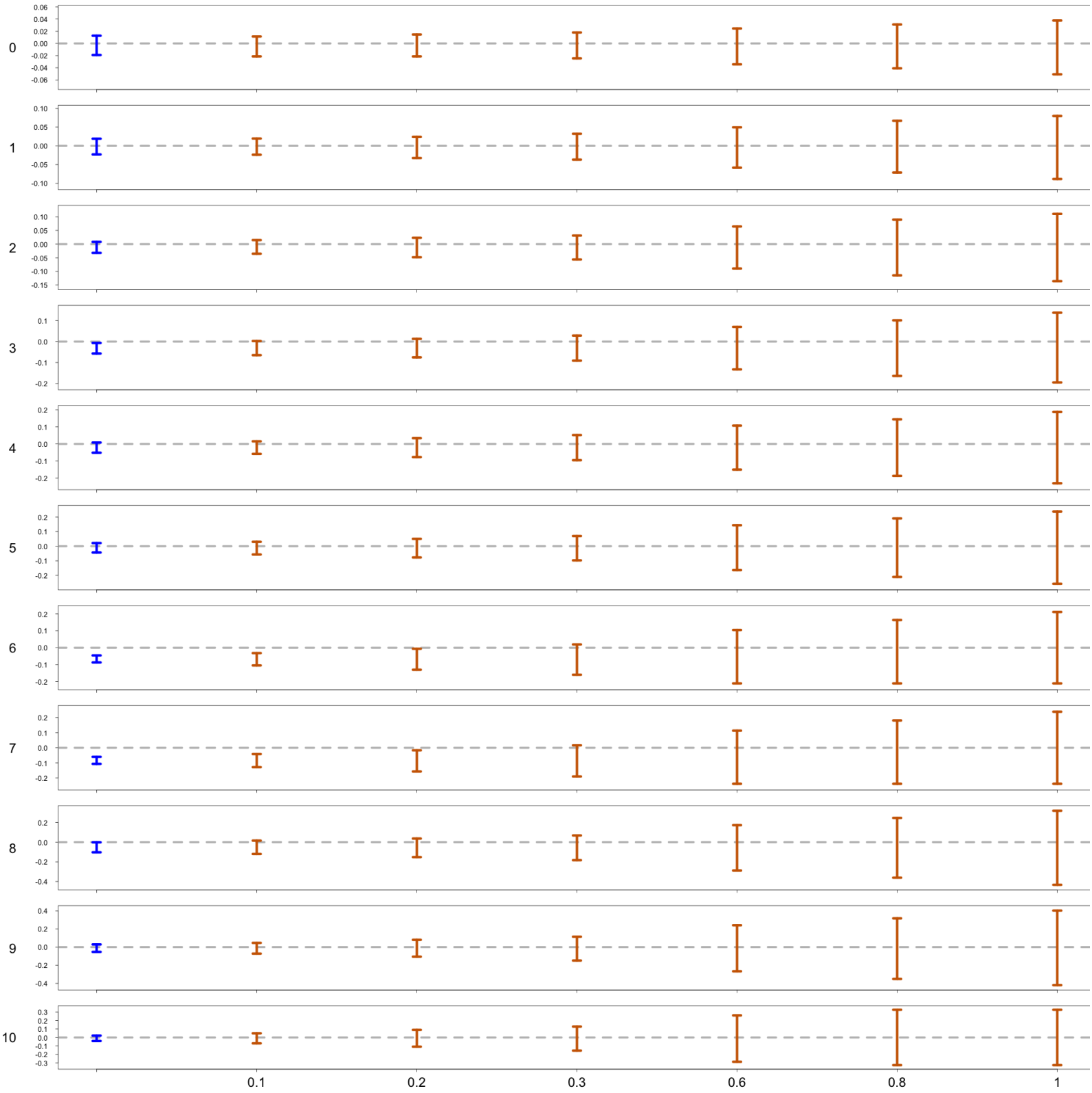


Figure D.3.8: 95% confidence intervals (CIs) following Rambachan and Roth (2023) for the effect of IBLI on the share of bare ground (BG) in all rangelands at the HUC-12 level and exposure to ≥ 500 cumulative IDW TLUs insured. The y-axis captures post-treatment event time period CIs. Blue CIs are original and orange CIs vary based on the proportion (x-axis) of the maximum M pre-treatment violation of parallel trends that is applied to bound maximum potential post-treatment violations of parallel trends between consecutive time periods.

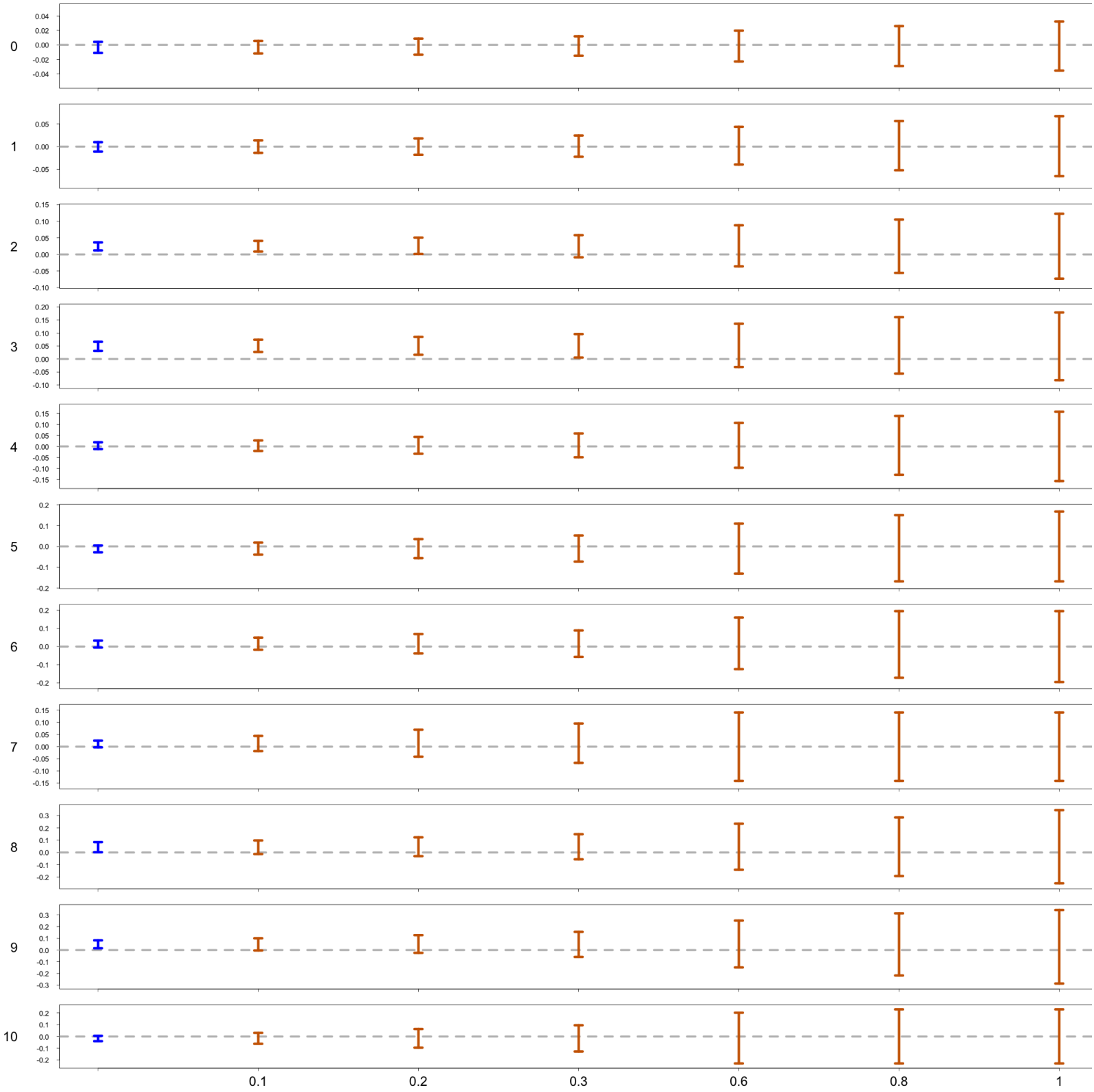


Figure D.3.9: 95% confidence intervals (CIs) following Rambachan and Roth (2023) for the effect of IBLI on the share of photosynthetic vegetation (PV) in all rangelands at the HUC-12 level and exposure to $\geq$ 500 cumulative IDW TLUs insured. The y-axis captures post-treatment event time period CIs. Blue CIs are original and orange CIs vary based on the proportion (x-axis) of the maximum M pre-treatment violation of parallel trends that is applied to bound maximum potential post-treatment violations of parallel trends between consecutive time periods.

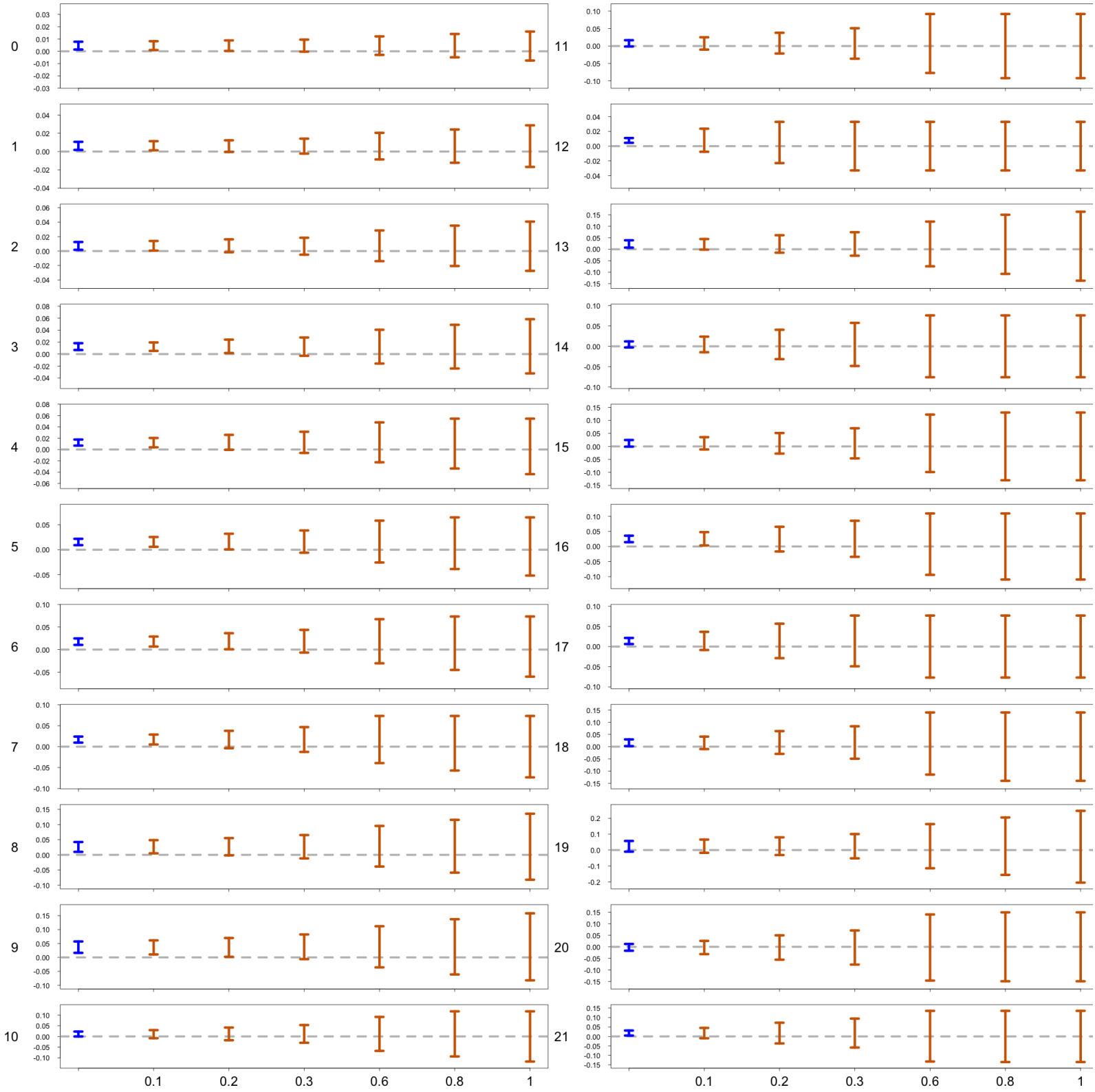


Figure D.3.10: 95% confidence intervals (CIs) following Rambachan and Roth (2023) for the effect of IBLI on mean enhanced vegetation index (EVI) in all rangelands at the HUC-12 level and exposure to ≥ 500 cumulative IDW TLUs insured. The y-axis captures post-treatment event time period CIs (periods 0 to 21). Blue CIs are original and orange CIs vary based on the proportion (x-axis) of the maximum M pre-treatment violation of parallel trends that is applied to bound maximum potential post-treatment violations of parallel trends between consecutive time periods.

References

Cattaneo, Matias D., Richard K. Crump, Max H. Farrell, and Yingjie Feng. 2024a. binsreg: Binscatter estimation and inference. R package version 1.1. Available at: https://cran.r-project.org/web/packages/binsreg/binsreg.pdf.

Cattaneo, Matias D, Richard K Crump, Max H Farrell, and Yingjie Feng. 2024b. On binscatter. *American Economic Review* 114 (5): 1488–1514. DOI: 10.1257/aer.20221576.

Clark, Patrick E, Douglas E Johnson, Mark A Kniep, Phillip Jermann, Brad Huttash, Andrew Wood, Michael Johnson, et al. 2006. An advanced, low-cost, gps-based animal tracking system. *Rangeland Ecology & Management* 59 (3): 334–340. DOI: https://doi.org/10.2111/05-162R.1.

Didan, Kamel, Armando Barreto Munoz, Ramón Solano, and Alfredo Huete. 2021. Modis/terra vegetation indices 16-day l3 global 250m sin grid v061 [dataset]. DOI https://doi.org/10.5067/MODIS/MOD13Q1.061.

Gardner, John, Neil Thakral, Linh T. Tô, and Luther Yap. 2025. Two-stage differences in differences. Working paper, Available at: https://neilthakral.github.io/files/papers/2sdd.pdf.

Jakiela, Pamela. 2021. Simple diagnostics for two-way fixed effects. Working paper, DOI: https://doi.org/10.48550/arXiv.2103.13229.

Lehner, Bernhard, and Günther Grill. 2013. Global river hydrography and network routing: baseline data and new approaches to study the world's large river systems. *Hydrological Processes* 27 (15): 2171–2186. DOI: https://doi.org/10.1002/hyp.9740.

Liao, Chuan, Patrick E Clark, and Stephen D DeGloria. 2018. Bush encroachment dynamics and rangeland management implications in southern ethiopia. *Ecology and evolution* 8 (23): 11694–11703. DOI: https://doi.org/10.1002/ece3.4621.

Liao, Chuan, Patrick E Clark, Stephen D DeGloria, and Christopher B Barrett. 2017. Complexity in the spatial utilization of rangelands: Pastoral mobility in the horn of africa. *Applied Geography* 86: 208–219. DOI: https://doi.org/10.1016/j.apgeog.2017.07.003.

Pellant, Mike, Patrick L. Shaver, David A. Pyke, Jeffrey E. Herrick, Nika Lepak, Gregg Riegel, Emily Kachergis, et al. 2020. Interpreting indicators of rangeland health, version 5: Technical reference 1734-6. U.S. Department of the Interior, Bureau of Land Management. Available at: https://pubs.er.usgs.gov/publication/70215720.

Rambachan, Ashesh, and Jonathan Roth. 2023. A more credible approach to parallel trends. *Review of Economic Studies* 90 (5): 2555–2591. DOI: https://doi.org/10.1093/restud/rdad056.

Soto, Gerardo E, Steven W. Wilcox, Patrick E Clark, Francesco P Fava, Nathaniel D Jensen, Njoki Kahiu, Chuan Liao, et al. 2024. Mapping rangeland health indicators in eastern africa from 2000 to 2022. *Earth System Science Data* 16 (11): 5375–5404. DOI: https://doi.org/10.5281/zenodo.7106166.